Activated interleukin-7 receptor signaling drives B-cell acute lymphoblastic leukemia in mice.

Kerri R. Thomas

A dissertation

submitted in partial fulfillment of the

requirements for the degree of

Doctor of Philosophy

University of Washington

2021

Reading committee

David J. Rawlings, chair

Richard G. James

Brian Iritani

Program Authorized to Offer Degree

Department of Immunology

University of Washington

Abstract

Activated interleukin-7 receptor signaling drives B-cell acute lymphoblastic leukemia in mice.

Kerri R. Thomas

Chair of the Supervisory Committee:

Adjunct Professor David J. Rawlings, M.D.

Department of Immunology

Philadelphia chromosome-like acute lymphoblastic leukemia (Ph-like ALL) is a high-risk subtype of B-ALL often associated with genetic variants that alter cytokine receptor signaling, including mutations in the interleukin-7 receptor (*IL7R*). Although gain-of-function mutations in *IL7R* are present in a subset of Ph-like ALLs, whether these lesions can initiate leukemic disease remains unknown. To investigate whether *IL7R* variants are leukemia-initiating, we built mouse models expressing activated *Il7r* (aIL7R). B-cell intrinsic aIL7R mice developed spontaneous B-ALL, demonstrating sufficiency of *Il7r* activating mutations in leukemogenesis. Concomitant introduction of a knock-out allele in the associated adapter protein Lnk (encoded by *Sh2b3*) or a dominant-negative variant of the transcription factor Ikaros (*Ikzf1*) increased disease penetrance. The resulting murine leukemias displayed monoclonality and recurrent somatic *Kras* mutations and efficiently engrafted into immunocompetent mice. Prior to transformation, aIL7R-expressing mice exhibited an expansion of late pro-B cells with elevated Bcl-xl expression and IL-7-independent survival. Phosphoproteomic analyses of aIL7R leukemic cells revealed constitutive Stat5 signaling and B cell receptor (BCR)-like signaling despite absence of surface pre-BCR. A human Ph-like ALL xenograft with mutant *IL7R*, loss of *SH2B3*, and *VPREB1* deletion recapitulated this signature. Finally, *in vitro*

treatment of aIL7R leukemic B-cells with Jak, mTOR, or Syk inhibitors blocked growth, confirming that each pathway is active in this model of *IL7R*-driven B-ALL.

TABLE OF CONTENTS

List of Figures

List of Tables

Acknowledgements

I would like to thank Eric Allenspach, Michelle Wray-Dutra, and Jacquelyn Gorman for assistance with designing, performing, and interpreting experiments. Thanks to Richard James and Nate Camp for assistance in designing, performing, and interpreting the mass spectrometry phosphoproteomics experiments. Thank you to the Northwest Genomics Center at the University of Washington for performing the whole exome sequencing and to Andrew Timms and Eric Allenspach for their assistance with the analysis. Thank you to the UW Histology and Imaging Core for performing the H&E staining and to Denny Liggitt for the histopathology analysis. Thank you to Joseph Loftus and Sarah Tasian for sharing Ph-like ALL xenografts for these studies and for performing the *in vivo* entospletinib treatment experiment. Thank you to Katia Georgopoulos for sharing the Ikzf1 exon 5 floxed mice. Finally, a big thank you to Eric Allenspach, Sarah Tasian, Beth Lawlor, Katia Georgopoulos, Richard James, and David Rawlings for critical review of the manuscript that resulted from these studies.

Chapter I. **Introduction**

I.1 **B cell lymphopoiesis**

The adaptive immune system consists of lymphocytes, specifically T and B cells, that function coordinately to orchestrate highly specialized and pathogen-specific responses to infection. The primary effector functions of B cells during an immune response are to recognize and internalize antigen via their B cell receptor (BCR), present antigen to T cells, and to produce opsonizing and/or neutralizing antibodies. Most B cells develop within in the bone marrow, where they arise from common lymphoid progenitors (CLPs) and then progress sequentially through the early pro-B, late pro-B, large pre-B, small pre-B, and immature B cell developmental stages. This process occurs in response to both external signals from bone marrow stromal cells as well as cell-intrinsic signals. Secreted cytokines like Flt3-ligand, stem cell factor (SCF), and IL-7 stimulate the proliferation and survival of early progenitor stages, while the chemokine CXCL12 aids in the retention of these progenitor cells in bone marrow microenvironment via CXCR4 chemoattraction[1-4]. From the large pre-B stage onward, surface pre-B cell receptor (pre-BCR) and BCR signals predominantly drive differentiation.

A key step in B cell lymphopoiesis is the generation of a functional BCR that becomes expressed on the B cell surface following VDJ or VJ rearrangement of the immunoglobulin (Ig) heavy and light chain loci, respectively. Successful rearrangement of the BCR is crucial to a mature B cell's ability to recognize pathogens and perform its effector functions during an immune response. The random nature of Ig gene rearrangement is necessary to assemble a diverse set of B cell receptors (BCRs)[1] and tight regulation of this process is required to maintain genomic integrity of a cell. Accordingly, Ig rearrangement is necessarily separate from proliferation. Heavy chain DNA rearrangement begins in the early pro-B stage, with D-J joining. Pro-B cells become pre-B cells with surface expression of the pre-BCR, a heterodimer of the rearranged μ heavy chain and the surrogate light chains (vpreB1 and λ5). The pre-BCR is expressed in a complex with the signal transduction molecules Igα and Igβ, that become phosphorylated in response to pre-BCR crosslinking. If this phosphorylation occurs, an event indicating productive heavy chain

rearrangement, large pre-B cells are positively selected to pass the pre-BCR checkpoint and undergo a clonal expansion. Cells with non-productively rearranged heavy chains undergo apoptosis and do not survive. Subsequently, light chain rearrangement proceeds during the small pre-B cell stage, resulting in immature B cells that express a rearranged Ig heavy chain-light chain pair (IgM). Surface IgM on immature B cells is then tested for reactivity to self-antigens prior to egress from the bone marrow. These positive and negative selection events during BM development ensure the production of a functional, non-autoreactive B cell pool.

Dysregulation of BM B lymphopoiesis can lead to primary immunodeficiencies or autoimmunity due to the absence of functional mature B cells or persistence of autoreactive B cell clones, respectively. One of the best described immunodeficiencies is X-linked agammaglobulinemia (XLA), where patients cannot produce antibodies (immunoglobulins) and are susceptible to recurrent bacterial infections. XLA patients have mutations that impair the function of the tyrosine kinase BTK downstream of the pre-BCR[5]. BTK mutations lead to a block in B cell development at the late pro-B to large pre-B transition and dramatically reduced peripheral B cells[6]. In contrast, defects in apoptotic pathways can impair negative selection at the immature B cell checkpoint, leading to the inappropriate survival of autoreactive B cells. This is best exemplified by the Bcl-2-Ig transgenic mouse model, where B cells that overexpress the apoptosis inhibitor Bcl-2 produce anti-nuclear antibodies, causing glomerulonephritis[7].

Aberrations in B cell development can also lead to B cell precursor acute lymphoblastic leukemias (B-ALLs). Normal pro- and pre-B cells have malignant phenotypic counterparts (pro-B and pre-B ALLs) that may reflect the developmental stage at which oncogenic transformation occurred. Dysregulation or loss-of-function mutations in transcription factors important for B cell specification or commitment are present in many B-ALLs. PAX5 and EBF1 deletion mutations are found in 24-30% and 4-6% of pediatric B-ALL cases, respectively[8, 9], and *Ebf1*$^{+/-}$*Pax5*$^{+/-}$ mice develop pro-B ALL[10], suggesting a causative role in leukemogenesis. Blocks in differentiation at the pre-BCR checkpoint can also lead to B-ALL via mutations that promote pro-proliferative signaling and evasion of cell cycle arrest. Mice deficient for the B cell linker protein Blnk, a key component of the pre-BCR signaling pathway, develop B-ALLs with high pre-BCR

expression and genetic disruption of Arf-Mdm2-p53 tumor suppressor pathway[11]. Activating mutations in other effector molecules downstream of pre-BCR, like those in the RAS-ERK pathway, are also frequently observed[12-16]. Apart from pre-BCR signals, another key component regulating early B cell development and the pre-BCR checkpoint is the interleukin-7 receptor, though its potential role in leukemia initiation in less clear.

I.2 **IL-7R signaling in lymphocyte development and maintenance**

The interleukin-7 receptor (IL-7R) is a heterodimeric cytokine receptor that consists of IL-7Ra (CD127) and the common gamma chain (IL2RG). Signaling through the IL-7R is crucial for the development of all lymphoid lineage cells, including T cells, B cells, and innate lymphoid cells (reviewed in [17]). CLPs are defined in part by IL-7Ra expression[18], and IL-7 signals are thought to play a role in directing progenitors towards a B cell rather than T cell fate[19]. In the thymus, IL-7R signaling aids the differentiation and proliferation of $CD4^-$ $CD8^-$ double-negative (DN) pre-T cells by inhibiting expression of the transcriptional repressor Bcl-6 and regulating cell growth genes[20]. $CD4^+CD8^+$ double-positive cells, by contrast, inactivate IL-7R signals while undergoing positive selection and then subsequently re-express the receptor[21, 22]. Mature T cells also use IL-7R signals for their long-term maintenance via modulation of apoptotic pathways[23], as well as for the formation of memory T cells[24].

Unlike T cells, IL-7R signaling is only transiently important in B cell progenitors. Starting at the late pro-B stage, signaling via the IL-7R regulates early B cell development and expands pre-B cells through coordinated signaling with the pre-BCR. IL-7R signals via the JAK-STAT (Janus kinase-signal transducer and activator of transcription) and PI3-kinase (PI3-K) pathways to activate cell proliferation and survival genes[1, 17, 25]. IL-7R signals are also known to block RAG1/2 activity and subsequent Ig light chain rearrangement. Thus, a critical step in pre-B cell development is to downregulate the IL-7R to allow for successful light chain recombination. This downregulation is coordinated via signals mediated by the pre-BCR, which initially cooperates with the IL-7R at the large pre-B cell stage, but subsequently suppresses STAT5 activation and IL-7R-induced proliferation at the small pre-B cell stage[1, 25, 26]. While the

mechanisms orchestrating this process remain unclear, this molecular crosstalk represents a critical checkpoint in early B cell development. Lack of the pre-BCR, or downstream effectors like Btk or Blnk, results in checkpoint loss and either failure to produce mature B cells or an uncontrolled expansion of the precursor population[27-29]. Dysregulation of these pathways can lead to precursor B-cell acute lymphoblastic leukemia (B-ALL) [30, 31].

I.3 **Philadelphia chromosome-like acute lymphoblastic leukemia**

B-ALL is characterized clinically by a very broad array of molecular defects, including aneuploidy (21-32%), chromosomal rearrangements (31-51%), and/or sequence mutations (up to 25%) [8, 32, 33]. Genome-wide sequencing and array-competitive genomic hybridization have been utilized to identify all sequence and structural variants that may be contributing to disease. While these efforts to identify mutations are comprehensive, previously uncharacterized mutations will often require further study to have prognostic impact. Due to this complexity, recent studies have also employed gene expression signatures to better characterize specific leukemic populations and to help to predict treatment outcomes[34-37]. Gene expression profiling can identify novel B-ALL subtypes and determine whether different genetic lesions may phenocopy one another at the molecular level.

One of the best described B cell leukemia subtypes is the Philadelphia chromosome ALL (Ph+ ALL), where a translocation between chromosomes 9 and 22 results in a gene fusion of BCR and ABL1. This BCR-ABL1 fusion creates a constitutively active tyrosine kinase which mimics pre-BCR signals by activating BTK, allowing cells to avoid the pre-BCR checkpoint and survive without undergoing normal differentiation[38]. In contrast, Philadelphia chromosome-like acute lymphoblastic leukemia (Ph-like ALL) is a separate clinical category of ALL that comprises 15-30% of National Cancer Institute high-risk B-ALL occurring in children, adolescents, and adults[39]. The Ph-like ALL subtype represents B-ALLs that share a similar transcriptional profile to Ph+ ALL but lack the canonical BCR-ABL1 chromosomal translocation. Instead, Ph-like ALLs contain diverse mutations predicted to augment cytokine receptor signals, promote

kinase activation, and limit cell differentiation. The mutational landscape of Ph-like ALLs include genetic events that lead to: overexpression of the TSLP receptor, CRLF2; gain-of-function (GOF) mutations in IL-7Ra or JAK1/2; and/or loss-of-function (LOF) mutations in SH2B3, a negative regulator of cytokine signaling, or the lymphoid transcription factor IKAROS [13, 37, 40 33, 34]. Nearly all genetic studies of Ph-like ALL also find additional lesions that are common across many forms of cancer (e.g. mutations in *RAS* and *TP53*/*RB1* pathways, and CDKN2A/B)[13, 41, 42].

The observation that Ph+ and Ph-like ALL share a similar transcriptional signature is surprising, as the Ph+ signature presumably reflects the outcome of enhanced ABL1 tyrosine kinase activation, while Ph-like ALLs are predominantly JAK-STAT-driven. Ph-like ALLs are arrested between the pro- and pre-B cell stages of development, where cytokine-driven proliferation may facilitate the build-up of additional mutations that ultimately result in oncogenic transformation. This hypothesis has not been definitively tested, however.

I.4 **IL-7R gain-of-function mutations in ALL**

Activating insertion/deletion (indel) mutations in the *IL7R* gene have been identified in approximately 12% of Ph-like ALL cases, as well as in 9% of T-ALL[13, 43, 44]. There are four defined "classes" of heterozygous somatic *IL7R* mutations found in leukemias, affecting either exon 6 (classes 1-3) or less frequently, exon 5 (class 4). The exon 5 mutations are all S185C variants that confer cytokine independence and enhanced sensitivity to TSLP when co-expressed with CRLF2[44]. The exon 6 mutations are insertion mutations in the transmembrane domain that either contain a cysteine residue (class 1), positively-charged residues like arginine or histidine (class 2), or tryptophans or SxxG motifs (class 3)[43-45]. Of these, class 1 mutations are the most common, where the cysteine residue leads to disulfide bond-mediated receptor homodimerization and cytokine-independent activation[44]. Ba/F3 cells or hematopoietic progenitors overexpressing *IL7R* gene class 1 mutants can induce B-ALL when transplanted into mice, suggesting a potential role for these mutations in leukemogenesis[44, 46]. *IL7R* mutations are presumed to

increase STAT5 signaling, leading to dysregulation of B cell development through inhibition of the pre-BCR pathway and thereby potentially promoting leukemic transformation[1, 26, 43, 44, 47-49]. However, this concept has not been definitively tested in a physiologic setting.

IL7R activating mutations co-occur in Ph-like ALL with other purported activating mutations in related cytokine receptors including events leading to *CRLF2* overexpression or *FLT3* indel mutations[13]. They can also co-occur with loss-of-function mutations in the negative signaling regulator *SH2B3* (encoding LNK), or alterations in the transcription factor *IKZF1* (encoding IKAROS)[13]. SH2B3 is a member of the Src homology 2-B family of adaptor proteins that negatively regulates the activation of multiple tyrosine kinases and cytokine signaling pathways. *Sh2b3*$^{-/-}$ mice exhibit reduced negative regulation of signaling mediated by stem cell factor, IL-7, GM-CSF, thrombopoietin, and erythropoietin, and are characterized by overproduction of stem cells, B cells, dendritic cells, erythrocytes, and megakaryocytes[50-55]. Mechanistic studies have shown that SH2B3 can directly interact with phosphorylated JAKs and likely functions to attenuate downstream JAK-mediated signals, including IL-7-induced JAK/STAT5 activation[56, 57].

Analysis of newly diagnosed adult B-ALL samples identified a high-risk subset with higher *IL7R* expression and lower *SH2B3* expression than in normal BM progenitors[58], suggesting these proteins may coordinate to promote leukemia persistence. B-ALLs with high expression of *IL7R* and low expression of *SH2B3* are associated with the BCR-ABL1 fusion gene, as well as *IKZF1* deletion[58]. IKAROS (encoded by *IKZF1*) is a member of the Ikaros family of zinc-finger proteins along with HELIOS (*IKZF2*), AIOLOS (*IKZF3*), EOS (*IKZF4*), and PEGASUS (*IKZF5*). IKAROS is a lymphoid-lineage transcription factor that plays a key role in lymphocyte development. Indeed, several mouse models of *Ikzf1* deletion displayed severe defects in all lymphocyte lineages (T, B, and NK cells)[59-61]. Early stages of B cell development, specifically the pro-B-to-pre-B transition, require Ikaros activity in mice[61]. Ikaros likely mediates this transition via its involvement in regulatory networks affecting both the pre-BCR and the IL-7R[26, 62-64]. Downstream of IL-7R activation, STAT5A and IKAROS compete for binding sites, with opposing effects

on target gene expression[65]. Of note, amongst these target genes, IKAROS promotes *SH2B3* transcription, while inhibiting *IL7R* transcription[58]. Thus, loss of IKAROS may lead to a reduction in SH2B3 expression and an increase in IL-7R, while also limiting differentiation to the pre-B cell stage, thereby compounding the effects of constitutive IL-7R signaling. Together, these data suggest a potential synergistic role for SH2B3 and/or IKAROS loss with activated IL-7R signals, but no study to date has specifically tested this relationship.

I.5 **Signaling programs in Ph-like ALL**

Comprehensive genomic and proteomic profiling of cancers can lead to the development of better precision medicine therapies and improved outcomes for patients[41, 66]. For many years, Ph+ ALL was associated with a very poor prognosis, but patient outcomes have improved significantly with the advent of targeted kinase inhibitor (TKI) therapies. Targeting the BCR-ABL1 mutation with the addition of the ABL inhibitor imatinib or related TKIs to an intensive chemotherapy regimen has led to increased remission rates for Ph+ ALL. Tyrosine kinase activity is also a hallmark of Ph-like ALL, and the hope is that these patients would similarly benefit from TKIs targeting JAK, SRC, FLT3, or other kinase pathways. Indeed, a handful of clinical trials are currently underway to evaluate the efficacy of dasatanib (SRC inhibitor) and ruxolitinib (JAK1/2 inhibitor) on Ph-like ALLs with ABL1 fusion mutations or CRLF2/JAK pathway mutations, respectively (NCT01406756, NCT03117751, NCT02420717, and NCT02723994). Preclinical studies with Ph-like ALL patient-derived xenografts (PDXs) have demonstrated *in vivo* effectiveness of JAK inhibitors, providing rationale for this clinical approach[67, 68]. However, these studies showed variability in the activity of ruxolitinib treatment, depending on the underlying lesions, and it remains unclear how well this therapy may translate to patients with alternative genetic lesions contributing to Ph-like ALL. Thus, a more complete understanding of the signaling programs active within this mutationally diverse subtype of B-ALL is likely to further inform potential treatment strategies.

Recent studies have found that, despite being leukemic cells, the signaling mechanisms of B cell negative selection are intact in primary Ph+ ALL[69]. Increasing BCR signaling through pharmacologic hyperactivation of SYK tyrosine kinase targets Ph+ ALL for negative selection [69]. Based on these findings, the pre-BCR is now recognized as a potential therapeutic target for B-ALL [47, 69, 70]. Ph-like ALL remains difficult to treat, perhaps due in part to distinct survival signaling not appreciated in the transcriptional profiles. Although counterintuitive, Ph-like ALLs with constitutive IL-7R signaling have been classified as transcriptionally similar to Ph+ (ABL1-driven) leukemias[37, 41]. However, assuming the counter-regulatory IL-7R and pre-BCR pathways present in normal early B cell development are intact, these subtypes (activated IL-7R versus pre-BCR-mimicking constitutive ABL1) would be predicted to exhibit distinct signaling programs. Likewise, whether malignant Ph-like ALL cells mimic canonical B cell development signals or engage a unique oncogenic signaling program remains unknown.

I.6 **Questions to address**

Previous genomic studies of Ph-like ALL have identified a constellation of mutations that are presumed to enhance cytokine signaling and/or reduce activity of transcription factors that drive B cell differentiation. A better understanding of the molecular pathways that regulate these oncogenic events is likely essential for guiding the development of targeted therapies and precision medicine for this high-risk leukemia subtype. Studies to determine the roles that individual mutations play in leukemogenesis has thus far primarily been conducted in patient-derived samples and/or cell line models, which are complicated by issues of mutational burden and questionable physiologic relevance, respectively.

Is activated IL-7R sufficient to drive oncogenic transformation in primary murine B cell progenitors?

As the activated IL-7R mutation is predicted to occur in early B cell progenitors, BM B cell development analysis is likely to improve our understanding Ph-like ALL biology. To evaluate the impact

of activated IL-7R on B cell development and leukemogenesis, we generated an inducible transgenic mouse model where the murine *Il7r* coding sequence contains a class 1 (cysteine-containing) patient leukemia mutation: a 4 amino acid insertion PPCL in the analogous location of the transmembrane domain (*Il7r* p.P243insPPCL; referred to as 'aIL7R'). This construct was introduced in association with a downstream T2A-linked GFP marker into the endogenous *Rosa26* locus. Crossing these mice to the mb1-cre and CD19-cre strains, that mediate expression in early B cell progenitors, gives rise to GFP^+ cells that co-express aIL7R. Importantly, this model was designed to induce aIL7R expression at levels similar to those in B-ALL patients with heterozygous somatic mutations. We used this model, as well as two lineage-specific models of loss-of-function mutations in *Sh2b3* and *Ikzf1*, to study the effect of these mutation(s) on B cell development and leukemogenesis. Our novel findings clearly demonstrate that B-intrinsic expression of aIL7R is sufficient to initiate bona fide B-ALL in mice and that heterozygous loss of either Sh2b3 or Ikaros significantly increases disease penetrance.

What signaling programs are altered in Ph-like ALL?

Ph-like ALLs have been extensively characterized by their transcriptional profile, but comprehensive proteomic strategies to characterize their signaling programs have been lacking. Our study utilized a combination of phosphoflow, mass-spectrometry-based phosphoproteomics, and *in vitro* viability assays with specific kinase inhibitors to investigate the signaling pathways that are active and vital in both our novel murine leukemias and in genetically relevant, patient-derived, Ph-like ALL xenograft models. Our data reveal activation of Stat5 and mTORC1 targets, as well as a unique "BCR-like" signature, that is blunted by Syk inhibition.

Can we make a genetically-engineered mouse model of B-ALL for studying relevant drug combinations in vivo?

Preclinical testing of novel drugs for the treatment of B-ALL is critical step to make sure that the most promising drugs are prioritized to enter clinical trials. Yet, the rate of successful translation of novel

therapeutics to the clinic remains quite low. Currently, most preclinical models of Ph-like ALL assess responsiveness to therapy *in vivo* using patient- or cell line-derived xenografts implanted immunodeficient animals. The lack of an immune-competent tumor microenvironment likely complicates bench-to-bedside translation. In our study, we successfully transplanted primary aIL7R leukemias into immunocompetent WT mice and utilized this serial transplantation system to demonstrate the partial efficacy of rapamycin therapy *in vivo*.

Chapter II. **Role of an activating IL-7R mutation in B cell leukemogenesis**

II.1 **Introduction**

Philadelphia chromosome-like acute lymphoblastic leukemia (Ph-like ALL) comprises 15-30% of National Cancer Institute high-risk B-ALL occurring in children, adolescents, and adults[39]. Although Ph-like ALLs share a similar transcriptional profile to Philadelphia chromosome-positive ALL[37], these leukemias exhibit diverse mutations predicted to augment cytokine signaling, promote kinase activation, and limit cell differentiation[13, 33, 37, 39, 41]. Activating insertion/deletion (indel) mutations in the *IL7R* gene have been identified in approximately 12% of Ph-like ALL cases, as well as in 9% of T-ALL[13, 43, 44]. A common *IL7R* mutation introduces a cysteine residue in the transmembrane domain that promotes receptor homodimerization and cytokine-independent activation[44]. IL-7R plays a critical role in early B progenitor growth and differentiation, where it signals via the JAK-STAT and PI3-kinase (PI3K) pathways to promote cell proliferation and survival prior to BCR rearrangement[1, 17, 25]. *IL7R* mutations are presumed to increase STAT5 signaling, leading to dysregulation of B cell development through inhibition of the pre-BCR pathway and thereby potentially promoting leukemic transformation[1, 26, 43, 44, 47-49]. However, this concept has not been definitively tested, and whether malignant B-ALL cells mimic canonical B cell development signals or engage a unique oncogenic signaling program remains unknown.

IL7R activating mutations co-occur in B-ALL with loss-of-function mutations in the negative signaling regulator *SH2B3* (encoding LNK) or alterations in the transcription factor *IKZF1* (encoding IKAROS) at rates of ~55% or 32%, respectively[13]. B lymphopoiesis is altered in *Sh2b3*$^{-/-}$ mice, with pro-B cell overproduction due to enhanced sensitivity to IL-7, resulting in increased Stat5 activation[50, 56]. By contrast, IKAROS controls multiple stages of B lymphopoiesis. Introduction of germline homozygous null or DNA-binding domain *Ikzf1* mutations results in a complete block in B lineage development[59, 60, 71]. In contrast, introduction of these homozygous changes post B-lineage specification results in a block in the transition from the highly proliferative large pre-B cell stage to the quiescent small pre-B cell stage[61, 72]. Importantly, STAT5 antagonizes IKAROS activity in murine pre-B cells and primary B-ALLs by reciprocally regulating many of the same target genes, including *IL7R*[58, 65]. Collectively, these data suggest that mutations in *IL7R* may collaborate with those in *SH2B3* and *IKZF1* to alter B cell development in ways that drive leukemic transformation.

Here, we present a genetically engineered mouse model (GEMM) of B-ALL that is driven by B-cell intrinsic expression of an activating mutation in *Il7r.* This model reproduces many of the hallmarks of Ph-like B-ALL, including monoclonal growth, B-precursor immunophenotype, *de novo* co-mutation of common tumor suppressors and oncogenes, and activation of canonical cytokine and BCR-like signaling. We carefully characterized the biology, leukemic transition, and drug responses in this aIL7R GEMM and propose that it will be broadly useful in future studies to characterize factors regulating Ph-like ALL onset and potential treatments.

II.2 **Results**

II.2.1 B-intrinsic expression of an insertion mutation in Il7r drives B cell precursor ALL.

Common *IL7R* mutations in B-ALL include cysteine insertions within the transmembrane domain[44]. Expression of murine *Il7r* containing the B-ALL-associated activating L243insPPCL (*Il7r* p.P243insPPCL) mutation, hereafter referred to as activated "aIL7R", in Ba/F3 cells permitted IL-3-

independent growth and constitutive Stat5 phosphorylation (Figure **II.S1**). To generate knock-in mice, we introduced aIL7R with a cis-linked GFP reporter downstream of the murine *Rosa26* promoter and a floxed stop cassette (Figure **II.1a**). Rosa26-aIL7R$^{+/wt}$ mice were crossed to Mb1-cre or CD19-cre strains (referred to as "aIL7R-Mb1" or "aIL7R-CD19," respectively) to turn on one copy of the mutant allele at the bone marrow (BM) pro-B stage (B220^{+} surface (s)μHC^{-} IgD^{-} CD24^{hi} BP-1^{-}; Figure **II.S2a**). In aIL7R-Mb1 mice, pro-B and all subsequent developmental BM and splenic B cell populations expressed GFP. Mature B cells (B220^{+} sμHC^{+} IgD^{+}) maintained surface IL-7R expression and co-expressed GFP, whereas IL-7R expression was absent in mature B cells from controls, demonstrating aIL7R is expressed on the cell surface (Figure **II.1b-c**). Total surface IL-7R in aIL7R-mb1 late pro-B cells (B220^{+} sμHC^{-} IgD^{-} CD24^{hi} BP-1^{+}) was not significantly changed relative to controls, while median IL-7R fluorescence in aIL7R-Mb1 mature B cells was approximately one-fifth of that in Mb1-cre late pro-B cells, suggesting that surface aIL7R expression is roughly 20% of endogenous IL-7R (Figure **II.1b-c**).

Longitudinal cohorts revealed that aIL7R-Mb1 and aIL7R-CD19 mice developed spontaneous leukemic disease with low penetrance (~20%) with a median time to euthanasia criteria of 16 or 12 weeks, respectively (Figure **II.1d**). Leukemic animals displayed lymphadenopathy, splenomegaly, and high levels of neoplastic B cells in peripheral blood (Figure **II.1e-h**). Disease manifestations included hind limb paralysis with leukemic infiltration of vertebral bone marrow, bone degeneration, and local nerve impingement (Figure **II.1g**, Tables **II.1** and **II.2**). Leukemia infiltration into liver and central nervous system meninges were also observed (Figure **II.S2b** and Table **II.2**). Leukemia cells (leukemias referred to as "aIL7R alone") expressed markers consistent with late pro-/large pre-B cells (CD19^{+} sμHC^{-} IgD^{-} CD24^{hi} BP-1^{+}) (Figure **II.1h-j**, Figure **II.S2c**). Further characterization revealed surface pre-BCR (sμHC^{+} VpreB1^{+} or sμHC^{+}) expression in primary leukemia cells from 5 of 6 mice, consistent with a pre-B cell immunophenotype (Table **II.1**). Finally, Ig heavy chain sequencing showed clonal leukemia with expression of one or two predominant V_H segments per animal (Figure **II.S2d**, Table **II.1**). Together, these data demonstrate that aIL7R can promote *de novo* leukemic transformation.

II.2.2 Loss of Sh2b3 or Ikzf1 exacerbates and accelerates aIL7R-driven leukemia.

Loss-of-function mutations in *SH2B3* and *IKZF1* are also associated with Ph-like ALL, including those with *IL7R* mutations[13, 56, 58, 65]. To model the genetic interaction between *Sh2b3* and aIL7R, we introduced an inducible knock-out allele of *Sh2b3*[73] onto the aIL7R background. Alternative breeding strategies produced compound heterozygous animals with either global or B-lineage-restricted loss of Sh2b3 (strains referred to as aIL7R-Mb1 $Sh2b3^{+/-}$ or aIL7R $Sh2b3^{fl/+}$ Mb1, respectively). To model leukemia-associated *IKZF1* deletions, we crossed aIL7R mice to animals expressing an exon 5 floxed dominant negative isoform of Ikaros in B cells[72] similar to the Ik6 isoform in human B-ALL[74] (strain hereafter referred to as "aIL7R $Ikzf1^{fl/+}$ CD19").

As in aIL7R-Mb1/-CD19 mice, aIL7R-Mb1 $Sh2b3^{+/-}$, aIL7R $Sh2b3^{fl/+}$ Mb1, and aIL7R $Ikzf1^{fl/+}$ CD19 animals also developed spontaneous B-ALL with features that closely resembled aIL7R alone leukemias (referred to as "aIL7R/Sh2b3" and "aIL7R/Ikzf1" leukemias) (Figure **II.1d-j**, Tables **II.1** and **II.2**, Figure **II.S2a-b**). B-intrinsic *Sh2b3* deletion increased leukemia penetrance to ~40% of aIL7R $Sh2b3^{fl/+}$ Mb1 mice, while co-expression of mutant *Ikzf1* resulted in complete penetrance of aIL7R $Ikzf1^{fl/+}$ CD19 animals by week 15 (Figure **II.1d**). In the absence of aIL7R, heterozygous *Sh2b3* deletion or *Ikzf1* mutant expression did not lead to disease (Figure **II.1d**). Disease presentation, tissue pathology, $CD24^{hi}$ $BP\text{-}1^{+}$ precursor phenotype, and leukemia clonality mirrored the features of aIL7R alone leukemias (Figure **II.1e-j**, Tables **II.1** and **II.2**, Figure **II.S2a-b**). Interestingly, hepatic infiltration with leukemia was more pronounced in aIL7R/Ikzf1 leukemias, suggesting potential genotype differences in leukemia localization (Figure **II.S2b**, Table **II.2**). Unlike the aIL7R alone leukemias, surface pre-BCR expression was not detected in most compound heterozygous leukemias (aIL7R/Sh2b3: only 1 of 8; aIL7R/Ikzf1: 3 of 14) (Table **II.1**, Figure **II.S2e**). However, some leukemias expressed c-kit and/or surrogate light chain in the absence of surface heavy chain ($s\mu HC^{-}$ $VpreB1^{+}$), which was similar to previously described studies of mouse and human "pro-BCR^{+}" pro-B ALL (Figure **II.S2e**, Table **II.1**)[75-77].

Next, we assessed the capacity to generate secondary leukemias via serial transplantation. Splenocytes from 12 independent aIL7R alone, aIL7R/Sh2b3, and aIL7R/Ikzf1 primary leukemias were transplanted into unirradiated immunocompetent C57BL/6 (B6) recipient mice (Figure **II.2a**). Regardless of leukemia genotype, all recipient animals rapidly succumbed to disease, although across all starting genotypes the time to required euthanasia varied depending on the specific murine donor (~2-6 weeks; Figure **II.2b-d**). Transplanted (GFP^+) cells were present at high proportions in BM, spleen, and peripheral blood and maintained their $CD24^{hi}$ BP-1^+ phenotype (Figure **II.2e-h**). Collectively, these findings are consistent with reproducible malignant transformation in animals with B-cell intrinsic expression of aIL7R.

II.2.3 aIL7R leukemias harbor somatic mutations in Kras, Trp53, and Bcor.

To determine which secondary mutations were associated with aIL7R-driven leukemia in these models, we performed whole exome sequencing on eight primary leukemias (2 aIL7R alone, 3 aIL7R/Sh2b3, 3 aIL7R/Ikzf1) and four paired tail DNA samples as controls. We used two somatic variant callers, Pisces and Mutect2 (Figure **II.S3a**), to identify somatic nucleotide variants (SNVs) present in leukemia and not tail DNA. *Kras* variants were highly prevalent irrespective of starting genotype (6 of 8 leukemias) with most located at codons 12, 13, 61, and 146, previously identified "hotspots" mutated in many cancers[78] (Figure **II.2i**, Figure **II.S3b**, Table **II.3**). Additional variants included mutations in the tumor suppressor, *Trp53* (encoding Tp53), and in the Bcl6 interacting corepressor (*Bcor*) (Figure **II.2i**, Table **II.3**). *Bcor* mutations (stop-gain variant or a 1bp frameshift variant in exon 8) were similar to mutations described in pro-B ALLs from *NUP98-PHF23* transgenic mice, a model that mirrors features of *cytokine receptor-like factor 2* (*CRLF2*)-rearranged Ph-like ALL[79]. Mutations in the E3 ubiquitin ligase *Cbll1* and the NOTCH1 receptor *Notch1* were also present in aIL7R/Sh2b3 leukemias (2 of 3 and 1 of 3, respectively; Figure **II.2i**, Table **II.3**). By contrast, all aIL7R/Ikzf1 leukemias displayed an ostensible loss of the remaining wild-type *Ikzf1* allele, as evidenced by absence of exon 5 sequence coverage (Figure **II.2i**, Figure **II.S3c**, Table **II.3**). Loss-of-heterozygosity analysis between paired tail and leukemia DNA indicated one aIL7R/Ikzf1 leukemia (7K7) possessed a large deletion in chromosome 11 encompassing

both *Ikzf1* and *Trp53* (Figure **II.2i**). These data show that aIL7R-driven leukemias acquire somatic mutations in multiple genes previously associated with B-ALL, events that may contribute directly to leukemogenesis.

II.2.4 aIL7R expression preferentially drives expansion of BM late pro-B cells.

To ascertain the effect of aIL7R on B cell development, we performed detailed immunophenotyping of bone marrow and splenic B cells prior to leukemogenesis. aIL7R-Mb1 mice displayed increased marrow cellularity with expansion of B220+ B cells (Figure **II.3a-c**). The percentage and absolute number of late pro B cells ($B220^{+}$ $s\mu HC^{-}$ IgD^{-} $CD24^{hi}$ $BP\text{-}1^{+}$; Figure **II.3d**) was specifically increased. However, mature B cells ($B220^{+}$ $s\mu HC^{+}$ IgD^{+}) were present in numbers equivalent to control mice, consistent with no significant impairment in overall B cell development (Figure **II.3d**). In the context of aIL7R, global loss of one *Sh2b3* allele led to an increase in early pro B and late pro B cells (Figure **II.3b**, **d**). Additionally, aIL7R-Mb1 and aIL7R-Mb1 $Sh2b3^{+/-}$ mice displayed a skewing towards increased splenic transitional B cells and reduced marginal zone B cells (Figure **II.S4a-d**). While aIL7R-CD19 and aIL7R $Ikzf1^{fl/+}$ CD19 animals did not exhibit an increase in total B cell numbers (Figure **II.3e**, Figure **II.S4e-g**), aIL7R $Ikzf1^{fl/+}$ CD19 mice displayed an increased proportion and absolute number of late pro-B cell progenitor cells (Figure **II.3f**). These studies show that B-intrinsic aIL7R expression specifically promotes a modest increase in the late pro-B cell compartment and that this phenotype is enhanced by either *Sh2b3* loss or expression of mutant *Ikzf1*.

II.2.5 aIL7R and loss of Sh2b3 promotes enhanced survival in normal and leukemic B cell progenitors.

IL-7R signaling promotes survival of normal B cell progenitors by upregulating anti-apoptotic BCL-2-like family members[80, 81]. As *Bcl2l1* (encoding the Bcl-xl protein) transgenic animals similarly develop a large expansion of pro-B cells and Bcl-xl is most highly expressed in pro-B and pre-B cells[82], we assessed intranuclear Bcl-xl protein expression by flow cytometry in non-leukemic (i.e. lacking in disease symptoms as defined by our IACUC protocol) mice. aIL7R-Mb1 $Sh2b3^{+/-}$ mice displayed elevated Bcl-xl

levels in bone marrow B cells ($B220^+$) and pro/pre-B cells ($B220^+$ $s\mu HC^-$ IgD^-) (Figure **II.4a-b**). Similarly, leukemic aIL7R/Sh2b3 B cells exhibited increased Bcl-xl protein expression relative to control pro/pre-B cells (Figure **II.4c-d**).

To assess the role of aIL7R-driven cell proliferation, we performed *in vivo* EdU labeling studies. While aIL7R-Mb1 and aIL7R-Mb1 $Sh2b3^{+/-}$ mice had a greater frequency of EdU^+ BM B cells, the rate of incorporation within the late pro-B cell compartment was not different from that of control mice (Figure **II.4e-f**). In contrast, *ex vivo* staining of B cells from leukemic aIL7R mice demonstrated increased Ki-67^+ cells in both bone marrow and spleen (Figure **II.4g-h**). Taken together, these experiments suggested that aIL7R with loss of Sh2b3 may promote enhanced survival of normally proliferating marrow progenitors in non-leukemic animals via upregulation of Bcl-xl. Further, aIL7R/Sh2b3 leukemic cells exhibit both upregulation in Bcl-xl, possibly due to conserved signaling events, and increased cell proliferation mediated via acquired leukemia-enhancing genetic lesions. However, as changes in Bcl-xl expression were not evident in non-leukemic or leukemic aIL7R $Ikzf1^{fl/+}$ CD19 mice, this pathway is not uniformly active across aIL7R-associated leukemias.

II.2.6 *aIL7R pro-B cells lack constitutive Stat5 activation yet are less sensitive to IL-7 depletion in vivo.*

We next assessed whether phosphorylated (p)-Stat5 was increased in flow cytometry-sorted late pro-B cells from littermate control, aIL7R-Mb1, and aIL7R $Sh2b3^{fl/+}$ Mb1 mice. Surprisingly, we observed no genotype-specific differences in basal or IL-7-induced pStat5 levels via intracellular phosphoflow cytometry (Figure **II.5a-b**). Alternatively, when analyzing splenic B cells, we found that IL-7 induced higher levels of pStat5 in aIL7R-expressing mature B cells relative to controls, although basal levels remained similar across genotypes (Figure **II.5c-d**). Overall, these data suggest that aIL7R is capable of transducing pStat5 signals in primary B cells in the presence of ligand but lacks evidence for constitutive Stat5 signaling as assessed by flow cytometry. The lack of measurable constitutive Stat5 signaling likely reflects the relatively low level of aIL7R expression in our Rosa-promoter based model.

We next tested whether the expansion of the pro-B cell compartment in aIL7R animals requires endogenous IL-7. In these experiments, we treated aIL7R Sh2b3$^{fl/+}$ Mb1 and control animals *in vivo* with IL-7 blocking or isotype negative control antibodies (Figure **II.5e**). Strikingly, treatment with the blocking antibody depleted both total BM B (B220+) and late pro-B cells in control animals, but had no effect upon aIL7R progenitors (Figure **II.5f-h**). These data imply that aIL7R provides an IL-7-independent signal that promotes pro-B cell growth in a non-leukemic setting.

To test whether aIL7R-driven leukemias require IL-7 for survival/maintenance, two aIL7R/Sh2b3 primary leukemias (7S4 and 7S5) were transplanted into B6 recipient animals that were subsequently treated with anti-IL-7 or isotype control antibodies and monitored for signs of disease (Figure **II.S5d**). Anti-IL-7- and isotype-treated animals developed disease with similar kinetics, and IL-7 blockade had no impact on survival (Figure **II.S5e**), indicating that IL-7 is not required for growth of aIL7R-derived leukemias *in vivo*. We performed parallel studies in human Ph-like ALL PDX models, including one with *IL7R* mutation and *SH2B3* deletion (PALJDL)[68], and assessed *in vitro* and *in vivo* dependencies upon IL-7 (n=11 PDX models; Table **II.4**). While cells from all PDX models showed increased pSTAT5 levels following *in vitro* stimulation with IL-7, *in vivo* treatment of the PALJDL PDX model with the IL-7 blocking antibody had no effect upon leukemia proliferation, as measured by longitudinal bioluminescent imaging (Figure **II.S5f-i**). In contrast, *in vivo* IL-7 blockade treatment of an aggressive PDX model that overexpresses TSLPR in association with an activating JAK2 mutation (*IGH-CRLF2 JAK2*^{R683G}; ALL121) resulted in decreased leukemia burden at sacrifice and the recovered leukemia cells exhibited reduced viability (Figure **II.S6**). Taken together, these data suggest that aIL7R promotes IL-7-independent growth of B cell progenitors and that IL-7 blockade is unlikely to control leukemic burden in B-ALL expressing aIL7R but may prove more effective with other Ph-like subtypes.

II.2.7 aIL7R murine leukemias are sensitive in vitro and in vivo to rapamycin.

Ph-like ALL cells have previously been shown to be sensitive to *in vitro* and *in vivo* treatment with JAK and/or mTOR pathway inhibitors, implying that survival may be, in part, dependent upon both signaling pathways[68, 83, 84]. To assess Jak/Stat and mTOR signaling activation in our aIL7R-driven mouse leukemias, we measured *ex vivo* phosphorylation of Stat5, as well as the PI3-K/Akt/mTORC1 targets ribosomal protein S6 and the translational repressor 4E-BP1. aIL7R alone and aIL7R/Ikzf1 leukemias showed a 1.5-fold increase in pStat5 levels in BM B (CD19+) cells and no significant differences in basal pS6 relative to control B cells from the BM and/or spleen (Figure **II.S5a-b**). Similar to our pStat5 findings, aIL7R/Ikzf1 bone marrow leukemia cells exhibited a ~2-fold increase in p4E-BP1 levels relative to control BM B cells and splenic cells from all types of aIL7R leukemias increased p4E-BP1 compared to control cells (~2-6-fold; Figure **II.6a**). Taken together, these data suggest that mTOR and likely also Stat5 signaling are activated in aIL7R leukemias and that our GEMMs recapitulate human Ph-like ALL biology.

Consistent with prior reports[68], we confirmed that rapamycin treatment of PALJDL PDX mice effectively inhibited *in vivo* leukemia proliferation (Figure **II.S5i**). To assess whether murine aIL7R leukemias were responsive to mTOR inhibition, we cultured leukemia cells with the mTOR inhibitor rapamycin and found it significantly reduced viability of aIL7R/Sh2b3 and aIL7R/Ikzf1 leukemias (Figure **II.6b**). To test the effect of mTOR inhibition *in vivo*, we transplanted an aIL7R alone leukemia (7R4) or aIL7R/Sh2b3 leukemias (7S5 and 7S6) into B6 mice and treated animals with rapamycin or vehicle for 4 weeks (Figure **II.6c**). Rapamycin treatment extended recipient survival for leukemias 7R4 and 7S6, but exerted minimal impact on 7S5 recipients (Figure **II.6d-i**). Five of 8 (62.5%) 7S6 leukemia recipients treated with vehicle succumbed to disease (median survival of 23 days), while all rapamycin-treated mice survived and showed no signs of leukemia at sacrifice (Figure **II.6e, h**). Similarly, 6 of 7 (85.7%) vehicle-treated 7R4 leukemia recipients met euthanasia criteria (median survival = 19 days), compared to only 2 of 7 (28.6%) receiving rapamycin (Figure **II.6f, i**). Together, these data demonstrate that the mTOR pathway is active in aIL7R leukemias and that rapamycin is partially effective at controlling leukemia burden *in*

vivo. The sensitivity of aIL7R leukemias to rapamycin further validates the response previously observed in our human Ph-like ALL PDX model (Figure **II.S5i**).

II.2.8 IL7R-mutant leukemias display activation of "BCR-like" effector molecules.

To identify signaling programs that might mediate IL-7 independence in aIL7R leukemia cells, we performed phospho-tyrosine immunoprecipitation coupled with mass spectrometry from cell lysates derived from surface pre-BCR$^-$ secondary murine leukemias (1 aIL7R alone - 7R4, 2 aIL7R/Sh2b3 - 7S5 and 7S6, and 2 aIL7R/Ikzf1 – 7K7 and 7K10). We identified 122 unique phospho-sites from 109 proteins (Table **II.5**). As anticipated, tyrosine phosphorylation of Stat5a/b and Stat3 were increased in leukemia cells isolated from secondary hosts (Figure **II.7a**, Tables **II.5** and **II.6**, Figure **II.S7**). Despite the absence of surface pre-BCR expression, we surprisingly observed phosphorylation of multiple canonical "BCR-like" effectors, including Syk, Cbl, Btk and others (Figure **II.7a**, Tables **II.5** and **II.6**, Figure **II.S7**). We next assessed whether this tyrosine phosphorylation signature was conserved in human Ph-like ALL PDX models. We performed phospho-tyrosine immunoprecipitation of cells harvested from 6 discrete Ph-like ALL PDX models (Table **II.4**) and quantified tyrosine phosphorylation by mass spectrometry (Table **II.7**). Similar to the aIL7R murine leukemias, we identified enrichment of pBTK and pSYK residues, as well as pSTAT5A and pJAK3, in the PALJDL model (Figure **II.7b**). Notably, a similar BCR-like signaling signature was detected in additional Ph-like ALL PDX models with other JAK pathway genetic alterations. These findings suggest that a common adaptation in *IL7R*-driven leukemia is activation of BCR-like signaling independent of surface pre-BCR expression that was recently reported in other Ph-like ALL cases[85].

II.2.9 aIL7R leukemias are sensitive to Syk inhibition in vitro.

To determine whether the BCR-like signaling program present in aIL7R murine leukemias and Ph-like ALL PDX models was directly associated with IL-7R activation, we used a targeted proteomic approach to monitor tyrosine phosphorylation of these substrates in the presence of acute stimulation with

IL-7. We also used entospletinib and ruxolitinib to assess whether phosphorylation of these peptides was associated with SYK- or JAK-dependent signaling, respectively. As expected, Stat5 phosphorylation was enhanced by IL-7 and diminished with exposure to the Jak1/2 inhibitor, ruxolitinib, but was minimally affected by treatment with the Syk inhibitor, entospletinib (Figure **II.7c-d**). Additionally, we found IL-7-independent phosphorylation of Syk that was abrogated by entospletinib, but minimally affected by ruxolitinib (Figure **II.7c, e**). Finally, Cbl and Pik3ap1 (BCAP) peptides were also inhibited by entospletinib, suggesting that these proteins are downstream of Syk in this BCR-like pathway (Figure **II.7b, f-g**). These results suggest that aIL7R leukemias manifest a unique IL-7-independent BCR-like program in addition to an IL-7-inducible Jak/Stat program.

We subsequently tested whether this BCR-like signaling program is essential for survival of aIL7R leukemias *in vitro*. We cultured aIL7R leukemia cells with ruxolitinib, entospletinib, the proteasome inhibitor bortezomib as a positive control, and compounds that target proteins downstream of Syk, including the PI3Kδ inhibitor idelalisib, the Btk inhibitor ibrutinib, or the MEK inhibitor trametinib. As predicted in prior reports[28], viability of aIL7R leukemic cells was sensitive to ruxolitinib (Figure **II.7h-i**), idelalisib (Figure **II.S8a-b**), and bortezomib (Figure **II.7j-k**). While individual leukemias showed varying degrees of sensitivity to these inhibitors, aIL7R leukemias were also sensitive to entospletinib *in vitro* (Figure **II.7l-m**). Finally, aIL7R/Ikzf1 leukemias displayed specific sensitivity to ibrutinib (Figure **II.S8c-d**) and trametinib (Figure **II.S8e-f**), which suggest that this genotype may rely on different essential pathways compared with aIL7R alone or aIL7R/Sh2b3. These data further validate that aIL7R leukemias exhibit active BCR-like signaling, especially via the Syk and PI3K pathways, and suggest that these compounds could be effective as part of combinations with Jak and/or mTOR inhibitors to target aIL7R-driven leukemias.

II.2.10 IL-7R-mutant patient-derived xenograft is not controlled by Syk inhibition in vivo.

Given the *in vitro* data demonstrating a sensitivity of aIL7R murine leukemias to Syk inhibition, we next tested whether entospletinib treatment would control IL-7R-mutant leukemia burden *in vivo*. We

utilized the PALJDL PDX model and treated recipient mice with vehicle, the Src kinase inhibitor dasatanib, or entospletinib-formulated rodent chow. We found that neither treatment had an inhibitory effect on leukemia engraftment kinetics nor final leukemia burden, indicating that entospletinib treatment as a monotherapy is insufficient to inhibit IL-7R-mutant Ph-like ALL *in vivo* (Figure **II.S9**).

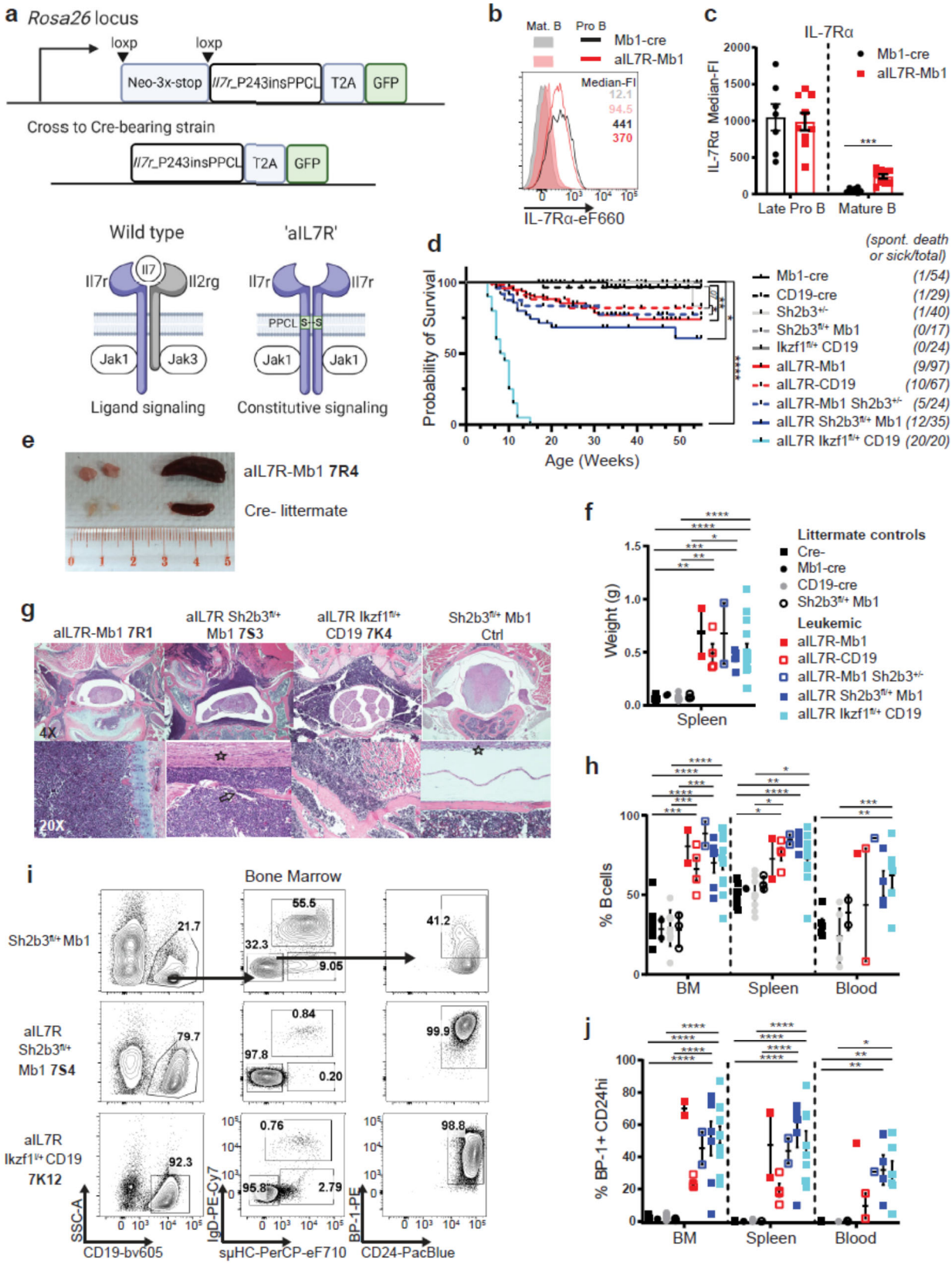
a Rosa26 locus
loxp
loxp
Neo-3x-stop
Il7r_P243insPPCL
T2A
GFP
Cross to Cre-bearing strain
Il7r_P243insPPCL
T2A
GFP
Wild type
'aIL7R'
Il7
Il7r
Il2rg
Il7r
Il7r
PPCL
S-S
Jak1
Jak3
Jak1
Jak1
Ligand signaling
Constitutive signaling
b
Mat. B
Pro B
Mb1-cre
aIL7R-Mb1
Median-FI
12.1
94.5
441
370
IL-7Rα-eF660
c
IL-7Rα
Mb1-cre
aIL7R-Mb1
IL-7Rα Median-FI
2000
1500
1000
500
0
***
Late Pro B
Mature B
d
(spont. death or sick/total)
Probability of Survival
100
50
0
0
10
20
30
40
50
Age (Weeks)
Mb1-cre (1/54)
CD19-cre (1/29)
Sh2b3+/- (1/40)
Sh2b3fl/+ Mb1 (0/17)
Ikzf1fl/+ CD19 (0/24)
aIL7R-Mb1 (9/97)
aIL7R-CD19 (10/67)
aIL7R-Mb1 Sh2b3+/- (5/24)
aIL7R Sh2b3fl/+ Mb1 (12/35)
aIL7R Ikzf1fl/+ CD19 (20/20)
e
aIL7R-Mb1 7R4
Cre- littermate
f
Weight (g)
1.5
1.0
0.5
0.0
Spleen
Littermate controls
Cre-
Mb1-cre
CD19-cre
Sh2b3fl/+ Mb1
Leukemic
aIL7R-Mb1
aIL7R-CD19
aIL7R-Mb1 Sh2b3+/-
aIL7R Sh2b3fl/+ Mb1
aIL7R Ikzf1fl/+ CD19
g
aIL7R-Mb1 7R1
aIL7R Sh2b3fl/+ Mb1 7S3
aIL7R Ikzf1fl/+ CD19 7K4
Sh2b3fl/+ Mb1 Ctrl
4X
20X
h
% B cells
100
50
0
BM
Spleen
Blood
i
Bone Marrow
Sh2b3fl/+ Mb1
21.7
55.5
32.3
9.05
41.2
aIL7R Sh2b3fl/+ Mb1 7S4
79.7
0.84
97.8
0.20
99.9
aIL7R Ikzf1l/+ CD19 7K12
92.3
0.76
95.8
2.79
98.8
SSC-A
CD19-bv605
IgD-PE-Cy7
sμHC-PerCP-eF710
BP-1-PE
CD24-PacBlue
j
% BP-1+ CD24hi
100
80
60
40
20
0
BM
Spleen
Blood

Figure II.1.

Figure II.1. B-intrinsic aIL7R and heterozygous loss of Sh2b3 or Ikaros rapidly promote B cell precursor leukemias. (**a**) (*Top*) Schematic of strategy for generation of knock-in mice expressing B-intrinsic activated mouse aIL7R (Il7r_P243insPPCL). (*Bottom*) Schematic of protein dimers illustrating ligand-induced wildtype IL-7R (Il7ra-Il2rg) versus constitutive aIL7R homodimer. Other ligand-induced protein dimers could include Il7ra-aIL7R and Il2rg-aIL7R (not pictured). Images created with BioRender.com. (**b**) Surface IL-7Rα expression in late pro-B ($B220^+$ IgD^- $s\mu HC^-$ $CD24^{hi}$ $BP\text{-}1^+$; open histograms) and mature B ($B220^+$ $s\mu HC^+$ IgD^+; filled histograms) cells from Mb1-cre (black) and $aIL7R^{+/-}$ $Mb1\text{-}cre^{+/-}$ (aIL7R-Mb1; red) mice. (**c**) Quantification of IL-7Rα surface expression in late pro-B and mature B cells. Bar graphs depict mean ± SEM of data from 4 independent experiments. N = 7 Mb1-cre and 9 aIL7R-Mb1. Significance defined as *** = $P \leq 0.001$ by two-tailed Student's T test. (**d**) Survival curves for aIL7R-expressing mice relative to controls (Mb1-cre, CD19-cre, $Sh2b3^{+/-}$, $Sh2b3^{fl/+}$ Mb1 or $Ikzf1^{fl/+}$ CD19). Animals used experimentally prior to 15 weeks of age were excluded. Numbers on left side indicate the number of spontaneous death or disease events per total animals. Total N = 54 Mb1-Cre controls, 29 CD19-cre controls, 40 $Sh2b3^{+/-}$ (global), 17 $Sh2b3^{fl/+}$ Mb1 (B-intrinsic), 24 $Ikzf1^{fl/+}$ CD19, 97 aIL7R-Mb1, 67 aIL7R-CD19, 24 aIL7R-Mb1 $Sh2b3^{+/-}$, 35 aIL7R $Sh2b3^{fl/+}$ Mb1, and 20 aIL7R $Ikzf1^{fl/+}$ CD19 mice. Significance defined by Mantel-Cox test. ** = $P \leq 0.005$ and **** = $P \leq 0.0001$. (**e**) Representative spleen and inguinal lymph nodes from a leukemic aIL7R-Mb1 animal and a Cre^- littermate control. **7R4** (and similar nomenclature in subsequent panels) represents identifier for specific leukemic animal as detailed in Supplementary Table 1. (**f**) Quantification of spleen weights for leukemic animals and littermate controls. Significance defined as **** = $P \leq 0.0001$ by one-way ANOVA. (**g**) Representative H&E staining of vertebral bone sections from leukemic mice with indicated genotype and an $Sh2b3^{fl/+}$ Mb1 littermate control. N = 1 $Sh2b3^{fl/+}$ Mb1 littermate control, 1 $Ikzf1^{fl/+}$ CD19 littermate control, 1 aIL7R-Mb1, 1 aIL7R-CD19, 3 aIL7R $Sh2b3^{fl/+}$ Mb1, and 3 aIL7R $Ikzf1^{fl/+}$ CD19 mice analyzed. (**h**) Frequency of B cells in the bone marrow (BM), spleen, and peripheral blood from littermate control and leukemic mice with indicated genotypes. (**i**) Representative flow plots of B cell developmental subsets in the BM. (**j**) Frequency of $BP\text{-}1^+CD24^{hi}$ progenitor B cells in the BM, SPL, and peripheral blood. (**f, h, j**) Data points represent individual mice and bars represent mean ± SEM. N= 12 Cre^- controls (black squares), 2 Mb1-cre controls (black circles), 10 CD19-cre controls (grey circles), 3 $Sh2b3^{fl/+}$ Mb1 (open black circles), 2 aIL7R-Mb1 (red squares) 4 aIL7R-CD19 (open red squares), 2 aIL7R-Mb1 $Sh2b3^{+/-}$ (open blue squares), 6 aIL7R $Sh2b3^{fl/+}$ Mb1 (blue squares) and 13 aIL7R $Ikzf1^{fl/+}$ CD19 (teal squares). (**h, j**) Significance defined as ** = $P \leq 0.005$, *** = $P \leq 0.001$ and **** = $P \leq 0.0001$ by two-way ANOVA. *aIL7R-Mb1 $Sh2b3^{+/-}$* = B-intrinsic aIL7R & global Sh2b3 het; *aIL7R $Sh2b3^{fl/+}$ Mb1* = B-intrinsic aIL7R & Sh2b3 het; *$Ikzf1^{fl/+}$ CD19* = B-intrinsic mutant Ikzf1 het; *aIL7R $Ikzf1^{fl/+}$ CD19* = B-intrinsic aIL7R & mutant Ikzf1 het.

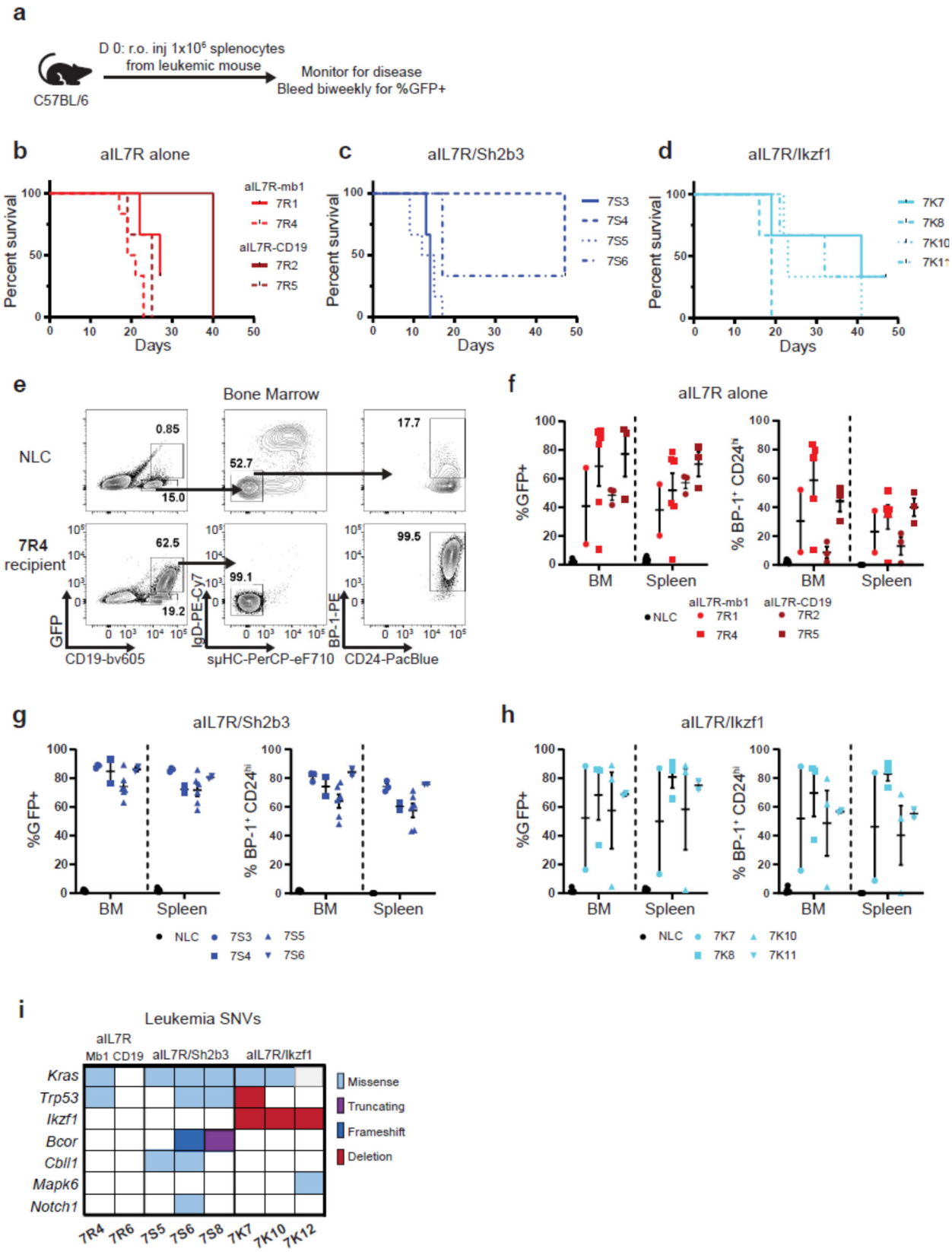
a
D 0: r.o. inj 1x10⁶ splenocytes
from leukemic mouse
Monitor for disease
Bleed biweekly for %GFP+
C57BL/6
b
aIL7R alone
Percent survival
Days
aIL7R-mb1
7R1
7R4
aIL7R-CD19
7R2
7R5
c
aIL7R/Sh2b3
7S3
7S4
7S5
7S6
d
aIL7R/Ikzf1
7K7
7K8
7K10
7K11
e
Bone Marrow
NLC
7R4
recipient
0.85
15.0
52.7
17.7
62.5
19.2
99.1
99.5
GFP
CD19-bv605
IgD-PE-Cy7
sμHC-PerCP-eF710
BP-1-PE
CD24-PacBlue
f
aIL7R alone
%GFP+
% BP-1⁺ CD24ʰⁱ
BM
Spleen
NLC
aIL7R-mb1
7R1
7R4
aIL7R-CD19
7R2
7R5
g
aIL7R/Sh2b3
NLC
7S3
7S4
7S5
7S6
h
aIL7R/Ikzf1
NLC
7K7
7K8
7K10
7K11
i
Leukemia SNVs
aIL7R
Mb1 CD19
aIL7R/Sh2b3
aIL7R/Ikzf1
Kras
Trp53
Ikzf1
Bcor
Cbll1
Mapk6
Notch1
7R4
7R6
7S5
7S6
7S8
7K7
7K10
7K12
Missense
Truncating
Frameshift
Deletion

Figure II.2.

Figure II.2. aIL7R leukemias are transplantable into immunocompetent hosts and acquire mutations in clinically relevant genes. (**a** - **h**) 1e06 primary leukemia cells were transferred retro-orbitally (r.o.) into wildtype C57BL/6 recipient mice. (**a**) Schematic of leukemia serial transfer experiments. (**b** - **d**) Survival curves for aIL7R alone (**b**), aIL7R/Sh2b3 (**c**), and aIL7R/Ikzf1 (**d**) leukemia recipient animals. (**e**) Representative flow plots of B cell subsets in the BM of an aIL7R-Mb1 leukemia (7R4) recipient and a no leukemia control (NLC) that did not undergo adoptive transfer. (**f** - **h**) Frequency of GFP+ (*left*) and BP-1^{+}CD24^{hi} (*right*) leukemia cells in the BM and spleen of aIL7R alone (**f**), aIL7R/Sh2b3 (**g**), and aIL7R/Ikzf1 (**h**) leukemia recipients. (**b** - **h**) Data points represent individual recipient mice and bars represent mean + SEM. N = 3 recipients for 7R1, 7R2, 7R5, 7S3, 7S4, 7S6, 7K7, 7K8, 7K10, and 7K11, 6 recipients for 7R4 and 7S5 (2 independent experiments), and 18 no leukemia controls (6 per graph). (**i**) Summary of somatic nucleotide variants (SNVs) identified by whole-exome sequencing and validated in IGV in a panel of 8 aIL7R leukemias.

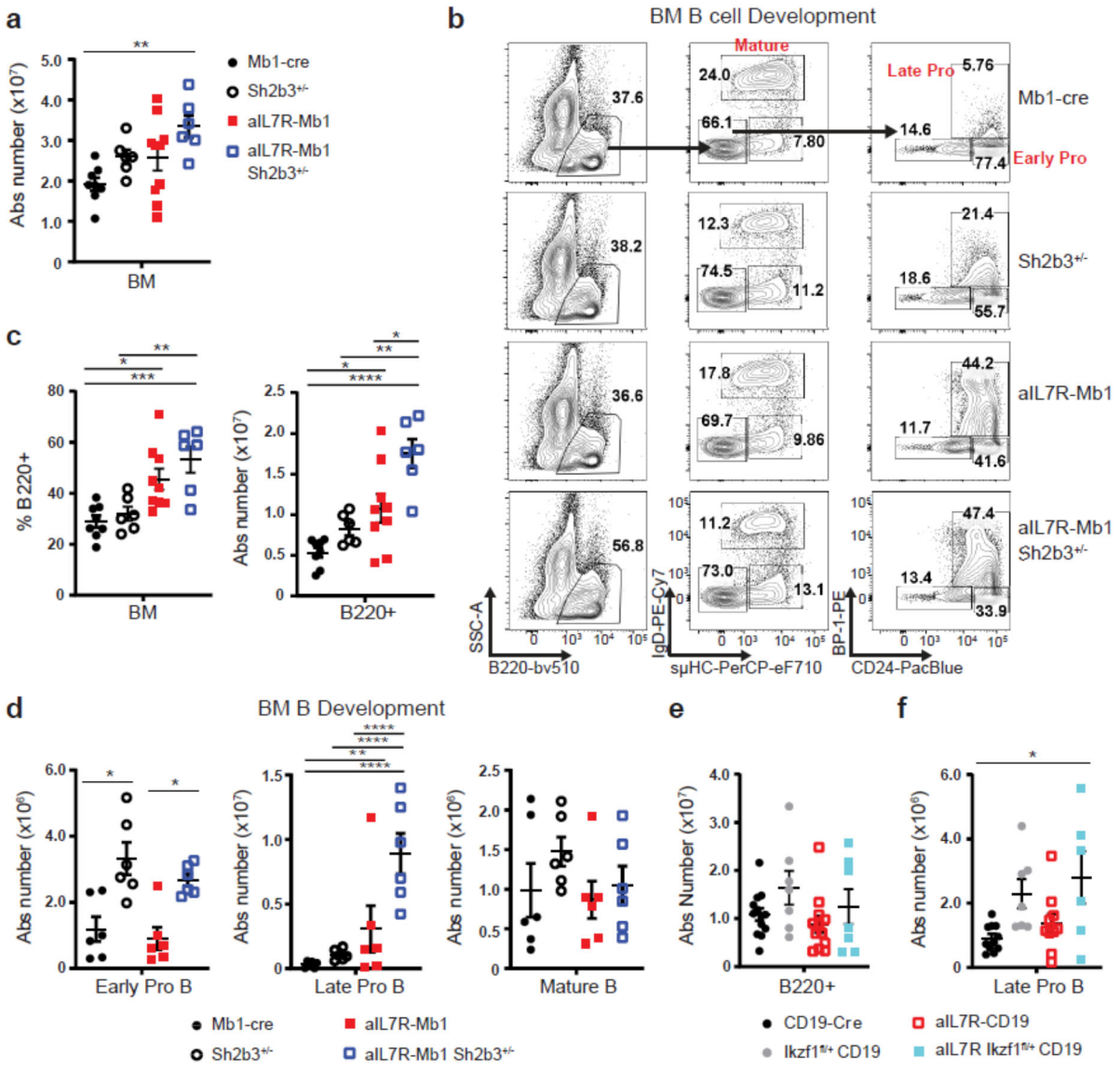

Figure II.3. B-lineage aIL7R cooperates with heterozygous loss of *Sh2b3* or *Ikzf1* to drive a specific expansion of late pro B cells. (**a**) Absolute number of total BM cells recovered from 1 tibia + femur for animals with indicated genotypes. (**b**) Representative flow plots of BM B cell developmental subsets: early pro-B ($B220^+$ $s\mu HC^-IgD^-CD24^{hi}BP\text{-}1^-$), late pro-B ($B220^+$ $s\mu HC^-IgD^-CD24^{hi}BP\text{-}1^+$), and mature B ($B220^+$ $s\mu HC^+IgD^+$) highlighted. (**c**) Frequency (*left*) and absolute number (*right*) of $B220^+$ B cells in the BM. (**a, c**) Data from 4 independent experiments. N = 8 Mb1-cre (black circles), 6 $Sh2b3^{+/-}$ (black open circles), 9 aIL7R-Mb1 (red squares) and 6 aIL7R-Mb1 $Sh2b3^{+/-}$ (open blue squares) mice. (**d**) Absolute number of early pro-B (*left*), late pro-B (*center*), and mature B (*right*) cells in the BM. N = 6 replicate mice per genotype. (**e**) Absolute number of $B220^+$ B cells in the BM in aIL7R animals with or without B-intrinsic heterozygous mutant Ikzf1 expression (aIL7R $Ikzf1^{fl/+}$ CD19). (**f**) Absolute number of late pro-B cells in the BM. (**e, f**) Data from 4 independent experiments. N = 13 CD19-cre (black circles), 7 $Ikzf1^{fl/+}$ CD19 (gray circles), 12 aIL7R-CD19 (open red squares), and 6 aIL7R $Ikzf1^{fl/+}$ CD19 (teal squares) mice. (**a, c-f**) Data points represent individual mice and bars represent mean ± SEM. Significance defined as * = $P \leq 0.05$, ** = $P \leq 0.005$, *** = $P \leq 0.001$, **** = $P \leq 0.0001$ by one-way ANOVA.

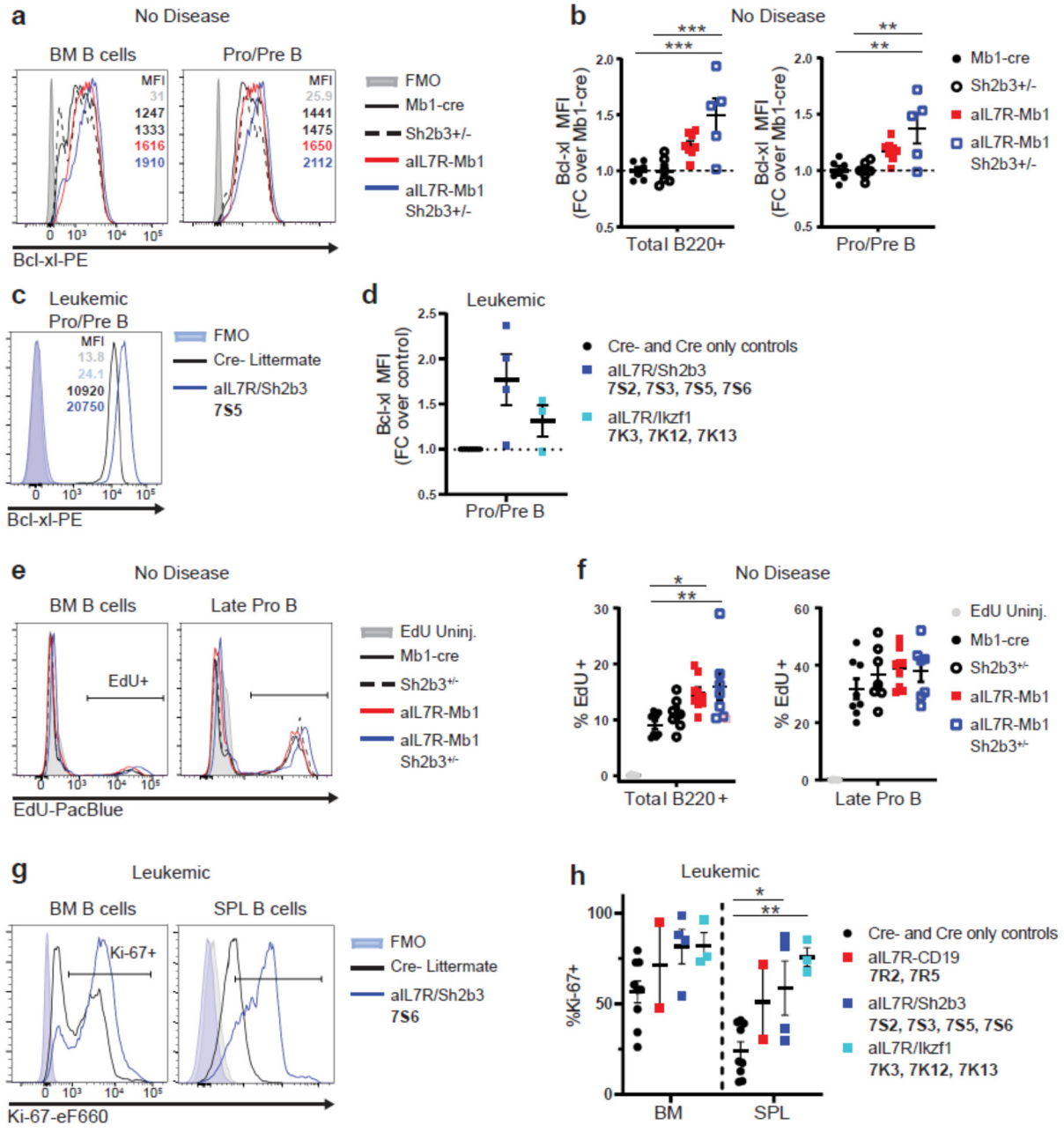

Figure II.4. aIL7R and loss of Sh2b3 promotes enhanced survival in normal and leukemic B cell progenitors. (**a**) Representative histograms of Bcl-xl expression in total B220$^+$ (*left*) and pro/pre-B cells (B220$^+$ sμHC$^-$IgD$^-$; *right*) in the BM of non-leukemic animals with the indicated genotypes. (**b**) Bcl-xl MFI normalized to the average fluorescence in Mb1-cre animals for total B220$^+$ (*left*) and pro/pre-B cells (*right*). Data from 3 independent experiments. N = 6 Mb1-cre, 6 Sh2b3$^{+/-}$, 8 aIL7R-Mb1, and 5 aIL7R-Mb1 Sh2b3$^{+/-}$ mice. FC = fold change. (**c**) Representative histogram of Bcl-xl expression in pro/pre-B cells in the BM from an aIL7R Sh2b3$^{fl/+}$ Mb1 leukemia (7S5) and a Cre$^-$ littermate control. (**d**) Relative fold-change in Bcl-xl MFI in leukemic cells normalized to MFI in pro/pre-B cells from Cre$^-$ and Cre only control animals. N = 8 controls (black circles), 4 aIL7R Sh2b3$^{fl/+}$ Mb1 (blue squares), and 3 aIL7R/Ikzf1 (teal squares) mice.

Figure II.4. cont'd. (**e** -**f**) 1 mg EdU was injected i.p. 1 hr prior to sacrifice. (**e**) Representative histograms showing the relative proportions of EdU^+ cells in total BM B and late pro-B cells. (**f**) Percentage of EdU+ cells in total BM B cells (left) and late pro B cells (right). Data from 3 independent experiments. N = 5 uninjected controls, 8 Mb1-cre, 7 $Sh2b3^{+/-}$, 9 aIL7R-Mb1, and 7 aIL7R-Mb1 $Sh2b3^{+/-}$ mice. (**b, f**) Significance defined as * = $P \leq 0.05$, ** = $P \leq 0.005$ and *** = $P \leq 0.001$ by one-way ANOVA. (**g**) Representative histograms of Ki-67 expression in BM B (CD19+; *left*) and SPL B (B220+; *right*) cells from an aIL7R/Sh2b3 leukemia (7S6) and a Cre^- littermate control. (**h**) Percentage of Ki-67+ cells in BM and SPL B cells in leukemic animals versus healthy Cre^- and Cre only littermate controls. N = 11 controls (black circles), 2 aIL7R-CD19 (red squares), 4 aIL7R $Sh2b3^{fl/+}$ Mb1 (blue squares), and 3 aIL7R/Ikzf1 (teal squares). Significance defined as * = $P \leq 0.05$ and ** = $P \leq 0.005$ by one-way ANOVA. (**b, d, f, h**) Data points represent individual mice and bars represent mean ± SEM.

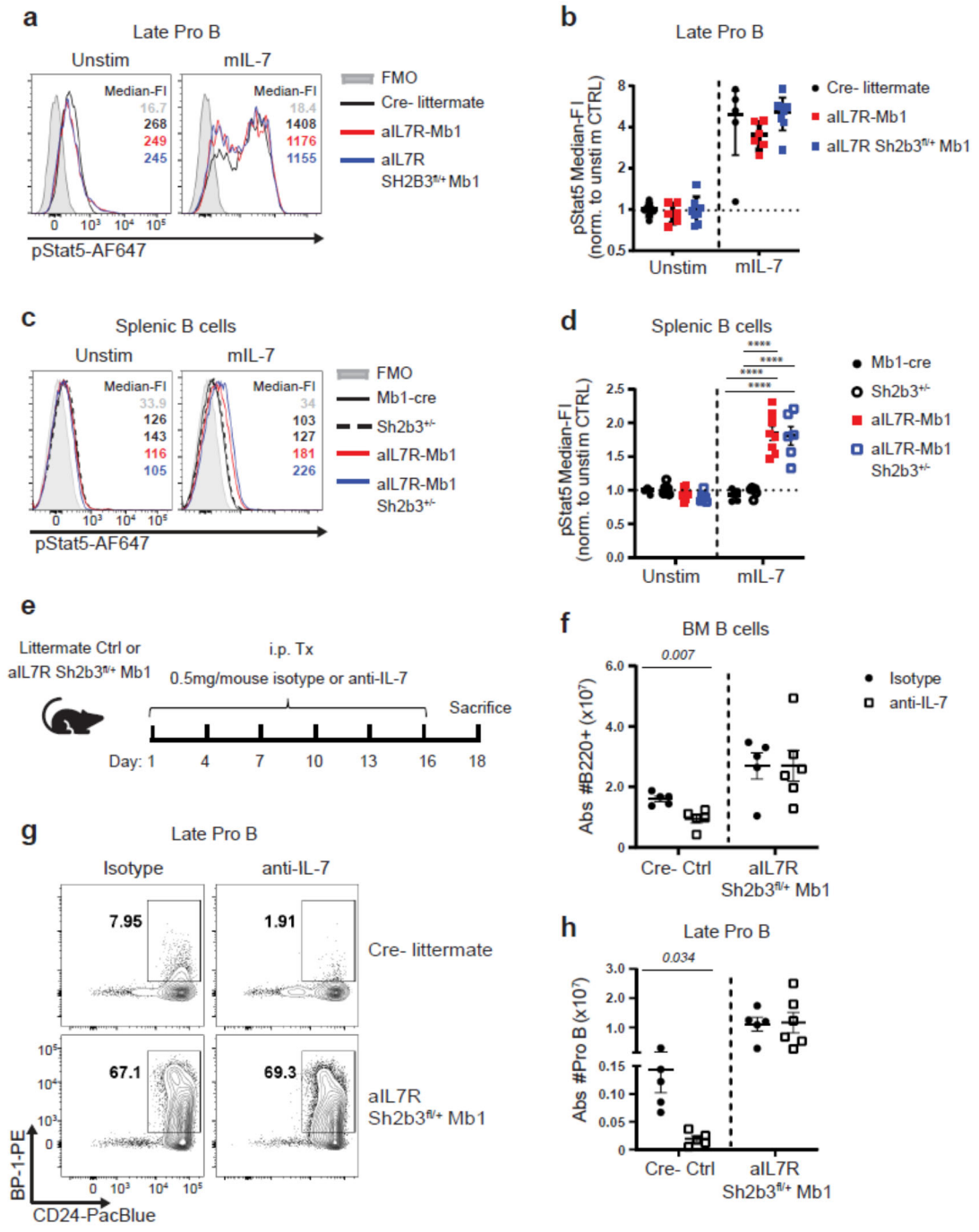

Figure II.5. aIL7R-expressing B cell progenitors are less sensitive to IL-7 depletion *in vivo*. (**a** - **b**) Late pro-B cells were sorted, rested, then stimulated with or without 10 ng/mL recombinant murine IL-7 (mIL-7). (**a**) Representative histograms of phosphorylated (p)Stat5 in unstimulated and mIL-7-stimulated late pro-B cells. (**b**) pStat5 Median-FI normalized to the average fluorescence of unstimulated pro-B cells from Cre$^-$ littermate control animals. Data from 3 independent experiments. N = 5 Cre$^-$ littermate, 6 aIL7R-Mb1, and 7 aIL7R Sh2b3$^{fl/+}$ Mb1 mice. (**c** - **d**) Naïve B cells were enriched from total splenocytes and

Figure II.5. cont'd. stimulated with 25 ng/mL mIL-7. (**c**) Representative histograms of pStat5 in unstimulated and IL-7 stimulated cells. (**d**) pStat5 Median-FI normalized to the average fluorescence of unstimulated B cells from Mb1-cre animals. Data from 3 independent experiments. N = 6 Mb1-cre, 6 $Sh2b3^{+/-}$, 8 aIL7R-Mb1, and 6 aIL7R-Mb1 $Sh2b3^{+/-}$ mice. Significance defined by **** = $P \leq 0.0001$ by two-way ANOVA. (**e - j**) aIL7R $Sh2b3^{fl/+}$ Mb1 and Cre^{-} littermate control mice were treated i.p. with 0.5 mg/mouse isotype control or neutralizing anti-IL-7 mAb every third day for 16 days (6 injections) and sacrificed on day 18. (**e**) Schematic of *in vivo* blocking antibody treatment. (**f**) Absolute number of $B220^{+}$ B cells in the BM from 1 tibia + femur in isotype- (black circles) and anti-IL-7-treated (open squares) animals. (**g**) Representative flow cytometry plots showing the frequency of late pro-B cells in isotype- and anti-IL-7-treated animals. (**h**) Absolute number of late pro-B cells in the BM from isotype- and anti-IL-7-treated animals. (**f, h**) Data from 2 independent experiments. N = 5 Cre^{-} controls per treatment group and 5 (isotype) or 6 (anti-IL-7) aIL7R $Sh2b3^{fl/+}$ Mb1 mice. Significance defined by multiple t tests using the Holm-Sidak method. (**b, d, f, h**) Data points represent individual mice and bars represent mean ± SEM.

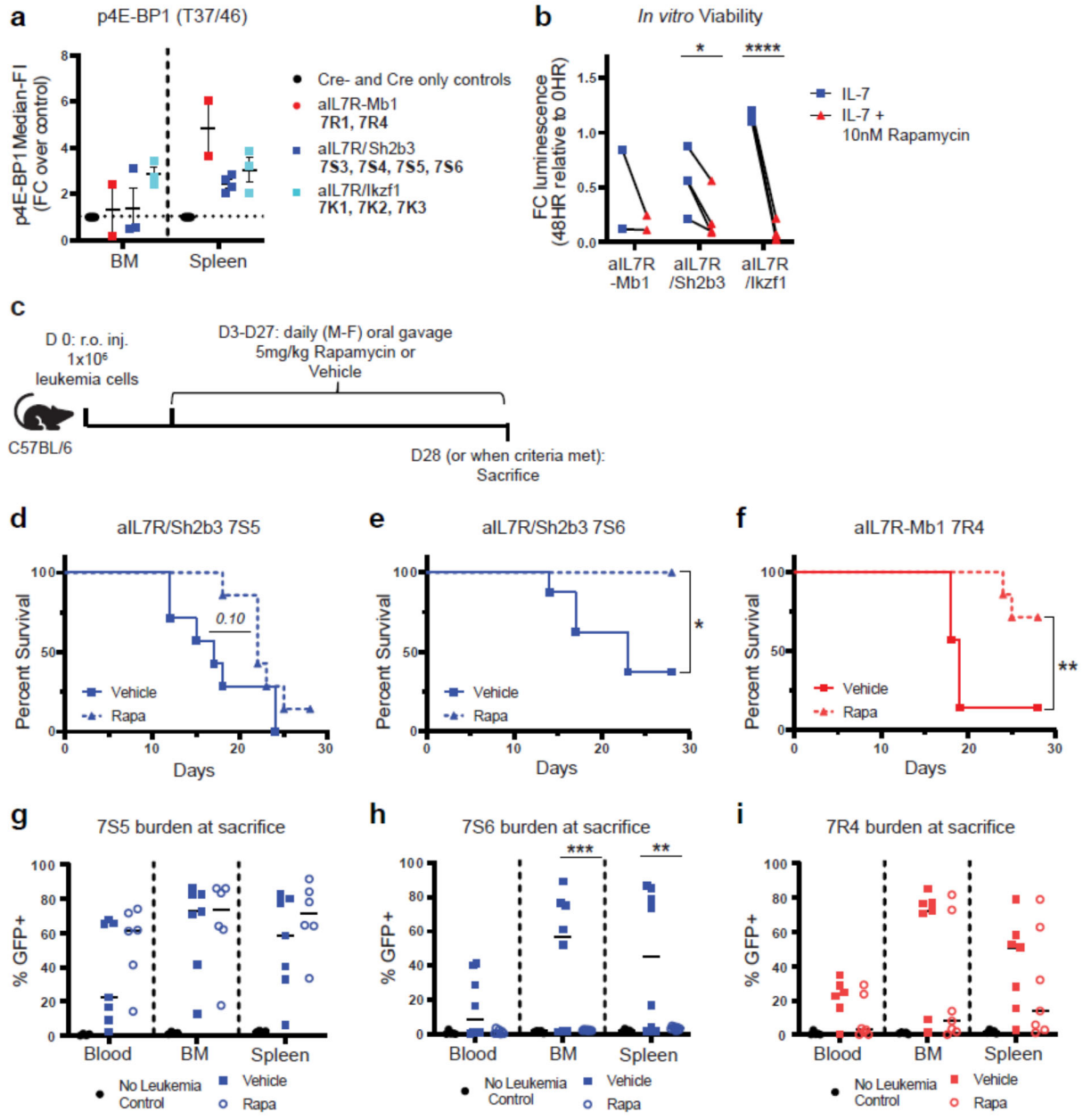

Figure II.6. aIL7R leukemias are responsive to rapamycin therapy *in vivo*. (**a**) Fold-change median-FI of p4E-BP1 in BM and spleen B cells ($CD19^+$) *ex vivo* from aIL7R leukemic animals relative to Cre^- or Cre only littermate controls. N = 8 controls, 2 aIL7R-Mb1, 4 aIL7R $Sh2b3^{fl/+}$ Mb1, and 3 aIL7R/Ikzf1. (**b**) CellTiter-Glo luminescent cell viability of aIL7R leukemias cultured for 48 hrs with IL-7 with (red triangle) or without (blue square) rapamycin (Rapa). Luminescence reported as fold change relative to *ex vivo* (0 hr) levels. Significance defined as *: P = 0.024 and ****: P < 0.0001 by two-tailed paired t tests. N = 2 aIL7R-Mb1, 4 aIL7R $Sh2b3^{fl/+}$ Mb1 and 4 aIL7R/Ikzf1. (**c** - **i**) Primary aIL7R leukemia cells were transferred retro-orbitally (r.o.) into C57BL/6 recipient mice and then given rapamycin or vehicle by oral gavage daily for 4 weeks. (**c**) Schematic of *in vivo* rapamycin treatment experiments. (**d** - **f**) Survival curves for recipients of murine leukemias 7S5 (**d**), 7S6 (**e**), and 7R4 (**f**) treated with vehicle (solid line) or rapamycin (dashed

Figure II.6. cont'd. line). Significance defined by Mantel-Cox test. *: P = 0.023 and **: P = 0.0084. Data from 2 independent experiments. (**g-i**) Frequency of GFP+ leukemic 7S5 (**g**), 7S6 (**h**), and 7R4 (**i**) cells in peripheral blood, BM, and spleen of recipient animals at sacrifice. Closed squares = vehicle and open circles = rapamycin. Data points represent individual mice and lines represent mean. N = 7 7S5, 8 7S6, and 7 7R4 recipients per treatment group. N = 5 no leukemia controls per graph.

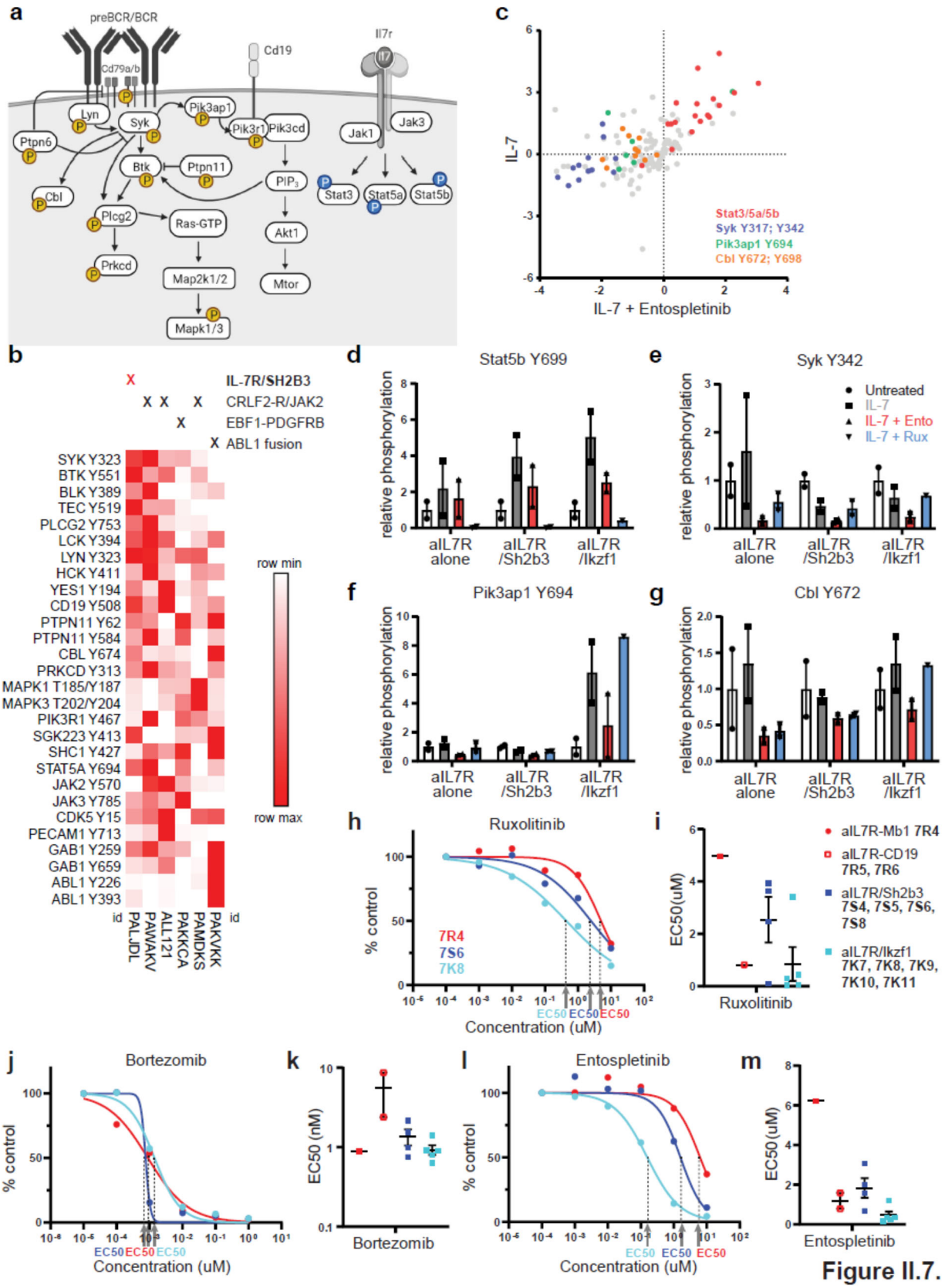
a
preBCR/BCR
Cd79a/b
Cd19
Il7r
Il7
Lyn
Syk
Pik3ap1
Pik3r1
Pik3cd
Jak1
Jak3
Ptpn6
Btk
Ptpn11
PIP3
Stat3
Stat5a
Stat5b
Cbl
Plcg2
Ras-GTP
Akt1
Prkcd
Map2k1/2
Mtor
Mapk1/3
b
IL-7R/SH2B3
CRLF2-R/JAK2
EBF1-PDGFRB
ABL1 fusion
SYK Y323
BTK Y551
BLK Y389
TEC Y519
PLCG2 Y753
LCK Y394
LYN Y323
HCK Y411
YES1 Y194
CD19 Y508
PTPN11 Y62
PTPN11 Y584
CBL Y674
PRKCD Y313
MAPK1 T185/Y187
MAPK3 T202/Y204
PIK3R1 Y467
SGK223 Y413
SHC1 Y427
STAT5A Y694
JAK2 Y570
JAK3 Y785
CDK5 Y15
PECAM1 Y713
GAB1 Y259
GAB1 Y659
ABL1 Y226
ABL1 Y393
id
PALJDL
PAVAKV
ALL121
PAKKCA
PAMDKS
PAKVKK
id
row min
row max
c
IL-7
IL-7 + Entospletinib
Stat3/5a/5b
Syk Y317; Y342
Pik3ap1 Y694
Cbl Y672; Y698
d
Stat5b Y699
relative phosphorylation
aIL7R alone
aIL7R /Sh2b3
aIL7R /Ikzf1
e
Syk Y342
Untreated
IL-7
IL-7 + Ento
IL-7 + Rux
f
Pik3ap1 Y694
g
Cbl Y672
h
Ruxolitinib
% control
7R4
7S6
7K8
EC50
Concentration (uM)
i
EC50(uM)
aIL7R-Mb1 7R4
aIL7R-CD19 7R5, 7R6
aIL7R/Sh2b3 7S4, 7S5, 7S6, 7S8
aIL7R/Ikzf1 7K7, 7K8, 7K9, 7K10, 7K11
Ruxolitinib
j
Bortezomib
k
EC50 (nM)
l
Entospletinib
m
Entospletinib

Figure II.7.

Figure II.7. IL-7R-mutant leukemias display activation of a "BCR-like" signaling program. (**a**) Diagram of phosphorylated "BCR-like" peptides (gold) and phosphorylated Stat peptides (blue) identified by phospho-tyrosine immunoprecipitation and mass spectrometry analysis of six secondary aIL7R murine leukemias (1 aIL7R-Mb1, 7R4 – 2 recipients; 2 aIL7R/Sh2b3 – 7S5 and 7S6; 2 aIL7R/Ikzf1 – 7K7 and 7K10). Created with BioRender.com. (**b**) Quantification of peptides identified by phospho-tyrosine immunoprecipitation in six Ph-like ALL patient-derived xenograft models directly harvested from spleens of NSG mice. PDX models included an activating *IL7R/SH2B3*-null (IL-7R/SH2B3; PALJDL), three independent *CRLF2*-overexpressing/*JAK2* gain-of-function ALLs (CRLF2-R/JAK2; ALL121, PAMDKS, and PAWAKV), a *NUP214-ABL1* fusion (PAKVKK), and an *EBF1-PDGFRB* fusion (PAKKCA). (**c**-**g**) The murine aIL7R leukemias from (**a**) were cultured with or without 1 uM of entospletinib (Ento) or ruxolitinib (Rux) for 30 mins and then stimulated with or without 10 ng/mL mIL-7 for an additional 15 mins. Phospho-tyrosine residues were immunoprecipitated and analyzed by mass spectrometry. (**c**) Scatter plot of all pY peptides for the IL-7 alone vs entospletinib + IL-7 conditions. Data are presented as fold change relative to the average of untreated conditions for all peptides within each respective genotype. pStat3/Stat5 (red), pSyk (blue), pPik3ap1 (green), and pCbl (orange) peptides are highlighted. (**d**) Bar graph of pY699 Stat5b levels (in response to the indicated treatments) relative to the untreated conditions across genotypes. (**e**) Bar graph of pY342 Syk levels relative to untreated. (**f**) Bar graph of pY694 Pik3ap1 levels relative to untreated. (**g**) Bar graph of pY672 Cbl levels relative to untreated. (**d** - **g**) White bars = untreated; gray bars = IL-7 only; red bars = IL-7 + Ento; blue bars = IL-7 + Rux. Data points represent individual mice and bars represent mean with range. (**h** - **m**) Splenocytes harvested *ex vivo* from primary or secondary murine aIL7R leukemias were cultured with ruxolitinib (**h** - **i**), bortezomib (**j** - **k**), or entospletinib (**l** - **m**) for 24 hr in the presence of 10ng/mL mIL-7 and cell viability was assessed via CellTiter-Glo luminescence. Representative dose curves for leukemias 7R4 (red), 7S6 (blue) and 7K8 (teal) treated with ruxolitinib (**h**), bortezomib (**j**), or entospletinib (**l**). Data points represent luminescence values at specific inhibitor doses normalized to the luminescence at the lowest dose (100 pM or 10 pM (bortezomib)). Summary of EC50s for aIL7R leukemias at 24 hr treated with ruxolitinib (**i**), bortezomib (**k**), or entospletinib (**m**). Data points represent individual leukemias and lines represent means. N = 1 aIL7R-Mb1, 2 aIL7R-CD19, 4 aIL7R Sh2b3$^{fl/+}$ Mb1, and 5 aIL7R/Ikzf1 leukemias.

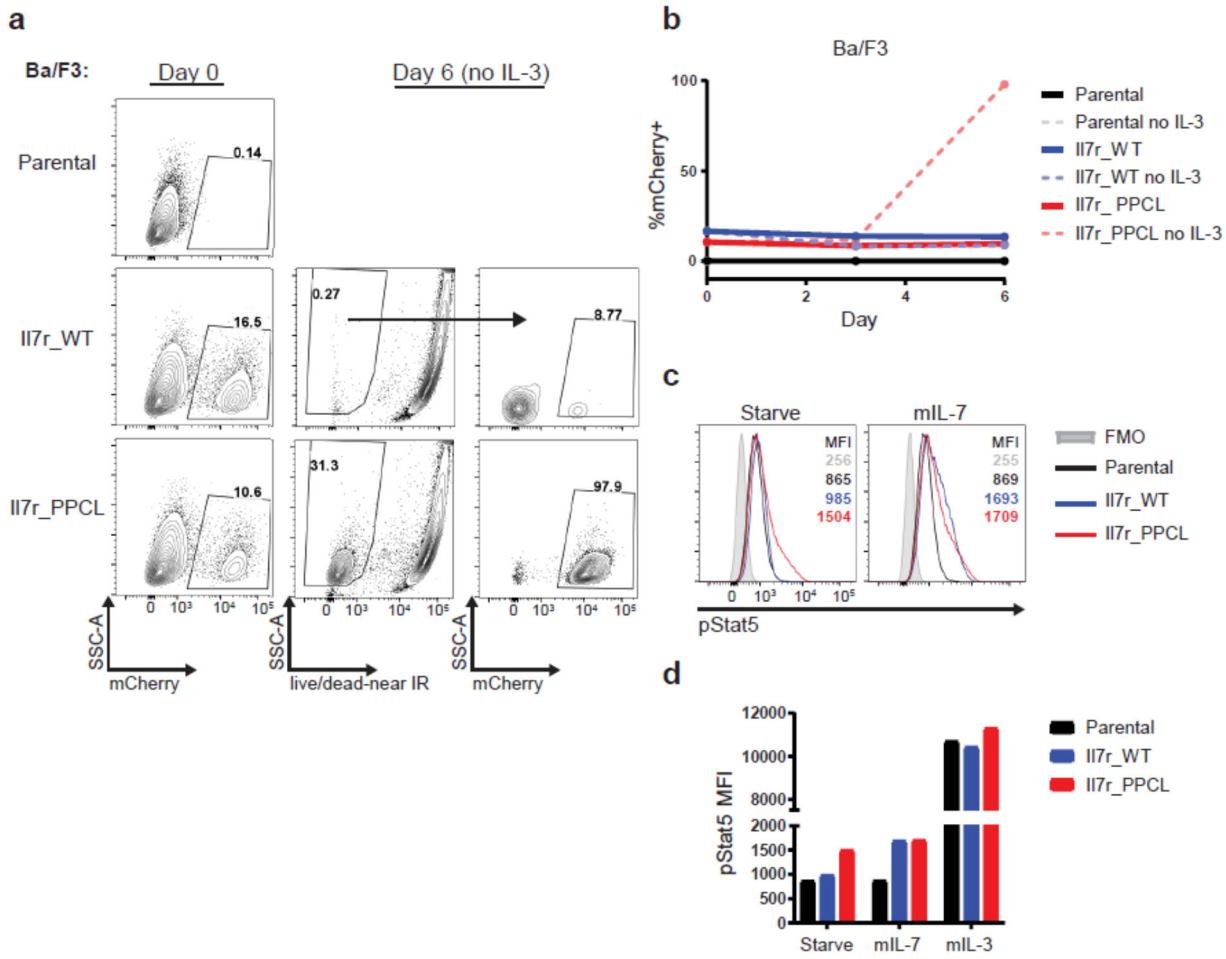

Figure II.S1. Overexpression of murine aIL7R confers cytokine independence and induces constitutive STAT5 phosphorylation in Ba/F3 cells. (**a**-**b**) Ba/F3 cells were transduced with a lentiviral vector containing wildtype (Il7r_WT) or mutant "activated" aIL7R (Il7r_PPCL) followed by a cis-linked mCherry reporter. Parental, Il7r_WT, and Il7r_PPCL Ba/F3 cells were cultured without IL-3 for 6 days. (**a**) Representative flow plots of %mCherry+ cells on Day 0; and viability and %mCherry+ cells on Day 6 for Parental, Il7r_WT, and Il7r_PPCL Ba/F3 cells. (**b**) Frequency of mCherry+ cells over time. (**c** - **d**) Il7r_WT and Il7r_PPCL transduced Ba/F3 cells were sorted on mCherry expression and maintained in culture with 10ng/mL recombinant murine IL-3. Parental and sorted Il7r_WT and Il7r_PPCL cells were washed, cultured without mIL-3 for 5hours (Starve) and then stimulated with either 10ng/mL mIL-7 or 10ng/mL mIL-3 for 20mins. Cells were then fixed, permeabilized, and stained for phospho-flow analysis. (**c**) Representative histograms of unstimulated (Starve; *left*) and mIL-7 (*right*) conditions. Filled gray histogram = fluorescence-minus-one (FMO); open histograms = parental (black), Il7r_WT (blue), and Il7r_PPCL (red). (**d**) MFI of pStat5 expression per condition. Representative data from one of two independent experiments.

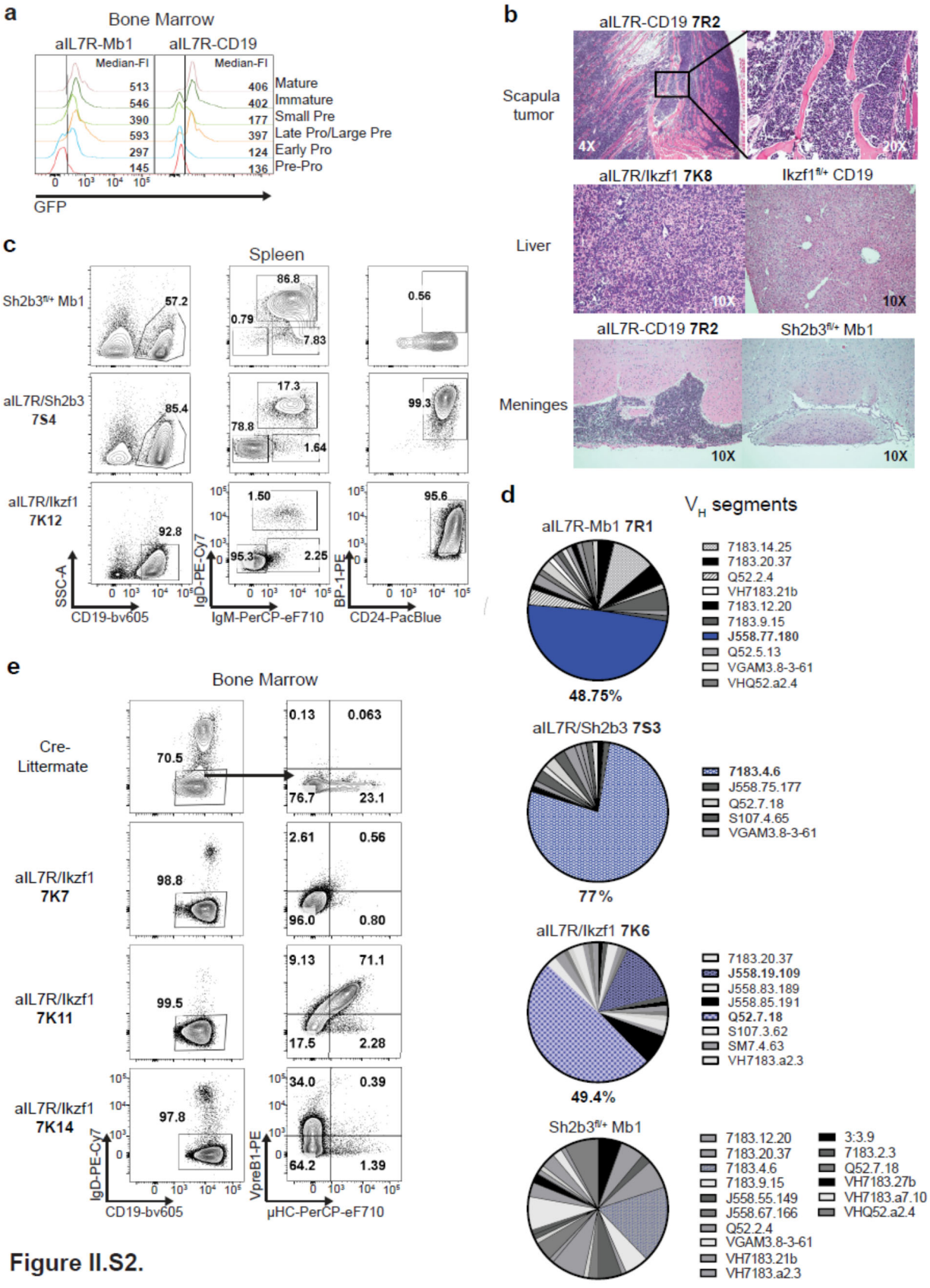
a
Bone Marrow
aIL7R-Mb1
aIL7R-CD19
Median-FI
513
546
390
593
297
145
406
402
177
397
124
136
Mature
Immature
Small Pre
Late Pro/Large Pre
Early Pro
Pre-Pro
GFP
b
aIL7R-CD19 7R2
Scapula tumor
4X
20X
aIL7R/Ikzf1 7K8
Ikzf1fl/+ CD19
Liver
10X
10X
aIL7R-CD19 7R2
Sh2b3fl/+ Mb1
Meninges
10X
10X
c
Spleen
Sh2b3fl/+ Mb1
57.2
86.8
0.79
7.83
0.56
aIL7R/Sh2b3 7S4
85.4
17.3
78.8
1.64
99.3
aIL7R/Ikzf1 7K12
92.8
1.50
95.3
2.25
95.6
SSC-A
CD19-bv605
IgD-PE-Cy7
IgM-PerCP-eF710
BP-1-PE
CD24-PacBlue
d
VH segments
aIL7R-Mb1 7R1
7183.14.25
7183.20.37
Q52.2.4
VH7183.21b
7183.12.20
7183.9.15
J558.77.180
Q52.5.13
VGAM3.8-3-61
VHQ52.a2.4
48.75%
aIL7R/Sh2b3 7S3
7183.4.6
J558.75.177
Q52.7.18
S107.4.65
VGAM3.8-3-61
77%
aIL7R/Ikzf1 7K6
7183.20.37
J558.19.109
J558.83.189
J558.85.191
Q52.7.18
S107.3.62
SM7.4.63
VH7183.a2.3
49.4%
Sh2b3fl/+ Mb1
7183.12.20
7183.20.37
7183.4.6
7183.9.15
J558.55.149
J558.67.166
Q52.2.4
VGAM3.8-3-61
VH7183.21b
VH7183.a2.3
3:3.9
7183.2.3
Q52.7.18
VH7183.27b
VH7183.a7.10
VHQ52.a2.4
e
Bone Marrow
Cre-Littermate
70.5
0.13
0.063
76.7
23.1
aIL7R/Ikzf1 7K7
98.8
2.61
0.56
96.0
0.80
aIL7R/Ikzf1 7K11
99.5
9.13
71.1
17.5
2.28
aIL7R/Ikzf1 7K14
97.8
34.0
0.39
64.2
1.39
IgD-PE-Cy7
CD19-bv605
VpreB1-PE
μHC-PerCP-eF710

Figure II.S2.

Figure II.S2. aIL7R murine leukemias infiltrate peripheral organs and display clonality and variable pre-BCR expression. (**a**) Representative histograms comparing the GFP expression in the B cell developmental subsets between aIL7R-Mb1 and aIL7R-CD19 BM. Open histograms: red = pre-pro-B, blue = early pro-B, orange = late pro-B/large pre-B, light green = small pre-B, dark green = immature B, and pink = mature B. (**b**) Representative H&E staining of the liver (*top*) and meninges (bottom) from leukemic mice from indicated genotype and littermate controls. N = 1 $Sh2b3^{fl/+}$ Mb1 littermate control, 1 $Ikzf1^{fl/+}$ CD19 littermate control, 1 aIL7R-Mb1, 1 aIL7R-CD19, 3 aIL7R $Sh2b3^{fl/+}$ Mb1, and 3 aIL7R $Ikzf1^{fl/+}$ CD19 mice. (**c**) Representative flow plots of B cell developmental subsets in the spleen of leukemic animals compared to control. (**d**) Representative heavy chain V segment families present in bulk splenocytes from three primary aIL7R leukemias (7R1, 7S3, and 7K6) and a littermate control. V_H segments representing < 1% of total sequences were excluded from legend. N = 1 aIL7R-Mb1, 4 aIL7R/Sh2b3, 4 aIL7R/Ikzf1, and 5 Cre^- or Cre only littermate controls sequenced. (**e**) Representative flow plots of normal and leukemic bone marrow with gating schema to measure pre-BCR expression ($CD19^+IgD^-s\mu HC^+vpreB1^+$) in three aIL7R/Ikzf1 leukemias (7K7, 7K11, and 7K14) and a littermate control.

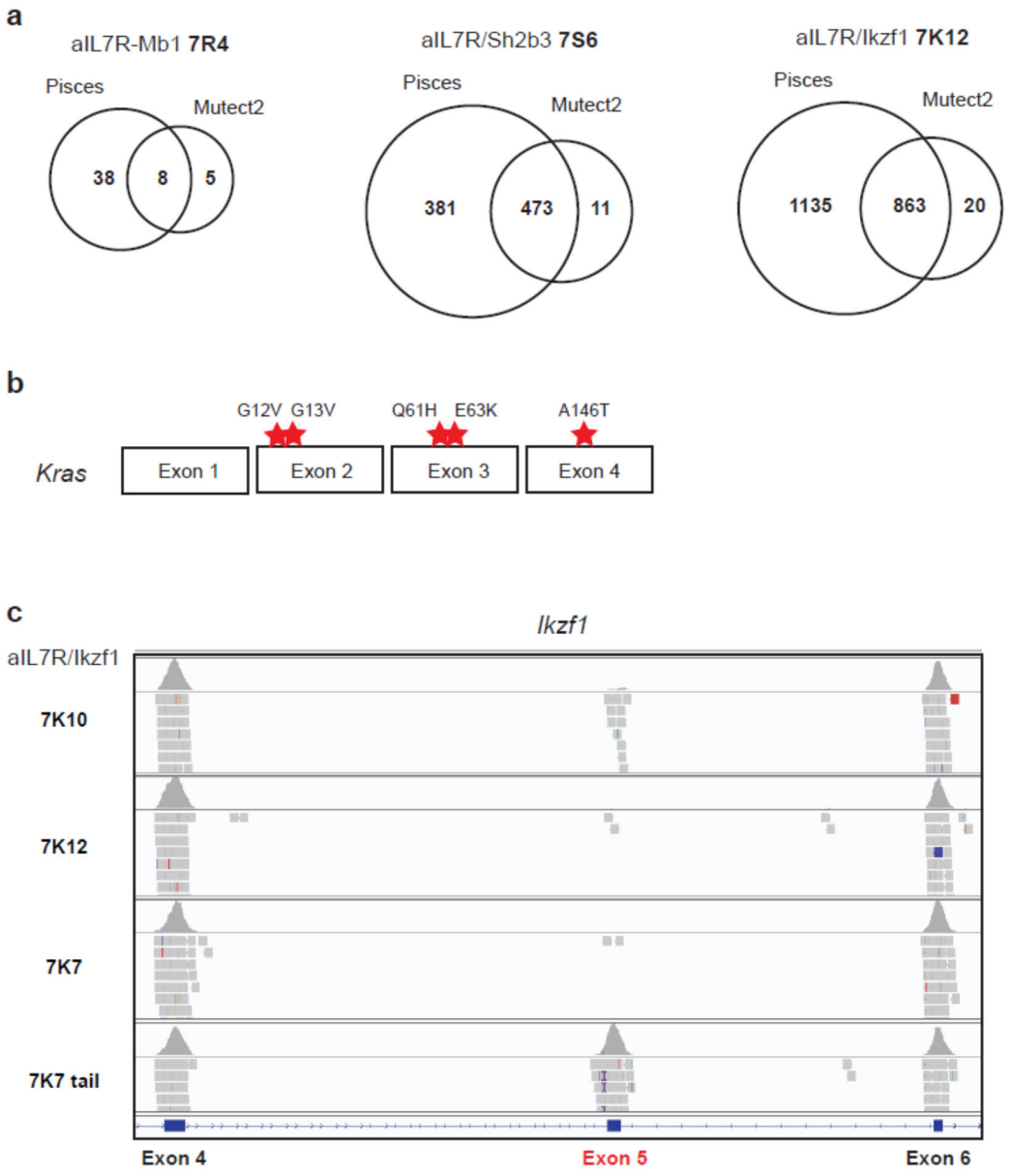

Figure II.S3. aIL7R leukemias display somatic mutations in known oncogenes (*Kras*) and tumor suppressors (*Ikzf1*). (**a**) SNVs identified by two variant caller methods, Pisces and Mutect2, were combined and overlapping SNVs were considered high-confidence variants. Representative Venn diagrams showing the number of variants identified in three primary leukemias (7R4, 7S6, and 7K12). Data representative of N = 1 aIL7R-Mb1, 1 aIL7R-CD19, 3 aIL7R Sh2b3$^{fl/+}$ Mb1, and 3 aIL7R/Ikzf1 leukemias. (**b**) Schematic of the cod ng exons for *Kras* and the amino acid substitutions caused by SNVs identified in the whole-exome sequencing. (**c**) IGV alignment snapshot of *Ikzf1* Exon 5 sequence coverage in aIL7R/Ikzf1 leukemias 7K7, 7K10, and 7K12 compared to paired tail gDNA (7K7).

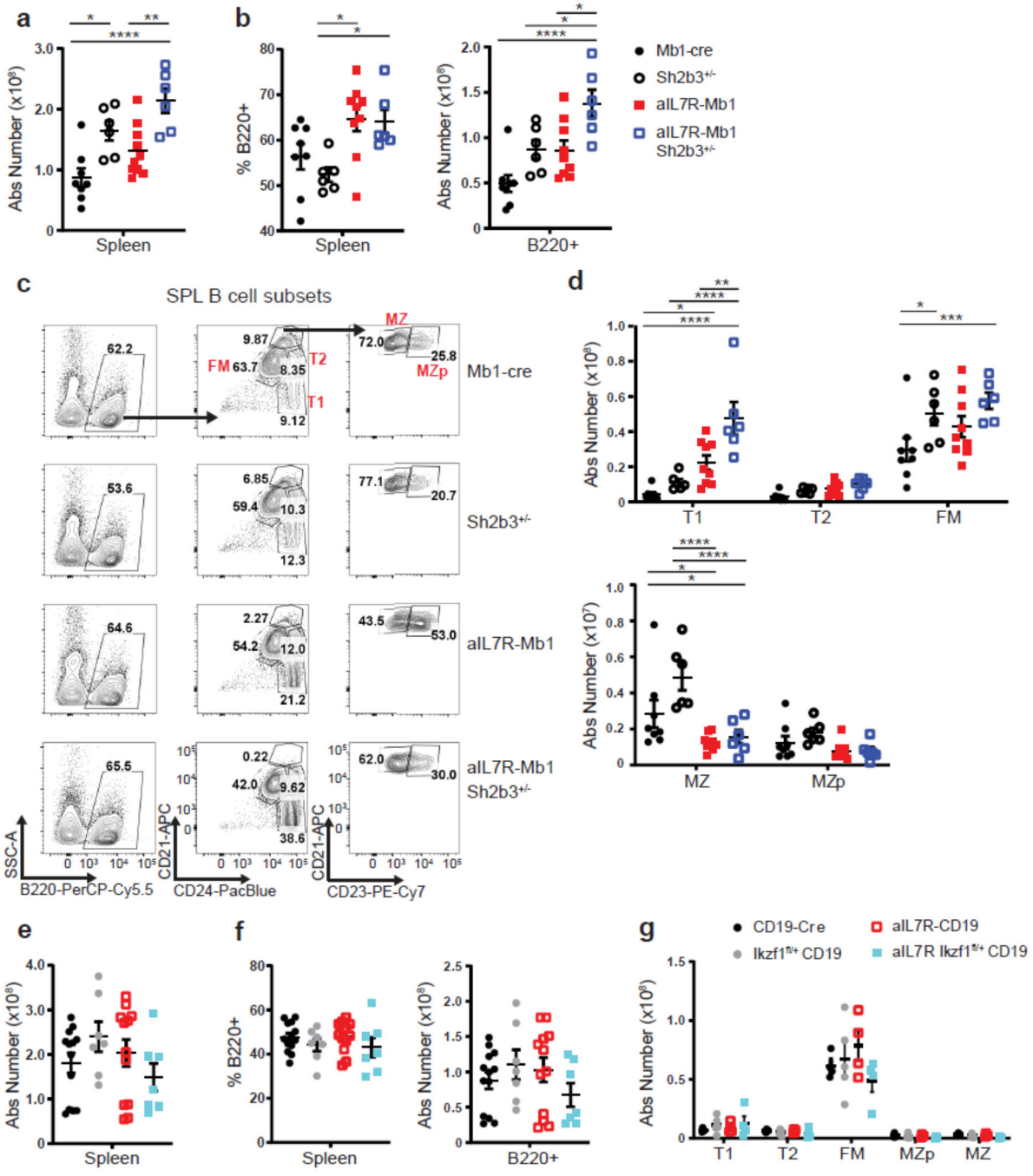

Figure II.S4. B-intrinsic aIL7R (with or without heterozygous loss of Sh2b3) skews peripheral B cell subsets. (**a**) Absolute cell counts of the spleen in mice of the indicated genotypes. (**b**) Frequency (*Left*) and absolute number (*Right*) of B220^{+} B cells in the spleen. (**a** -**b**) Significance defined as * = P ≤ 0.05, ** = P ≤ 0.005, and **** = P ≤ 0.0001 by one-way ANOVA. (**c**) Representative flow plots of splenic B cells subsets with gating schema to identify: transitional T1 (B220^{+}CD24^{hi}CD21^{lo}) and T2 (B220^{+}CD24^{hi}CD21^{mid}) cells, follicular mature (FM; B220^{+} CD24^{mid}CD21^{mid}) B cells, marginal zone (MZ; B220^{+}CD24^{mid}CD21^{hi}CD23^{-}) B cells and MZ precursors (MZp; B220^{+}CD24^{mid}CD21^{hi}CD23^{+}).

Figure II.S4. cont'd. (**d**) Absolute number of T1, T2, FM (*Top*) and MZ and MZp (*Bottom*) cells in the spleen. Significance defined by * = $P \leq 0.05$, ** = $P \leq 0.005$, *** = $P \leq 0.001$, and **** = $P \leq 0.0001$ by two-way ANOVA. (**a, b, d**) N = 8 Mb1-cre, 6 $Sh2b3^{+/-}$, 9 aIL7R-Mb1, and 6 aIL7R-Mb1 $Sh2b3^{+/-}$ mice. (**e**) Absolute cell count of the spleen in mice of the indicated genotypes. (**f**) Frequency (*Left*) and absolute number (*Right*) of $B220^{+}$ B cells in the spleen. (**e, f**) N = 13 CD19-cre, 7 $Ikzf1^{fl/+}$ CD19, 12 aIL7R-CD19, and 7 aIL7R $Ikzf1^{fl/+}$ CD19 mice. (**g**) Absolute number of T1, T2, FM, MZp, and MZ cells in the spleen. N = 4 CD19-cre, 4 $Ikzf1^{fl/+}$ CD19, 4 aIL7R-CD19, and 4 aIL7R $Ikzf1^{fl/+}$ CD19 mice. (**a, b, d – g**) Data points represent individual mice and bars represent mean + SEM.

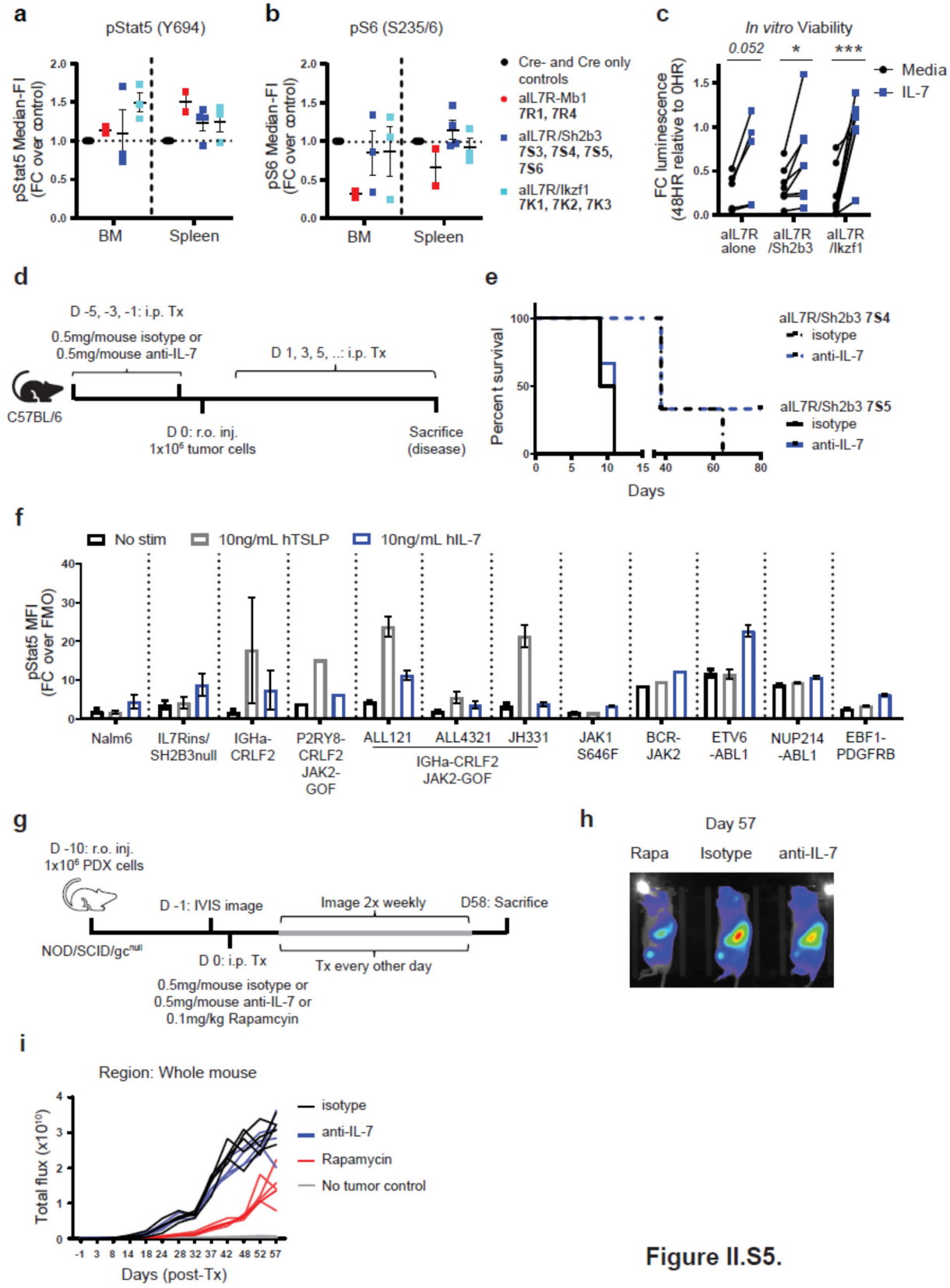
a
pStat5 (Y694)
pStat5 Median-FI (FC over control)
BM
Spleen
b
pS6 (S235/6)
pS6 Median-FI (FC over control)
Cre- and Cre only controls
aIL7R-Mb1 7R1, 7R4
aIL7R/Sh2b3 7S3, 7S4, 7S5, 7S6
aIL7R/Ikzf1 7K1, 7K2, 7K3
c
In vitro Viability
0.052
*
***
Media
IL-7
FC luminescence (48HR relative to 0HR)
aIL7R alone
aIL7R /Sh2b3
aIL7R /Ikzf1
d
D -5, -3, -1: i.p. Tx
0.5mg/mouse isotype or
0.5mg/mouse anti-IL-7
D 1, 3, 5, ..: i.p. Tx
C57BL/6
D 0: r.o. inj.
1x10⁵ tumor cells
Sacrifice (disease)
e
Percent survival
Days
aIL7R/Sh2b3 7S4
isotype
anti-IL-7
aIL7R/Sh2b3 7S5
isotype
anti-IL-7
f
No stim
10ng/mL hTSLP
10ng/mL hIL-7
pStat5 MFI (FC over FMO)
Nalm6
IL7Rins/ SH2B3null
IGHa-CRLF2
P2RY8-CRLF2 JAK2-GOF
ALL121
ALL4321
JH331
IGHa-CRLF2 JAK2-GOF
JAK1 S646F
BCR-JAK2
ETV6-ABL1
NUP214-ABL1
EBF1-PDGFRB
g
D -10: r.o. inj.
1x10⁶ PDX cells
D -1: IVIS image
Image 2x weekly
D58: Sacrifice
NOD/SCID/gc^null
D 0: i.p. Tx
Tx every other day
0.5mg/mouse isotype or
0.5mg/mouse anti-IL-7 or
0.1mg/kg Rapamcyin
h
Day 57
Rapa
Isotype
anti-IL-7
i
Region: Whole mouse
Total flux (x10¹⁰)
isotype
anti-IL-7
Rapamycin
No tumor control
Days (post-Tx)

Figure II.S5.

Figure II.S5. IL-7 enhances murine and human B-ALL viability and signaling *in vitro* but is not required for their survival *in vivo*. (**a**-**b**) Splenocytes and BM harvested *ex vivo* from primary or secondary aIL7R leukemias and littermate controls were fixed, permeabilized, and stained for phospho-flow cytometry. N = 8 Cre^- or Cre only controls, 2 aIL7R-Mb1, 4 aIL7R $Sh2b3^{fl/+}$ Mb1, and 3 aIL7R/Ikzf1. (**a**) Fold change median-FI of pStat5 in BM and SPL B cells ($CD19^+$). (**b**) Fold change median-FI of pS6 in BM and SPL B cells. (**c**) CellTiter-Glo luminescent cell viability of aIL7R leukemias cultured for 48 hr with or without mIL-7. Luminescence reported as fold change relative to *ex vivo* (0 hr) levels. N = 5 aIL7R alone, 8 aIL7R/Sh2b3, and 10 aIL7R/Ikzf1 leukemias. Significance defined as *: P = 0.0382 and ***: P = 0.0008 by two-tailed paired t tests. (**d** - **e**) B6 mice were pre-treated i.p. with 0.5 mg/mouse isotype or anti-IL-7 every other day for 6 days (3 injections) and then injected r.o. with $1x10^6$ splenocytes from aIL7R/Sh2b3 leukemias 7S4 & 7S5. Starting 1 day after implantation, recipient mice were treated every other day with isotype or anti-IL7 until sacrifice. N= 3 recipient animals per group. (**d**) Schematic of leukemia transfer and *in vivo* IL-7 blockade. (**e**) Survival curves for recipient animals. (**f**) pSTAT5 expression in 11 Ph-like ALL PDX models stimulated *ex vivo* with either 10 ng/mL recombinant human TSLP (hTSLP) or recombinant human IL-7 (hIL-7). Nalm6 (non-Ph+, non-Ph-like) B-ALL cells were included as a control. Data presented as fold change over fluorescence minus one (FMO). (**g** - **i**) NSG mice were injected r.o. with $1x10^6$ IL-7Rins/SH2B3null (PALJDL) PDX cells transduced to express a firefly luciferase construct. 8 days later (after leukemic cells were detectable by bioluminescent imaging), mice were injected i.p. with 0.5 mg/mouse isotype or anti-IL-7, or with 0.1 mg/kg rapamycin as a positive control. Mice were treated every other day and in vivo bioluminescent imaging was used ~2x weekly to track leukemia burden over time. N = 5 NSG recipients per treatment group and 1 no tumor control. (**g**) Schematic of treatment and imaging schedule. (**h**) Representative luminescent image of mice treated with rapamycin (Rapa), isotype, or anti-IL-7. (**i**) Total flux (photons/second) for the whole mouse over time.

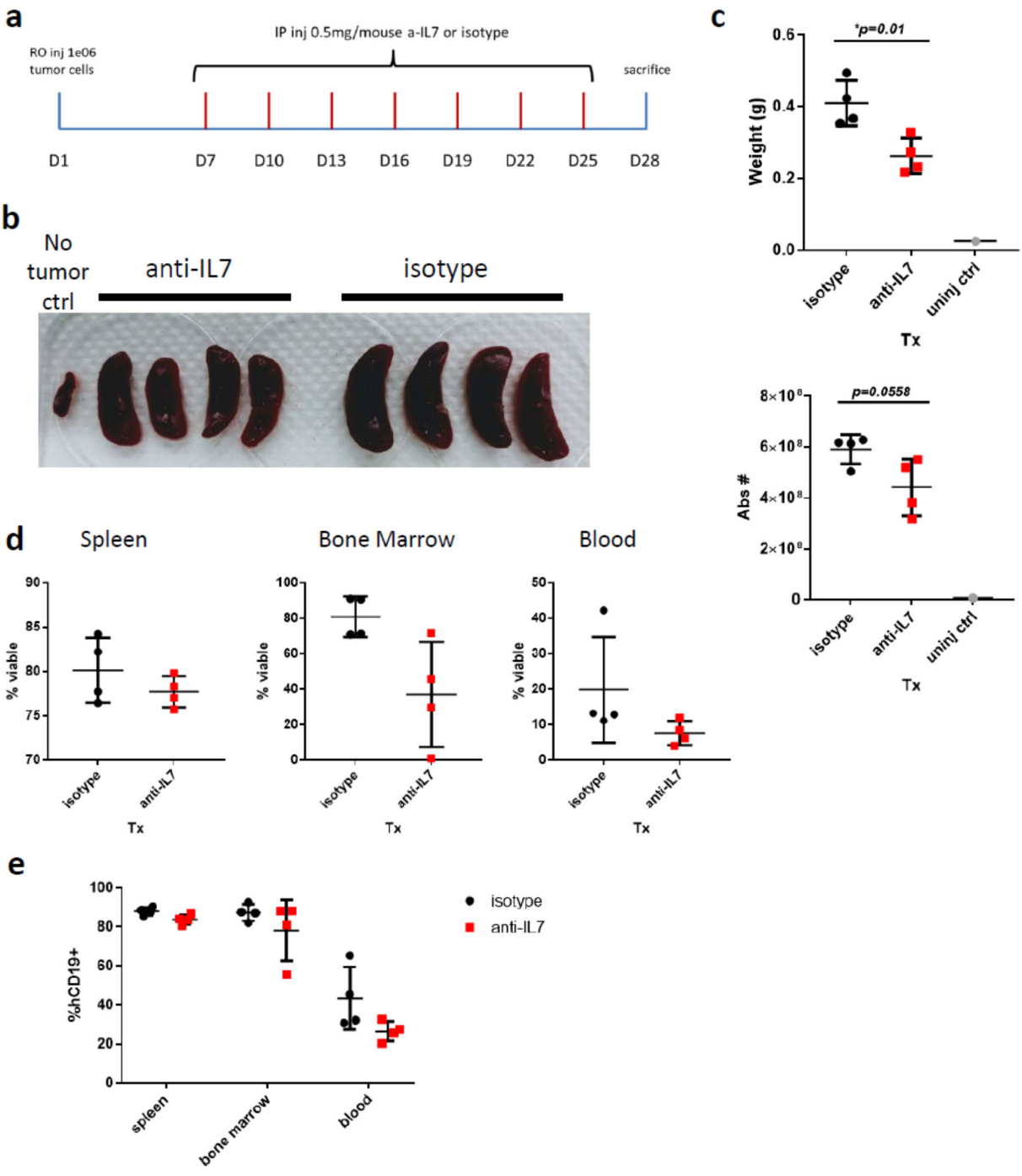

Figure II.S6. IL-7 blockade can modestly inhibit growth of a CRLF2-rearranged Ph-like xenograft *in vivo*. (**a**) Schematic of experimental approach. NSG mice were injected retroorbitally (r.o.) with 1e06 ALL121 cells. Starting 7 days post-implantation, mice were injected intraperitoneally (i.p.) with 0.5mg of anti-IL7 or isotype control every third day. Mice were sacrificed after 4 weeks. (**b**) Spleen size comparison between anti-IL7 or isotype-treated animals. (**c**) Spleen weight and total cell count. (**d**) Cell viability as measured by Live/Dead Near IR Fixable Dye (Thermo Fisher). (**e**) Frequency of human CD19-positive cells. Statistics calculated using unpaired student's T-test.

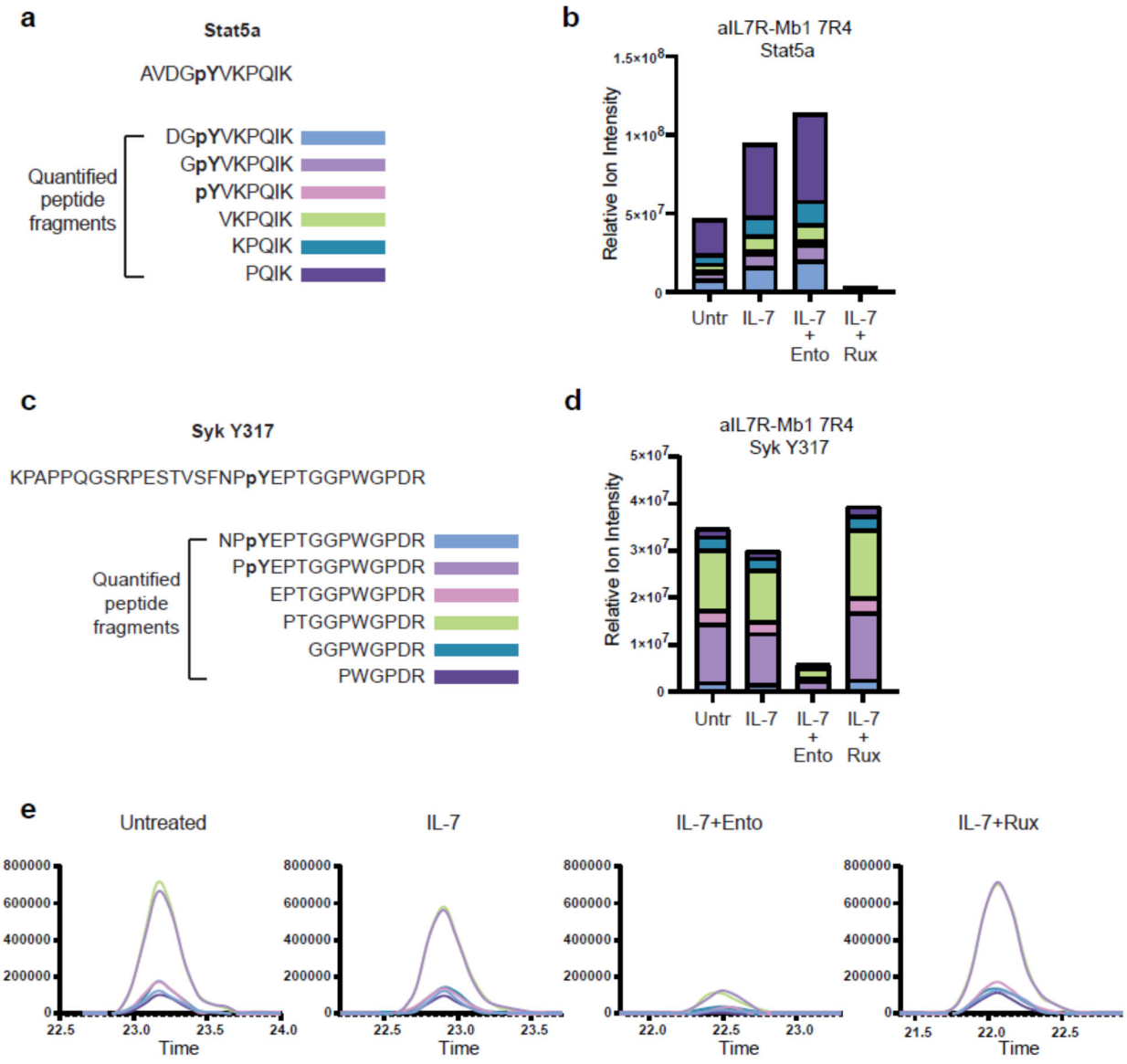

Figure II.S7. Representative examples of pY proteomic data for Stat5a and Syk peptides. (**a**) Diagram of quantified peptide fragments for Stat5a. (**b**) Bar graph representing the relative ion intensity of each peptide fragment of Stat5a per culture condition for aIL7R-Mb1 leukemia 7R4. (**c**) Diagram of quantified peptide fragments for Syk Y317. (**d**) Bar graph representing the relative ion intensity of each peptide fragment of Syk Y317 per culture condition for aIL7R-Mb1 leukemia 7R4. (**e**) Representative Syk Y317 peptide fragment elution profiles across culture conditions.

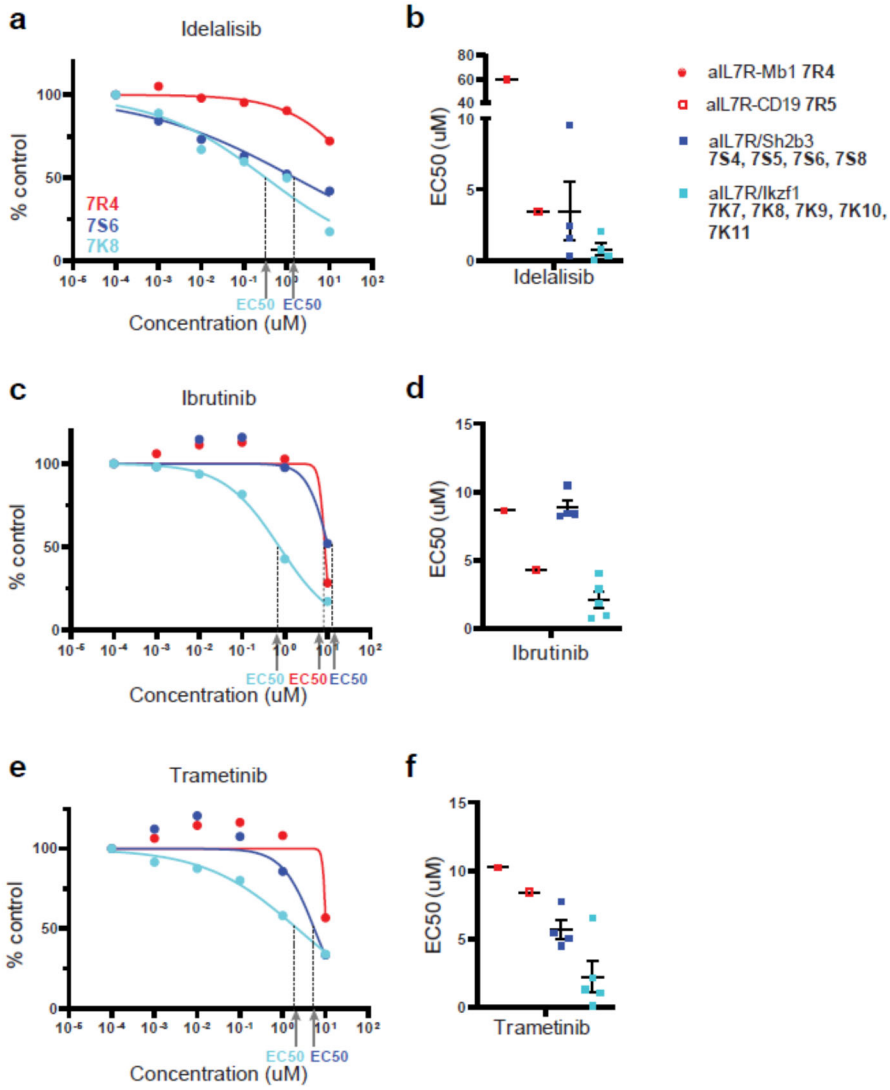

Figure II.S8. aIL7R leukemias are sensitive to "BCR-like" inhibition *in vitro*. (**a** - **f**) Splenocytes harvested *ex vivo* from primary or secondary murine aIL7R leukemias were cultured with idelalisib (**a** - **b**), ibrutinib (**c** - **d**), or trametinib (**e** - **f**) for 24 hr in the presence of 10ng/mL mIL-7 and cell viability was assessed via CellTiter-Glo luminescence. (**a** - **f**) Representative dose curves for leukemias 7R4 (red), 7S6 (blue) and 7K8 (teal) treated with idelalisib (**a**), ibrutinib (**c**), or trametinib (**e**). Data points represent luminescence values at specific inhibitor doses normalized to the luminescence at the lowest dose (100 pM). Summary of EC50s for aIL7R leukemias at 24 hr treated with idelalisib (**b**), ibrutinib (**d**), or trametinib (**f**). Data points represent individual leukemias and lines represent means. N = 1 aIL7R-Mb1, 1 aIL7R-CD19, 4 aIL7R Sh2b3$^{fl/+}$ Mb1, and 5 aIL7R/Ikzf1.

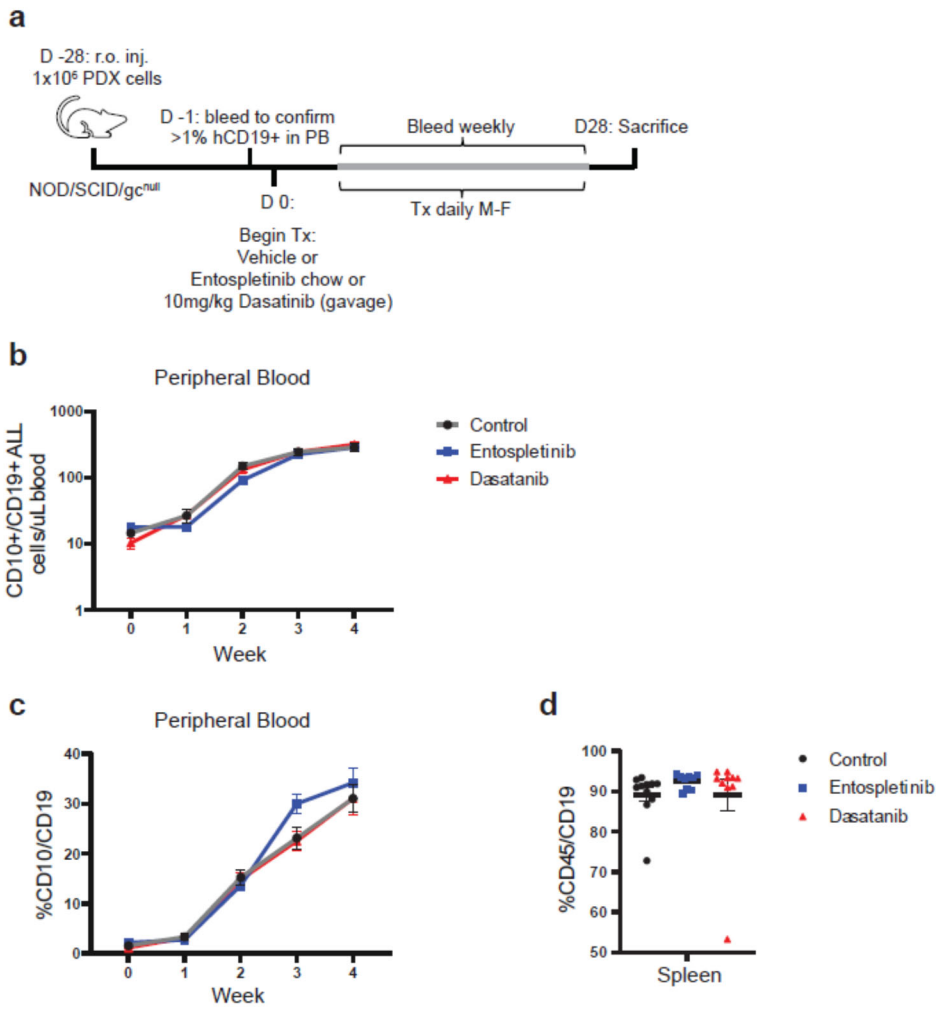

Figure II.S9. (**a** – **d**) NSG mice were injected r.o. with 1x10^6 IL7Rins/SH2B3null (PALJDL) human xenograft cells. When >1% hCD10+/hCD19+ were detectable in the peripheral blood, recipient animals were assigned to their treatment group (vehicle chow, entospletinib chow, or 10mg/kg dasatanib by oral gavage) and treated daily for 4 weeks. (**a**) Schematic of treatment schedule. (**b**) Peripheral hCD10+/hCD19+ ALL count over time. (**c**) Frequency of hCD10+/hCD19+ cells in peripheral blood over time. (**d**) Frequency of hCD45+/hCD19+ ALL cells in the spleen.

aIL7R alone															
Mouse #	Genotype	Sex	Age (wks)	Condition	Surface phenotype*	Transplanted	Ki-67	Bcl-xl	pFlow	H&E	IgH seq	If Y, dominant clone? (VH and %)	CellTiter-Glo	Phospho-proteomics	WES
7R1	aIL7R-Mb1	M	15.14	abdominal masses and poor ambulation	VpreB+ μHC+							J558.77.180; 48.75%			
7R2	aIL7R-CD19	F	11.14	cranial swelling and shoulder tumor	μHC+										
7R3	aIL7R-CD19	M	11.14	hunched/bloated	μHC+										
7R4	aIL7R-Mb1	M	7	thin/hunched and neck swelling	c-kit- VpreB- μHC-										
7R5	aIL7R-CD19	F	10	thin/hunched	VpreB+ μHC+										
7R6	aIL7R-CD19	M	12	shoulder tumor	μHC+										
aIL7R/Sh2b3															
Mouse #	Genotype	Sex	Age (wks)	Condition	Surface phenotype*	Transplanted	Ki-67	Bcl-xl	pFlow	H&E	IgH seq	If Y, dominant clone? (VH and %)	CellTiter-Glo	Phospho-proteomics	WES
7S1	aIL7R-Mb1 Sh2b3+/-	M	12.14	cranial swelling	μHC-										
7S2	aIL7R Sh2b3 fl/+ Mb1	F	11.28	hunched	μHC-							J558.11; 85%			
7S3	aIL7R Sh2b3 fl/+ Mb1	M	10.14	hind limb paralysis	μHC-							7183.4.6; 77%			
7S4	aIL7R Sh2b3 fl/+ Mb1	F	14.29	hind limb paralysis	μHC-							7183.4.6; 29.1%			
7S5	aIL7R Sh2b3 fl/+ Mb1	M	10	hind limb paralysis	c-kit- VpreB- μHC-							SM7.2.49; 33.3%			
7S6	aIL7R Sh2b3 fl/+ Mb1	F	11.14	forelimb paralysis	c-kit- VpreB- μHC-										
7S7	aIL7R-Mb1 Sh2b3+/-	M	7	cranial swelling	VpreB+ μHC+										
7S8	aIL7R Sh2b3 fl/+ Mb1	F	14	abdominal masses	VpreB+ μHC-										
aIL7R/Ikzf1															
Mouse #	Genotype	Sex	Age (wks)	Condition	Surface phenotype*	Transplanted	Ki-67	Bcl-xl	pFlow	H&E	IgH seq	If Y, dominant clone? (VH and %)	CellTiter-Glo	Phospho-proteomics	WES
7K1	aIL7R Ikzf1 fl/+ CD19	F	9.14	hind limb paralysis	μHC-							J558.72.173; 63%			
7K2	aIL7R Ikzf1 fl/+ CD19	F	9.57	hind limb paralysis	μHC-										
7K3	aIL7R Ikzf1 fl/+ CD19	M	9	thin/hunched	μHC+										
7K4	aIL7R Ikzf1 fl/+ CD19	M	9.28	hunched	μHC-							7183.4.6; 92.7%			
7K5	aIL7R Ikzf1 fl/+ CD19	M	9.28	hunched/bloated	μHC-							7183.4.6; 19.4%			
7K6	aIL7R Ikzf1 fl/+ CD19	F	7.14	runted/bloated	μHC-							Q52.7.18; 49.4%			
7K7	aIL7R Ikzf1 fl/+ CD19	M	6.85	hunched	c-kit+ VpreB+ μHC-										
7K8	aIL7R Ikzf1 fl/+ CD19	F	7.14	runted/hunched	c-kit- VpreB+ μHC-										
7K9	aIL7R Ikzf1 fl/+ CD19	F	11	hunched/poor ambulation	c-kit- VpreB+ μHC+										
7K10	aIL7R Ikzf1 fl/+ CD19	M	6.43	hind limb paralysis	c-kit+ VpreB+ μHC-										
7K11	aIL7R Ikzf1 fl/+ CD19	F	6	>50% GFPhi in peripheral blood	c-kit- VpreB+ μHC+										
7K12	aIL7R Ikzf1 fl/+ CD19	M	7	hind limb paralysis	c-kit+ VpreB+ μHC-										
7K13	aIL7R Ikzf1 fl/+ CD19	F	6	>50% GFPhi in peripheral blood	c-kit- vpreB+ μHC-										
7K14	aIL7R Ikzf1 fl/+ CD19	M	11	hind limb paralysis	VpreB+ μHC-										

*If not listed, the expression status is unknown.

Table II.1. Summary of spontaneous murine leukemias.

Mouse	Genotype	Spine	Brain (meninges)	Liver	Kidney	Lung	Lymph node	Other
7R1	aIL7R-Mb1	3+	wnl	1-2+	wnl	wnl	3+	
7R2	aIL7R-CD19	3+	2+	1+	wnl	wnl	3+	Scapula 3++
7S2	aIL7R SH2B3 fl/+ Mb1	wnl p	wnl	wnl	wnl	wnl	np	
7S3	aIL7R SH2B3 fl/+ Mb1	3+	scant	1+ pv	wnl	wnl	1+	
7S4	aIL7R SH2B3 fl/+ Mb1	3+	wnl	1-2+	wnl	wnl	np	
7K2	aIL7R Ikzf1 fl/+ CD19	1-2+	1+	1+ pv	wnl	wnl	np	
7K4	aIL7R Ikzf1 fl/+ CD19	3+	1+	3+	wnl	wnl	1+ (minimal tissue sample)	
7K8	aIL7R Ikzf1 fl/+ CD19	3+	2+ (poor section)	3++	1+ (scant)	wnl	np	
Littermate control 1 (7S3)	SH2B3 fl/+ Mb1	wnl (see note)	wnl	wnl	wnl	wnl	np	
Littermate control 2 (7K2)	Ikzf1 fl/+ CD19	wnl	wnl	wnl	wnl	wnl	np	

KEY
wnl – within normal limits
pv = perivascular
np - no tissue present

Scale (relative)
1 - mild
2 - moderate
3 - marked

Note - Littermate control 1 bone marrow is hyperplastic, but no evidence of neoplasia.

Table II.2. Summary of aIL7R murine leukemia histopathology.

ALL #	Strain	Kras	Tp53	Cbll1	Notch1	Bcor	Mapk6	Ikzf1	Other lesions
7R4	aIL7R-Mb1	Kras_Q61H	Trp53_N236D						Znrf3_R560S
7R6	aIL7R-CD19								Fmnl1_T797I; Atf6b_H453P; Mavs_C79W; Psmd4_A93T
7S5	aIL7R SH2B3fl/+ Mb1	Kras_A146T		Cbll1_A193T					
7S6	aIL7R SH2B3fl/+ Mb1	Kras_E63K	Trp53_V271F	Cbll1_A193T	Notch1_C449W	Bcor_S1226fs			
7S8	aIL7R SH2B3fl/+ Mb1	Kras_G13V	Trp53_R279H			Bcor_E1229X			Ufl1_G75S
7K7	aIL7R Ikzf1fl/+ CD19	Kras_G12V; Kras_A146T	deletion					deletion	
7K10	aIL7R Ikzf1fl/+ CD19	Kras_E63K						deletion	
7K12	aIL7R Ikzf1fl/+ CD19						Mapk6_E574K	deletion	

Table II.3. aIL7R murine leukemia somatic variants.

Xenograft #	Specimen ID	COG USI	Surface Phenotype	Rearrangement	Major Lesion(s)	Additional Lesions	Ph-like?	B cell pathway lesion description	p53 pathway lesions
1	NL482B	PALJDL	CD38+ CD24+ vpreB-		IL7R L242>FPGVC and SH2B3 e1-2 deletion		Y	PAX5 deletion; VPREB deletion	CDKN2A/B deletion
2	NH362	PALTWS	CD38+ CD24+/- vpreB-	IGH-CRLF2		FLT3 N609ins23aa	N	IKZF1 deletion; PAX5 deletion, homozygous; VPREB deletion	CDKN2A/B deletion; RB1 deletion
3	JH331	PAMDKS	CD38+/- CD24- vpreB-	IGH-CRLF2	JAK2 R683G	KRAS G12D	Y	IKZF1 deletion; PAX5 deletion; VPREB deletion	CDKN2A/B deletion
4	JL491	PAKMVD	CD38+ CD24+ vpreB-		JAK1 S646F	NRAS G12D, PAX5-ELN	Y	PAX5 deletion; RAG1/2 deletion	CDKN2A/B deletion
5	NL482A	PAKYEP	CD38+/- CD24+/- vpreB+	BCR-JAK2			Y	EBF1 deletion; IKZF1 deletion; VPREB deletion	CDKN2A/B deletion
6	NL432	PAKKCA	CD38+ CD24+/- vpreB+	EBF1-PDGFRB			Y	EBF1 deletion; IKZF1 deletion; VPREB deletion	CDKN2A/B deletion
7	NH011	PAKVKK	CD38+ CD24+/- vpreB+	NUP214-ABL1			Y	IKZF1 deletion, S402fs IKZF1 mutation; PAX5 deletion; G24R PAX5 mutation; VPREB deletion	CDKN2A/B deletion
8	PHL3	PANSFD	CD38- CD24- vpreB-	ETV6-ABL1			Y	IKZF1 deletion; PAX5 deletion; RAG1/2 deletion	CDKN2A/B deletion
9	ALL121	N/A	CD38+ CD24+/- vpreB-	IGH-CRLF2	JAK2 R683G		Y		CDKN2A/B deletion
10	ALL4321	N/A		IGH-CRLF2	JAK2 R683G		Y		
11	ALL4364	PAWAKV	CD38+ CD24- vpreB+	P2RY8-CRLF2	JAK2 R683G		Y		

Table II.4. Ph-like ALL patient-derived xenograft models. [Adapted from Roberts KG, *et al. NEJM*. (2014) and Tasian SK, *et al. Blood*. (2017)]

Protein	pY site(s)	Spectral counts		Protein	pY site(s)	Spectral counts
Abi1	Y213	8		Map4k1	Y569	3
Abl2	Y393	4		Mapk1	Y185	23
Ablim1	Y417	2		Mapk14	Y182	140
Actb	Y166	5		Mapk3	Y205	12
Alkbh3	Y127	4		Mapk7	Y221	6
Arhgap27	Y227	39		Mapk8	Y185	2
Btk	Y551	4		Mapk9	Y185	6
Carkd	Y81	2		Mela	Y129	8
Caskin2	Y253	3		Nedd9	Y260	4
Cbl	Y698	25		Pag1	Y224, Y414	30
Cd22	Y857	11		Pik3ap1	Y694	18
Cd244	Y266	3		Pik3r1	Y452, Y580	26
Cd247	Y153	3		Pkm2	Y148	4
Cd5	Y452	2		Plcg2	Y680, Y759	6
Cd79a	Y204	5		Pls3	Y127	18
Cdk16	Y176	4		Prkcd	Y332, Y311	17
Cdk1/2/3	Y15	197		Prmt1	Y309	4
Cep55	Y377	3		Prpf4b	Y849	114
Cfl1	Y68	6		Ptbp1	Y126	10
Cfl2	Y89	12		Ptpn11	Y62, Y580	10
Crkl	Y207	8		Ptpn18	Y381	9
Dapp1	Y139	4		Ptpn6	Y536	47
Dbf4	Y591	2		Ptpra	Y825	29
Ddx20	Y757	2		Ptpre	Y695	6
Dok1	Y450, Y361	17		Ranbp2	Y1349	6
Dok3	Y343	13		Rplp0	Y24	6
Dyrk1a	Y321	21		Rps10	Y12	14
Dyrk4	Y379	7		Sash3	Y189	4
Eef1a2	Y29	8		Setdb1	Y644	4
Eef2	Y443	2		Shmt1	Y28	6
Eno1	Y443	7		Siglecg	Y682	6
Esyt1	Y809	3		Sit1	Y73	5
Fcer1g	Y65	3		Skap2	Y260	7
Fcgr2b	Y326	3		Slamf6	Y319	10
Fes	Y713	4		Slamf7	Y302	10
Fgr	Y196, Y400	16		Snd1	Y109	5
G3bp1	Y125, Y56	10		Snrnp70	Y126	11
Gm6180	Y140	3		Spna2	Y1020	5
Gm6316	Y316	6		Stat3	Y704/5	15
Gmds	Y324	4		Stat5a	Y694	15
Gpx1	Y147	13		Stat5b	Y699	8
Gsk3b	Y216	48		Stk4	Y41	4
Hck	Y50	2		Sykb	Y130, Y202	40
Hipk1	Y352	8		Tjp2	Y1095	4
Hist1h2b	Y43	43		Tnk2	Y518, Y842, Y284	17
Hist1h4	Y51	17		Top1	Y725	2
Hsp90aa1	Y61	3		Top2a	Y804	2
Hsp90ab1	Y484	12		Tyrobp	Y92	6
Ikzf3	Y96	16		Vasp	Y39	5
Itsn2	Y922	28		Vav1	Y844	69
Lck	Y192	61		Vcl	Y692	10
Ldha	Y239	7		Vim	Y53, Y61	5
Lmo7	Y133	3		Was	Y293	13
Lrrc25	Y289	8		Yes1/Src/F	Y424/424/420/394	9
Lyn	Y397	12				

Table II.5. aIL7R murine leukemia tyrosine-phosphorylated peptides identified by DDA.

Mass [m/z]	CS [z]	Polarity	Start [min]	End [min]	NCE	Comment
758.828724	2	Positive	13	20	28	Abl2 LMTGDTY[+79.966331]TAHAGAK (light)
718.318495	3	Positive	18	26	28	Btk HYVVC[+57.021464]STPQSQY[+79.966331]YLAEK (light)
821.847833	2	Positive	17	25	28	Btk YVLDDEY[+79.966331]TSSVGSK (light)
798.086794	3	Positive	25	34	28	Cbl IKPSSSANAIY[+79.966331]SLAARPLPMPK (light)
873.902366	4	Positive	16	24	28	Cbl LPPGEQGESEEDTEY[+79.966331]MTPTSRPVGVQKPEPK (light)
1083.175775	3	Positive	20	29	28	Cd19 VTPPSGNGTQNQY[+79.966331]GNVLSLPTSTSGQAHAQR (light)
811.719716	3	Positive	24	32	28	Cd79a GLQGTY[+79.966331]QDVGNLHIGDAQLEKP (light)
673.277477	2	Positive	18	26	28	Cdk3-ps IGEGT[+79.966331]Y[+79.966331]GVVYK (light)
630.784642	2	Positive	15	23	28	Fcer1g ADAVY[+79.966331]TGLNTR (light)
719.623412	3	Positive	15	24	28	Fcgr2b HPEALDEETEHDY[+79.966331]QNHI (light)
751.829778	2	Positive	20	29	28	Fes EEADGIY[+79.966331]AASAGLR (light)
799.35779	3	Positive	32	36	28	Fes ISDFGMSREEADGIY[+79.966331]AASAGLR (light)
670.300125	2	Positive	19	27	28	Fgr LDTGGY[+79.966331]YITTR (light)
738.6875	3	Positive	16	28	28	Fgr LIEDNEY[+79.966331]NPQQGTKFPIK
681.281409	2	Positive	17	25	28	Gsk3b GEPNVSY[+79.966331]IC[+57.021464]SR (light)
707.318515	2	Positive	17	25	28	Hck GPVY[+79.966331]VPDPTSSSK (light)
595.964715	3	Positive	22	32	28	Ikzf1 SGLIY[+79.966331]LTNHINPHAR (light)
537.902787	3	Positive	18	26	28	Ikzf3 EYSDY[+79.966331]ESIKLER (light)
716.816474	2	Positive	24	32	28	Lck NLDNGGFY[+79.966331]ISPR (light)
1061.953892	2	Positive	37	49	28	Lck SVLDDFFTATEGQY[+79.966331]QPQP (light)
711.308481	2	Positive	18	28	28	Lyn SLDNGGYY[+79.966331]ISPR (light)
645.274107	2	Positive	10	20	28	Lyn VIEDNEY[+79.966331]TAR (light)
768.650512	3	Positive	22	32	28	Mapk1 VADPDHDHTGFLT[+79.966331]EY[+79.966331]VATR (light)
777.994279	3	Positive	22	32	28	Mapk3 IADPEHDHTGFLT[+79.966331]EY[+79.966331]VATR (light)
724.334499	2	Positive	17	25	28	Pik3ap1 VEFGVY[+79.966331]ESGPRK (light)
548.918772	3	Positive	10	20	28	Pik3r1 KLHEY[+79.966331]NTQFQEK (light)
554.928502	3	Positive	27	36	28	Pik3r1 TRDQY[+79.966331]LMWLTQK (light)
922.391362	2	Positive	21	31	28	Plcg2 MY[+79.966331]VDPSEINPSMPQR (light)
896.394231	2	Positive	27	37	28	Plcg2 NPGFY[+79.966331]VEANPMPTFK (light)
908.377289	2	Positive	19	29	28	Ptpn11 IQNTGDY[+79.966331]YDLYGGEK (light)
930.911831	2	Positive	19	29	28	Ptpn6 GQESEY[+79.966331]GNITYPPAVR (light)
832.361423	3	Positive	15	23	28	Stat3 YC[+57.021464]RPESQEHPEADPGAAPY[+79.966331]LK (light)
649.331228	2	Positive	12.5	21.5	28	Stat5a AVDGY[+79.966331]VKPQIK (light)
635.315578	2	Positive	12	20	28	Stat5b AADGY[+79.966331]VKPQIK (light)
657.631185	3	Positive	22	30	28	Sykb ARDNSGSY[+79.966331]ALC[+57.021464]LLHEGK (light)
920.410108	3	Positive	22.5	33.5	28	Sykb EALPMDTEVYESPY[+79.966331]ADPEEIRPK (light)
622.307753	2	Positive	17	26	28	Sykb ENLIREY[+79.966331]VK (light)
1096.841845	3	Positive	22	31	28	Sykb KPAPPQGSRPESTVSFNPY[+79.966331]EPTGGPWGPDR (light)
1119.424111	2	Positive	37	53	28	Vav1 IGWFPSNYVEEDYSEY[+79.966331]C[+57.021464] (light)
652.281932	2	Positive	11	21	28	Yes1 LIEDNEY[+79.966331]TAR (light)

Table II.6. aIL7R murine leukemia tyrosine-phosphorylated peptide isolation list.

Mass [m/z]	CS [z]	Polarity	Start [min]	End [min]	NCE	Comment
508.89297	3	Positive	12	19	28	ABL1 LMTGDTY[+80.0]TAHAGAK (heavy)
506.22157	3	Positive	12	19	28	ABL1 LMTGDTY[+80.0]TAHAGAK (light)
557.26194	3	Positive	16	22	28	ABL1 NKPTVY[+80.0]GVSPNYDK (heavy)
554.59054	3	Positive	16	22	28	ABL1 NKPTVY[+80.0]GVSPNYDK (light)
756.83909	2	Positive	15	21	28	BLK IIDSEY[+80.0]TAQEGAK (heavy)
752.83199	2	Positive	15	21	28	BLK IIDSEY[+80.0]TAQEGAK (light)
1108.5114	2	Positive	97	109	28	BTK VVALYDYMPMNANDLQLR (heavy)
1103.5073	2	Positive	97	109	28	BTK VVALYDYMPMNANDLQLR (light)
825.85493	2	Positive	23	32	28	BTK YVLDDEY[+80.0]TSSVGSK (heavy)
821.84783	2	Positive	23	32	28	BTK YVLDDEY[+80.0]TSSVGSK (light)
820.7302	3	Positive	96	108	28	CARKD IGVVGGCQEYTGAPYFAAISALK (heavy)
818.0588	3	Positive	96	108	28	CARKD IGVVGGCQEYTGAPYFAAISALK (light)
790.10084	3	Positive	55	70	28	CBL IKPSSSANAIY[+80.0]SLAARPLPVPK (heavy)
787.42944	3	Positive	55	70	28	CBL IKPSSSANAIY[+80.0]SLAARPLPVPK (light)
596.31169	2	Positive	42	55	28	CD19 GILY[+80.0]AAPQLR (heavy)
591.30756	2	Positive	42	55	28	CD19 GILY[+80.0]AAPQLR (light)
807.0593	3	Positive	72	86	28	CD79A GLQGTY[+80.0]QDVGSLNIGDVQLEKP (heavy)
804.3879	3	Positive	72	86	28	CD79A GLQGTY[+80.0]QDVGSLNIGDVQLEKP (light)
630.29359	2	Positive	26	37	28	CDK5 IGEGTY[+80.0]GTVFK (heavy)
626.28649	2	Positive	26	37	28	CDK5 IGEGTY[+80.0]GTVFK (light)
556.26191	3	Positive	42	54	28	GAB1 APSASVDSSLY[+80.0]NLPR (heavy)
552.92582	3	Positive	42	54	28	GAB1 APSASVDSSLY[+80.0]NLPR (light)
640.80432	2	Positive	17	24	28	GAB1 VDY[+80.0]VVVDQQK (heavy)
636.79722	2	Positive	17	24	28	GAB1 VDY[+80.0]VVVDQQK (light)
686.28554	2	Positive	19	31	28	GSK3B GEPNVSY[+80.0]IC[+57.0]SR (heavy)
681.28141	2	Positive	19	31	28	GSK3B GEPNVSY[+80.0]IC[+57.0]SR (light)
650.27824	2	Positive	11	20	28	HCK VIEDNEY[+80.0]TAR (heavy)
645.27411	2	Positive	11	20	28	HCK VIEDNEY[+80.0]TAR (light)
565.2747	2	Positive	31	44	28	INPPP5D EKLYDFVK (heavy)
561.2676	2	Positive	31	44	28	INPPP5D EKLYDFVK (light)
563.918	3	Positive	20	32	28	IZKF3 EYNEYENIKLER (heavy)
560.5819	3	Positive	20	32	28	IZKF3 EYNEYENIKLER (light)
494.6953	2	Positive	18	26	28	JAK1 GMDY[+80.0]LGSR (heavy)
489.69117	2	Positive	18	26	28	JAK1 GMDY[+80.0]LGSR (light)
639.97435	3	Positive	49	60	28	JAK2 EVGDY[+80.0]GQLHETEVLLK (heavy)
637.30295	3	Positive	49	60	28	JAK2 EVGDY[+80.0]GQLHETEVLLK (light)
652.2819	2	Positive	13	26	28	LCK LIEDNEY[+80.0]TAR (light)
657.2861	2	Positive	13	26	28	LCK LIEDNEY[+80.0]TAR (heavy)
461.22494	3	Positive	15	23	28	LYN TIY[+80.0]VRDPTSNK (heavy)
458.55354	3	Positive	15	23	28	LYN TIY[+80.0]VRDPTSNK (light)
771.9866	3	Positive	40	54	28	MAPK1 VADPDHDHTGFLT[+80.0]EY[+80.0]VATR (heavy)
768.65051	3	Positive	40	54	28	MAPK1 VADPDHDHTGFLT[+80.0]EY[+80.0]VATR (light)
781.33037	3	Positive	43	56	28	MAPK3 IADPEHDHTGFLT[+80.0]EY[+80.0]VATR (heavy)
777.99428	3	Positive	43	56	28	MAPK3 IADPEHDHTGFLT[+80.0]EY[+80.0]VATR (light)
707.8207	2	Positive	13.4	21	28	PECAM1 DTETVY[+80.0]SEVRK (heavy)
703.8136	2	Positive	13.4	21	28	PECAM1 DTETVY[+80.0]SEVRK (light)
649.2942	3	Positive	27	39	28	PIK3AP1 SQERPGNFYVSSESIR (heavy)
645.9581	3	Positive	27	39	28	PIK3AP1 SQERPGNFYVSSESIR (light)
626.6235	3	Positive	36	49	28	PIK3CD GSGELYEHEKDLVWK (heavy)
623.9521	3	Positive	36	49	28	PIK3CD GSGELYEHEKDLVWK (light)
464.87268	3	Positive	9	17	28	PIK3CD RGSGELY[+80.0]EHEK (heavy)
462.20128	3	Positive	9	17	28	PIK3CD RGSGELY[+80.0]EHEK (light)
623.9396	3	Positive	19	31	28	PIK3R1 SREYDRLY[+80.0]EEYTR (heavy)
620.6035	3	Positive	19	31	28	PIK3R1 SREYDRLY[+80.0]EEYTR (light)
527.2181	2	Positive	14	22	28	PIK3R1 LY[+80.0]EEYTR (light)
532.2222	2	Positive	14	22	28	PIK3R1 LY[+80.0]EEYTR (heavy)
636.28078	2	Positive	26	38	28	PLCG2 DINSLY[+80.0]DVSR (heavy)
631.27665	2	Positive	26	38	28	PLCG2 DINSLY[+80.0]DVSR (light)
567.918	3	Positive	30	40	28	PLCG2 IGTAEPDY[+80.0]GALYEGR (heavy)
564.5819	3	Positive	30	40	28	PLCG2 IGTAEPDY[+80.0]GALYEGR (light)
826.37075	2	Positive	16	25	28	PRAG1 EATQPEPIY[+80.0]AESTK (heavy)
822.36365	2	Positive	16	25	28	PRAG1 EATQPEPIY[+80.0]AESTK (light)
682.30828	3	Positive	27	38	28	PRKCD RSDSASSEPVGIY[+80.0]QGFEK (heavy)
679.63688	3	Positive	27	38	28	PRKCD RSDSASSEPVGIY[+80.0]QGFEK (light)

912.38439	2	Positive	32	43	28	PTPN11 IQNTGDY[+80.0]YDLYGGEK (heavy)
908.37729	2	Positive	32	43	28	PTPN11 IQNTGDY[+80.0]YDLYGGEK (light)
762.85402	2	Positive	21	32	28	PTPN11 VY[+80.0]ENVGLMQQQK (heavy)
758.84692	2	Positive	21	32	28	PTPN11 VY[+80.0]ENVGLMQQQK (light)
546.5985	3	Positive	18	27	28	PTPN18 SAEEAPLYSKVTPR (heavy)
543.2624	3	Positive	18	27	28	PTPN18 SAEEAPLYSKVTPR (light)
936.9019	2	Positive	31	45	28	PTPN6 GQESEYGNITYPPAMK (heavy)
932.8948	2	Positive	31	45	28	PTPN6 GQESEYGNITYPPAMK (light)
534.2464	3	Positive	9	18	28	PTPN6 HKEDVYENLHTK (heavy)
531.575	3	Positive	9	18	28	PTPN6 HKEDVYENLHTK (light)
992.44498	2	Positive	64	79	28	SHC1 ELFDDPSY[+80.0]VNVQNLDK (heavy)
988.43788	2	Positive	64	79	28	SHC1 ELFDDPSY[+80.0]VNVQNLDK (light)
864.0435	3	Positive	17	26	28	STAT3 YCRPESQEHPEADPGSAAPYLK (heavy)
861.3721	3	Positive	17	26	28	STAT3 YCRPESQEHPEADPGSAAPYLK (light)
653.33833	2	Positive	15	23	28	STAT5A AVDGY[+80.0]VKPQIK (heavy)
649.33123	2	Positive	15	23	28	STAT5A AVDGY[+80.0]VKPQIK (light)
848.69696	3	Positive	61	73	28	SYK EALPMDTEVY[+80.0]ESPYADPEEIR (heavy)
845.36087	3	Positive	61	73	28	SYK EALPMDTEVY[+80.0]ESPYADPEEIR (light)
823.03634	3	Positive	74	91	28	SYK QESTVSFNPY[+80.0]EPELAPWAADK (heavy)
820.36494	3	Positive	74	91	28	SYK QESTVSFNPY[+80.0]EPELAPWAADK (light)
811.34728	2	Positive	18	27	28	TEC YVLDDQY[+80.0]TSSSGAK (heavy)
807.34018	2	Positive	18	27	28	TEC YVLDDQY[+80.0]TSSSGAK (light)
655.77567	2	Positive	11	21	28	TYK2 AVPEGHEY[+80.0]YR (heavy)
650.77154	2	Positive	11	21	28	TYK2 AVPEGHEY[+80.0]YR (light)
478.72746	2	Positive	21.5	31.5	28	YES1 GAY[+80.0]SLSIR (heavy)
473.72333	2	Positive	21.5	31.5	28	YES1 GAY[+80.0]SLSIR (light)

Table II.7. Ph-like ALL PDX tyrosine-phosphorylated peptide isolation list.

II.3 **Discussion**

To date, preclinical modeling of Ph-like ALL has been performed predominantly using cell lines or patient-derived xenografts implanted into immunodeficient animals. While these models have contributed substantively to the understanding of Ph-like ALL, each have limitations (*i.e.* cell passage limits, lack of an immune-competent tumor microenvironment, etc.) that may impact translation. Here, we report a new activated *IL7R* GEMM as a model of human Ph-like ALL and other leukemia subtypes and demonstrate that B cell-intrinsic expression of aIL7R is sufficient to initiate B-ALL in mice. Importantly, the resultant leukemias reproducibly acquire mutations in oncogenes and tumor suppressors commonly associated with Ph-like ALL. Furthermore, concomitant heterozygous loss of *Sh2b3* or co-expression of a dominant-negative *Ikzf1* variant that frequently occur in human ALL markedly increased leukemia penetrance. Notably, our GEMM effectively mirrors key signaling programs in human *IL7R*-mutant ALL, including constitutive STAT5 and mTOR signaling, as well as a unique BCR-like signaling program despite absence of surface pre-BCR, which resulted in rapid, penetrant, and spontaneous disease in immune-

competent animals. Finally, based on our initial *in vitro* and *in vivo* studies, we predict that this preclinical aIL7R GEMM can effectively model candidate therapeutic interventions in an immune-competent setting and is representative of this high-risk human B-ALL subtype.

Leukemogenic potential has previously been described for primary murine hematopoietic cells or lymphoid progenitors overexpressing aIL7R mutant proteins following adoptive transfer into immunocompromised mice[17, 49, 86]. In these studies, mutant *IL7R*, alone or in combination with those in *NRAS* or *NOTCH1*, led to T-cell ALLs, myeloproliferative disorders, or IgM^+ B cell lymphomas[49, 86]. More recently, Geron *et al*. has demonstrated a similar leukemogenic potential for human hematopoietic progenitors overexpressing the PPCL mutant version of IL-7R[46]. In contrast, our study provides the first demonstration that B lineage-restricted expression of aIL7R at or below endogenous IL-7R levels is sufficient to initiate B-ALL in primary B cell progenitor cells. We speculate that leukemic transformation in the aIL7R model requires aIL7R-induced signaling and stereotypical secondary genetic hits. While additional work is needed to determine how *SH2B3* or *IKZF1* deletions specifically contribute to disease, our genetic studies demonstrate that some acquired lesions in aIL7R leukemias appear genotype-specific with aIL7R/Ikzf1 leukemias consistently exhibiting total loss of functional *Ikzf1*. Our findings showing co-occurrence of mutant *Trp53* in primary aIL7R/Sh2b3 leukemias also provide direct demonstration of previously-modeled synergistic impacts of Sh2b3 and Tp53 in mouse cancer mortality[56]. These observed genomic landscapes suggest that although aIL7R-Mb1/-CD19, aIL7R $Sh2b3^{fl/+}$ Mb1, and aIL7R $Ikzf1^{fl/+}$ CD19 animals all develop B-ALL, their journey to leukemia transformation may indeed be quite distinct.

In addition to associated genetic alterations, we predict that active IL-7R signaling may additionally play a direct role in ALL progression. Prior to disease, the pro-B cell expansion observed in aIL7R mice mirrors the effects of *in vivo* exogenous IL-7 administration to wildtype animals[87-89]. IL-7 hypersensitivity of pre-leukemic B cells and preferential expansion at the expense of normal progenitor cells has been reported by several groups[56, 90-92]. IL-7R has also been shown to be required for the leukemogenesis of BCR-ABL1-transduced murine pre-B cells *in vivo*, while IL-7 can diminish the inhibitory effect of

dasatanib treatment on similarly derived BCR-ABL1^{+} leukemogenic cells *in vitro*[93, 94]. Indeed, our *in vitro* cytokine stimulation studies using both aIL7R mouse leukemias and Ph-like ALL PDX cells suggest that endogenous IL-7 may provide an important survival signal for Ph-like leukemogenesis and maintenance. However, our limited studies of *in vivo* IL-7 antibody blockade did not appreciably affect leukemia proliferation in either our aIL7R mouse or human PALJDL models. Notably, recent work by Abdelrasoul *et al*. demonstrated a suppressive effect of *in vivo* IL-7 receptor blockade on BCR-ABL1^{+} xenograft models[94]. These findings suggest that combinatorial therapy using anti-IL-7/IL-7R in association with an additional target pathway may be a valuable next step in preclinical studies.

Ph-like ALL is characterized by a kinase-activated gene expression profile driven by JAK/STAT, PI3K pathway, and other signaling networks. Strikingly, our quantitative phospho-proteomic analyses independently identified multiple canonical "BCR-like" effectors in all aIL7R mouse leukemias and in our human *IL7R*-mutant/*SH2B3*-deleted and several other primary Ph-like ALL PDX models. Our findings are concordant with recent studies by Hurtz and colleagues, who reported BCR-like activation in *CRLF2*-rearranged Ph-like ALL cell lines and PDX cells lacking μHC surface expression via orthogonal transcriptional analysis and targeted immunoblotting to support the concept that BCR-like signaling was orchestrated via CD79A/B and SRC family kinases[85]. Upstream events mediating the BCR-like signaling program in aIL7R Ph-like and other leukemias remain to be determined; however, alternative non-BCR pathway proteins potentially capable of scaffolding Syk activation include integrins, C-type lectins, Fc or complement receptors (reviewed in [95]), and the surrogate light chain-only pro-BCR complex[75, 77]. Integrins comprise an important candidate, as large pre-B cells from Ikzf1$^{fl/fl}$ CD19 mice have enhanced expression of integrins α5, α6, and activated β1, and show an increase in FAK activation[72]. While technically challenging, it will also be important to determine whether this BCR-like program is active in aIL7R-expressing progenitors prior to overt disease development, or whether this phenomenon is a feature of transformation and/or secondary mutation acquisition. Regardless, consistent with recent data in *CRLF2*-rearranged Ph-like ALL[85] and *KMT2A*-rearranged infant B-ALL[96], our results suggest that targeting this

BCR-like program with Syk inhibitors (in parallel with other pathway agents) could potentially provide therapeutic benefit for aIL7R leukemias *in vivo* in preclinical models and in patients.

In summary, our aIL7R GEMM provides the first definitive demonstration of the leukemia-initiating role of aIL7R, a robust new platform for detailed and iterative investigation of combinatorial therapies to treat primary aIL7R B-ALL, and a system for identifying additional biochemical and genetic events that facilitate B cell leukemic transformation, growth, and survival. Our inducible strain should further permit analogous lineage-restricted modeling of other aIL7R-driven leukemias, including T-ALL.

II.4 **Methods**

Cell lines

Nalm6 (human pre-B; ATCC) and Ba/F3 (murine pro-B; Immunex, Seattle, WA, USA) cells were maintained in RPMI-1640 (HyClone) supplemented with 10% fetal calf serum (Omega Scientific), 1X GlutaMAX (Invitrogen), 20 mM N-2-hydroxyethylpiperazine-N'-2-ethanesulfonic acid (HEPES), 55 μm 2-mercaptoethanol (2ME; GIBCO), sodium pyruvate, and 10 ng/mL recombinant murine IL-3 (mIL-3 – Ba/F3 only; R&D Systems). Nalm6 cells were validated by surface immunophenotyping. Ba/F3 cells were authenticated by their inability to grow in the absence of murine IL-3.

Ba/F3 assays

Parental Ba/F3 cells were transduced with pRRL-MND-2A-mCherry lentiviral vectors containing WT or mutant murine *Il7r* (Il7r_P243insPPCL) followed by a self-cleaving T2A-linked mCherry reporter. Transduction efficiency (%mCherry+) was measured after 4 days. For assessment of cytokine independence, parental, Il7r_WT, and Il7r_PPCL Ba/F3 cells were subjected to mIL-3 withdrawal for 6 days. Cell counts, viability, and %mCherry+ were quantified at days 3 and 6.

Patient-derived xenografts

Secondary Ph-like ALL xenograft samples were provided by S. Tasian (Children's Hospital of Philadelphia, Philadelphia, PA). 1e06 splenocytes were injected retro-orbitally (r.o.) into NOD.Cg-*Prkdc*^{scid} *Il2rg*^{tm1Wjl}/SzJ (NSG) animals. Leukemia burden (% hCD19^{+}) was assessed biweekly by flow cytometric analysis of peripheral blood. Recipient animals were euthanized when ill according to standard parameters set on the IACUC protocol.

Animals

Murine Il7r_P243insPPCL coding region was cloned into the pRosa26-DEST vector (Gateway) with an upstream loxp-flanked 3×-stop codon and a downstream self-cleaving T2A linked GFP reporter. This targeting vector was then inserted into the *Rosa26* locus via homologous recombination after electroporation into C57BL6/J ES cells (Biocytogen). These activated Il7r "aIL7R" mice were crossed to Mb1-Cre[97] and CD19-Cre[98] mice. aIL7R-Mb1 mice were also crossed to Sh2b3 knockout and floxed mice[73] and aIL7R mice were crossed to B-intrinsic Ikzf1 exon 5 floxed animals[72]. NSG (005557), Mb1-Cre (020505), CD19-Cre (006785), and C57BL/6J (000664) mice were purchased from Jackson Laboratories. All mice were bred and maintained in a specific pathogen-free animal facility, and studies were performed in accordance with the Institutional Animal Care and Use Committee (IACUC) of Seattle Children's Research Institute. Mice were sorted into experimental groups based on genotype and matched for age and sex. Experimental groups were co-housed whenever possible. aIL7R and littermate mice used for immunophenotyping, cell cycle analysis, phospho-Stat5 assays, and *in vivo* IL-7 blockade were 6-11 weeks old. aIL7R mice were monitored for signs of spontaneous disease and were euthanized when ill according to standard parameters set on the IACUC protocol.

Reagents and antibodies

The LIVE/DEAD Fixable Near-IR Dead Cell Stain Kit (Invitrogen) was used according to the manufacturer's instructions. Anti-mouse and anti-human antibodies used in the study are described in detail below in Table II.8.

Mouse antibodies	Clone	Vendor	Catalog #	Lot #
PE anti-mouse IgD	11-26	Southern Biotech	1120-09	G0815-TF35R
Biotin Rat Anti-Mouse CD43	S7	BD	553269	7257995
PE-Cy7 anti human / mouse B220	RA3-6B2	BioLegend	103222	B270362
PE-Cy7 anti-mouse CD19	1D3	BD	552854	0009122
Pacific Blue anti-mouse CD24	M1/69	BioLegend	101820	B271348
Alexa 700 Streptavidin		Thermo Fisher	S21383	2047151
PE-Cy7 anti-mouse CD23	B3B4	BioLegend	101614	B259283
APC anti-mouse CD21	7 E9	BioLegend	123412	B210793
PerCP-Cy5.5 anti-mouse B220	RA3-6B2	BioLegend	103236	B285069
IgM Rat anti-Mouse, PerCP-eFluor™ 710	II/41	Thermo Fisher	46-5790-82	2185098
Brilliant Violet 605 anti-mouse CD19	6D5	BioLegend	115540	B289096
Biotin anti-mouse LY-51 / BP-1	6C3	BioLegend	108304	B193235
PE anti-mouse LY-51 / BP-1	6C3	BioLegend	108308	B297470
PE anti-mouse CD179a (VpreB)	R3	BioLegend	143604	B195300
PE-Cy7 anti-mouse IgD	11-26C	Thermo Fisher	25-5993-82	4323733
EF 660 anti-mouse CD127 / IL-7Ra	A7R34	Thermo Fisher	50127182	1919524
BV 510 anti-mouse/human CD45R/B220	RA3-6B2	BioLegend	103247	B260375
APC Rat Anti-Mouse CD43	S7	BD	560663	9017742
Purified Rat Anti-Mouse CD16/CD32 (Mouse BD Fc Block™)	2.4G2	BD	553142	148675
PE anti-mouse CD117 (c-kit)	2B8	Thermo Fisher	12-1171-82	E028962
Intracellular/Intranuclear antbodies				
Alexa Fluor® 647 Mouse Anti-Stat5 (pY694)	47/Stat5 (pY694)	BD	612599	9192735
Phospho-S6 Ribosomal Protein (Ser235/236) XP® Rabbit m	(D57.2.2E)	Cell Signaling Tech	4851S	26
Phospho-4E-BP1 Rabbit mAb	236B4	Cell Signaling Tech	5123S	8
PE anti-human/mouse Bcl-xL	54H6	Cell Signaling Tech	13835S	8
eFluor 660 anti-mouse Ki-67	SolA15	Thermo Fisher	501124387	1977755
Human antibodies				
FITC anti-human CD38	T16	Beckman Coulter	IM0775U	61
bv605 anti-human CD24	ML5	BioLegend	311123	B196581
APC anti-human CD10	HI10a	BioLegend	312210	B246897
PE anti-human CD179a (VpreB)	HSL96	BioLegend	347404	B209133
PE-Cy7 anti-human CD19	HIB19	BioLegend	302216	B278096
Pacific Blue anti-human IgM	MHM-88	BioLegend	314514	B223924
Alexa Fluor647 anti-human IL7Ra (CD127)	A019D5	BioLegend	351318	B220642
Fc Receptor Binding Inhibitor Polyclonal Antibody		Thermo Fisher	501129053	2075565
In vivo antibodies				
InVivoMAb anti-mouse/human IL-7	M25	Bio X Cell	BE0048	648417M1
InVivoMAb mouse IgG2b isotype control	MPC-11	Bio X Cell	BE0086	645417J3

Table II.8. Antibodies used in this study.

Flow cytometric and cell cycle analysis

Single-cell suspensions of peripheral blood, spleen, and BM were obtained and stained with fluorescently-labeled antibodies as previously described[99]. Transcription factor labeling was performed following surface staining for 20 min at 4°C by using the True-Nuclear Transcription Factor Buffer Set (BioLegend) according to the manufacturer's instructions. For Ki-67 staining, cells were fixed for 30 min at 4°C with

fixation/permeabilization solution (BD Biosciences), followed by staining with Ki-67 under the same conditions. All flow cytometric data were collected on an LSR II (BD) and analyzed by using FlowJo software (TreeStar).

Cell cycle analysis using in vivo EdU labeling

In vivo EdU labeling for cell cycle analysis was performed as previously described[100]. Briefly, 5-ethynyl-2'-deoxyuridine (EdU, Thermo Fisher) was dissolved in sterile DMSO and 1mg in a volume of 100ul was injected i.p. 1 hr prior to sacrifice. EdU detection was performed with the Click-iT Plus EdU Pacific Blue Flow Cytometry Assay Kits (Thermo Fisher). Cells are stained for surface markers for 15min at 4℃, followed by fixation and incubation with the Click-iT Plus reaction cocktail according to manufacturer's instructions.

In vitro cytokine stimulations and Phospho-flow analysis

Mouse splenic B cells were enriched using CD43 depletion (Miltenyi) and purified B cells were cultured in supplemented RPMI-1640 at 37°C. B cells were seeded at 5e05 cells/well in a 96-well plate with or without recombinant murine IL-7 (mIL-7)[101] (25 ng/mL) for 25 mins and fixed with 2% PFA in PBS for 10 min at 37°C. Cells were resuspended in cold Perm Buffer III (BD Biosciences) and stained with surface and phospho-site antibodies for 35 min at 4°C in the dark. For *ex vivo* aIL7R leukemia analysis, 1e06 cells harvested from BM and spleen were directly fixed, permeabilized, and stained as above for phospho-flow analysis. Mouse bone marrow late pro-B cells were FACS-sorted into 96 well plates at a density of 1.5e04 cells/well in supplemented RPMI-1640 medium, rested for 2 hours at 37°C and stimulated with mIL-7 (10 ng/mL) for 25 mins. Cells were then fixed, permeabilized, and stained for phospho-flow analysis

Il7r_WT and Il7r_PPCL expressing Ba/F3 cells cells were sorted on mCherry expression and maintained in supplemented RPMI-1640 with 10 ng/mL mIL-3. Cells were washed to remove cytokine, starved for 5 hours, stimulated with 10 ng/mL mIL-7 or 10 ng/mL mIL-3 for 20mins, fixed and stained for phospho-flow analysis.

For human xenografts, splenocytes from NSG recipients were plated at a density of 5e05 cells/well in a 96-well plate in supplemented RPMI-1640 with or without recombinant human IL-7 (PeproTech) or human TSLP (R&D Systems) (10 ng/mL) for 25 mins at 37°C. Cells were then fixed, permeabilized, and stained for phospho-flow analysis.

Histopathology

Tissues were fixed in 10% neutral buffered formalin, embedded in paraffin, and tissues sections stained with Hematoxylin and eosin (H&E) according to standard practices. Histology images were acquired using a Nikon OptiPhot-2 microscope and a Canon Eos 5D Mark II camera. Tissue sections were examined by a board-certified veterinary pathologist (H.D.L.) who was blinded to study design.

Igh sequencing

Murine *Igh* gene transcripts were amplified from leukemic splenocyte cDNA as described previously, using only the first round PCR of the nested PCR strategy[102]. Amplified sequences were purified using the NucleoSpin Gel & PCR Cleanup Kit (Macherey-Nagel), cloned into pJET1.2 plasmid DNA using the CloneJET PCR Cloning Kit (Thermo Fisher Scientific) and Sanger sequencing of individual transformed bacterial colonies was performed using the pJET1.2 forward and reverse sequencing primers. 96 colonies were sequenced per leukemia sample.

Exome sequencing and analysis

Genomic DNA (gDNA) from sorted primary aIL7R leukemia samples (spleen) and paired tail gDNA was submitted for whole exome sequencing using Twist Mouse Exome Panel with paired end 100bp NGS reads on NovaSeq (Illumina). FASTQ files were aligned using BWA to mm10 reference mouse genome. Unique leukemia somatic variants were identified by either Mutect2[103] or Pisces[104]. Mutect2 variants were subsequently filtered using FilterMutectCalls and annotated using ANNOVAR[105]. Pisces variants in the tumor sample were annotated using ANNOVAR and then filtered for coverage and if present in more than

one read in the normal sample. Variants were visualized using Integrated Genome Viewer (IGV; Broad Institute).

aIL7R leukemia serial transfer studies

1e06 splenocytes from aIL7R animals with spontaneous disease were injected r.o. into C57BL/6 mice. Leukemic burden was assessed biweekly by flow cytometric analysis of peripheral blood. Recipient animals were euthanized when ill according to IACUC protocol.

In vivo IL-7 blockade and kinase inhibitor treatment

aIL7R Sh2b3$^{fl/+}$ Mb1 and cre-negative littermate control mice were treated i.p. with 0.5 mg/mouse isotype control or neutralizing anti-IL-7 mAb (Bio X Cell) every third day for 16 days (6 injections) and sacrificed on day 18. For murine leukemias, B6 recipient mice were pre-treated i.p. with isotype or anti-IL-7 every other day for 6 days (3 injections), then injected r.o. with 1e06 splenocytes from primary aIL7R/Sh2b3 leukemias. Recipient mice were treated every other day with isotype or anti-IL-7 until they met euthanasia criteria.

NSG mice were injected r.o. with 1e06 IL-7Rins/SH2B3null (PALJDL) PDX cells transduced to express a firefly luciferase-eGFP fusion protein (ffluc-GFP; gift from Michael Jensen). *In vivo* bioluminescent imaging of PALJDL-ffluc-GFP cells was performed as previously described[106] using an IVIS Spectrum Imager (PerkinElmer). 8 days post-injection (after leukemic cells were detectable by bioluminescent imaging), mice were injected i.p. with 0.5 mg/mouse isotype or anti-IL-7, or with 0.1 mg/kg rapamycin (Selleck Chemicals) as a positive control. Mice were treated every other day for 8 weeks and *in vivo* bioluminescent imaging was used ~2x weekly to track leukemia burden over time. All animals were sacrificed on day 58.

1e06 aIL7R primary leukemia cells were injected r.o. into C57BL/6 recipient mice. Three days later, recipients were treated by gavage with 5 mg/kg rapamycin or vehicle (5% dextrose in water) daily (Mon-

Fri) for up to 4 weeks or until euthanasia. Leukemic burden was assessed weekly by flow cytometric analysis of peripheral blood.

For testing entospletinib and dasatanib treatments, NSG mice were injected r.o. with 1e06 IL-7Rins/SH2B3null (PALJDL) PDX cells. When >1% hCD10+/hCD19+ were detectable in the peripheral blood, recipient animals were assigned to their treatment group (vehicle chow, 0.05% entospletinib chow (Gilead), or 10mg/kg dasatanib by oral gavage) and treated daily for 4 weeks. Mice were bled weekly to track leukemia burden (hCD10+ hCD19+) over time and then sacrificed after the 4 weeks of treatment.

In vitro drug sensitivity assay

Splenocytes from primary or secondary leukemic animals were plated in supplemented RPMI-1640 with 10 ng/mL mIL-7 in 96 well plates at a density of 5e04 cells/well. Cells were cultured for 24 hours with or without ruxolitinib, rapamycin, bortezomib, entospletinib, ibrutinib, idelalisib (Selleck Chemicals), or trametinib (Cayman Chemical). Inhibitors were tested at a 10-fold dilution curve ranging from 10 uM to 100 pM or 1 uM to 10 pM (Bortezomib). Viability of cells was measured at 24 and 48 hours by adding 10 uL of CellTiter-Glo reagent (Promega) per well and incubating for 10 mins with shaking at room temperature (RT) before luminescence is recorded. Luminescence was read by using a SpectraMax i3x microplate reader (Molecular Devices).

Mass spectrometry-based phosphoproteomic analysis

Secondary murine aIL7R leukemias were harvested *ex vivo* from spleen and plated into 10 cm dishes at a density of 1e07 cells/mL. Cells were incubated at 37°C with or without 1 uM entospletinib or ruxolitinib (Selleck Chemicals) for 30 mins, and then with or without 10 ng/mL mIL-7 for an additional 15 mins. Cells were harvested, washed with 1X PBS (HyClone), and lysed. For Ph-like PDX models, cells were harvested *ex vivo* from spleen and 1e08 cells/sample were directly lysed.

Cell pellets were lysed in 8M Urea containing phosphatase inhibitors and sonicated. Protein concentration was then determined by a BCA assay (Pierce). 1-2 mg of each sample was reduced with 5 mM DTT at 56 °C for 45 minutes, then alkylated with 15 mM iodoacetamide for 30 minutes at RT in the dark. Samples were diluted 4-fold with 100 mM ammonium acetate, pH 8.9, and digested with Lysyl endopeptidase (Lys-C, from Wako) for 4 hours at RT at a ratio of 1:100 (Lys-C to total protein), followed by sequencing grade modified trypsin (Promega) at a ratio of 1:100 (trypsin to total protein), overnight at room temperature. Following digestion, peptides were desalted and concentrated using Sep-Pak Plus C18 cartridges (Waters) according to the manufacturer's recommendations. Samples were then dried by vacuum centrifugation, lyophilized, and stored at −80 °C until further processing.

Protein-G agarose (Sigma) was reconstituted in water for 1 hour at room temperature and washed three times in IP buffer (100 mM Tris pH 7.4, 0.3% NP-40). Beads were resuspended in IP buffer containing three antibodies (4G10 from Sigma, pY100 and pY1000 from Cell Signaling Technologies) and placed on a rotator for 6-8 hours at 4 degrees. Beads were washed with IP buffer and added to lyophilized peptides in IP buffer, overnight at 4 degrees. Beads were washed with IP buffer, wash buffer (100 mM Tris pH 7.4), and with water. Peptides were eluted with 15% Acetonitrile containing 0.15% trifluoroacetic acid. For human PDX samples, heavy labeled peptides were added, and in all cases the acetonitrile was removed using vacuum centrifugation.

Online peptide separation coupled to MS/MS was performed with a nanoLC system (nanoAcquity UPLC system, Waters) and a Q-exactive mass spectrometer (Thermo Fisher Scientific). Peptide samples were loaded onto a trap column (Bruker C18 MAGIC beads, 200 A pore size, 4 cm packing length, 100 µm column inner diameter) connected to an analytical column (Bruker C18 MAGIC beads, 100 A pore size, 20 cm packing length, 75 µm column inner diameter) with an incorporated electrospray emitter. Peptide separation was achieved using a gradient from 3 to 40% (V/V) of ACN in 0.1% FA over 40 or 115 minutes at a flow rate of 250 nL/min.

A top 10 method was used for data-dependent/discovery acquisitions. Full MS scans were acquired at a resolution of 70,000, a target automatic gain control (AGC) value of 1e6, with a maximum fill time of 100 ms. MS2 scans were acquired at a resolution of 17,500 with an AGC target of 5e4 and a maximum fill time of 200 ms, and a normalized collision energy of 28.

Parallel Reaction Monitoring (PRM) methods were used to target specific phosphorylated peptides. The acquisition method combined 5 sequential PRM events followed by a full scan event. Precursor ions of the peptides were targeted in preliminary experiments without time-scheduling and confirmed precursors were targeted +/− 5 minutes of the observed elution times in the actual experimental runs. PRM events were acquired with an orbitrap resolution of 17,500, an AGC value of 2e5, and maximum fill times of 100 ms, and a normalized energy of 28. The precursor ion of each targeted peptide was isolated using a 2 m/z window. Full MS scans were acquired at a resolution of 70,000, an AGC value of 3e6, and maximum fill times of 240 ms.

Data Processing and Analysis

For DDA analysis, MS data files were searched using the COMET algorithm[107] and the output was imported into the Trans-Proteomic Pipeline[108] with the following parameters: variable oxidation of methionine (15.99 Da), variable phosphorylation (79.96 Da) of serine, threonine, or tyrosine, up to 4 variable modifications per peptide, fixed carbamidomethylation of cysteine (57.02 Da), two missed cleavages, maximum charge of 7. Peptide false discovery rate (FDR) was set to 1%.

Quantitative analysis of pY peptides was performed with Skyline software[109]. Quantifiable fragment ions for each peptide were confirmed and an intensity value was determined by summing the area under the curve gleaned from a subset of fragment ion and/or precursor ion isotopic peaks (minimum peak number = 3). For mouse pY quantification, the intensity value for each peptide was normalized to that for a phosphorylated peptide from Fgr within the same sample prior to assessing changes in relative peptide

abundance. For human PDX models, the intensity values for endogenous peptides were first normalized to that of the corresponding spiked-in heavy peptide and then to that of GSK3B pY216.

Statistical analysis

All statistical analyses were performed using graphPad Prism version 8.4.2 unless specified above. All specific statistical tests and P-values are indicated in the relevant figures. In all summary figures, a single data point represents an individual mouse, and bars indicate the mean ± SEM. One-way and two-way ANOVA tests were adjusted for multiple comparisons using the Tukey's (one-way) or Sidak's (two-way) multiple comparisons tests. No sample size calculations were performed. Experiments were generally repeated 2 or more times with at least two mice or leukemias per genotype/group. An exception is the characterization of the mice with spontaneous leukemia - those experiments typically contained just the sick mouse and a healthy littermate control, as it was infrequent that multiple animals with spontaneous disease would meet euthanasia criteria at the same time. Data were only excluded when there was a technical issue with administering the EdU i.p. injections and no labeling was detected upon flow cytometry analysis (Figure 4e-f).

Data availability

The mapped reads for the whole exome sequencing have been deposited in the Sequence Read Archive database (BioProject ID: PRJNA735253). The mass spectrometry proteomics data have been deposited to the ProteomeXchange Consortium via the PRIDE[110] partner repository with the dataset identifiers PXD026438 and PXD026322.

Chapter III. **Concluding Remarks**

Molecular profiling of cancers through genome sequencing can identify tumor-specific mutations that may inform treatment strategies. However, genomic data alone is not always clinically useful without additional studies. The identification of a mutation often does not indicate how protein function may be impacted nor how altered protein function impacts cell biology. Similarly, it is not known whether specific mutations are "drivers" versus "passengers" in either oncogenic transformation or disease progression in the absence of direct testing. Without this knowledge, it can be difficult to understand what is truly causing an individual's cancer and to predict patient outcomes (i.e. responses to therapy, likelihood of relapse, etc.). Furthermore, it is challenging to deconvolute the effects and roles of individual mutations in primary patient samples, where mutational load may be quite high, and disease may be advanced. Analysis of isolated mutations can help inform how single mutations alter normal cellular processes and identify which mutations are capable of initiating disease.

Previous work has examined IL-7R activating mutations in isolation using retroviral overexpression systems. These studies made important observations about the effects of these mutations on protein dimerization and function and suggested a possible role for these mutants in leukemogenesis, yet there were limitations to those models. Primarily, that expression levels of the mutant receptors were supraphysiological and that *in vivo* oncogenesis was only tested via adoptive transfer of transduced cells into immunodeficient hosts. Thus, it remained difficult to determine how well these results translate to defining the role of activated IL-7R in human leukemias. Similarly, while *SH2B3* and *IKAROS* deletion mutations have been observed in Ph-like leukemias with mutant IL-7R, no study has investigated specific combinations of these mutations to determine their sufficiency in driving disease.

Murine models of lineage-restricted expression of activated *Il7r*, *Sh2b3* loss, and *Ikzf1* dysfunction can provide insight into how these mutations may cooperate to alter normal B cell biology and contribute to disease. In our study, we utilize these novel models to demonstrate that an activating *Il7r* mutation can

initiate B-ALL when expressed alone and at a level below endogenous wildtype IL-7R. Our data also establishes the requirement of aIL7R for leukemic disease in the Sh2b3$^{+/-}$, Sh2b3$^{fl/+}$ Mb1, and Ikzf1$^{fl/+}$ CD19 models, as these mutations alone do not result in B-ALL. Future work is needed to define the mechanism(s) by which Sh2b3 and Ikaros dysfunction enhance the aIL7R disease phenotype. Loss of Sh2b3 clearly impacts signaling pathways in progenitor B cells beyond IL-7R that may synergize to drive B-ALL. Consistent with this, loss of SH2B3 is observed across a broad range of Ph-like ALLs, including leukemias with alterations in *CRLF2*, *JAK2*, *IKZF1* and others [13, 41, 111-113]. These leukemic cells retain expression of endogenous (wildtype) IL-7R. Thus, loss of SH2B3 in this setting likely impacts JAK activation via endogenous IL-7 (as well as in response to CRLF2 signaling). Indeed, Wei Tong's group has shown that loss of SH2B3 increases STAT5 activation and cell growth in response to IL-7 in pro/pre-B cells[56]. Therefore, SH2B3 loss likely cooperates with both wildtype and mutant IL-7R signals. Like *SH2B3*, *IKZF1* deletions or mutations are observed across multiple genetic subtypes of Ph-like ALL. Importantly, STAT5 antagonizes IKAROS activity in murine pre-B cells and primary B-ALLs by reciprocally regulating many of the same target genes, including the induction of *IL7R*[58, 65]. Collectively, these data suggest that both SH2B3 and IKAROS can negatively regulate IL-7R, albeit via different mechanisms (signaling vs transcriptional regulation), and that mutations in *IL7R* may collaborate with those in *SH2B3* and *IKZF1* to alter B cell development in ways that drive leukemic transformation.

Leukemic transformation after an early arrest of B cell development in the bone marrow has been reported in some mouse models. For example, B-ALL occurs in Blnk$^{-/-}$ and Btk$^{-/-}$ Blnk$^{-/-}$ [92, 114] but not in Rag1/2 KO, uMT, or IL-7R KO models [115-118]. While our aIL7R mice exhibit an expansion of late pro-B cells, B cell maturation is not altered prior to leukemia onset (Figures **II.3** and **II.S4**). Further, the degree of progenitor expansion is not correlated with the rate or penetrance of aIL7R-driven transformation. *Sh2b3*$^{-/-}$ mice have increased B cell progenitors, but do not develop B-ALL[50]. Similarly, while Ikzf1$^{fl/fl}$ CD19 B cells are blocked at the large pre-B stage and have leukemogenic potential in NSG mice[72], heterozygous Ikzf1$^{fl/+}$ animals lack progenitor expansion and do not develop spontaneous leukemias. Taken together,

these data suggest that simply blocking development is insufficient to drive B cell progenitor leukemogenesis. It is intriguing to speculate that the stage at which development is blocked or altered plays a role in the likelihood of transformation, due to the stage-specific differences in signaling, transcription, and proliferation.

While IL-7R activating mutations are relatively rare in B-ALL, they are more frequently observed in T-ALL. Like in B-ALL, IL-7 signaling promotes the survival and proliferation of T-ALL, and unlike normal thymocytes, it does so regardless of the stage at which development in blocked[119]. In T-ALL, IL-7R mutations occur in all subtypes, but appear to be enriched in early T cell precursor ALL (ETP-ALL), as well as leukemias with *HOXA* or *TLX* overexpression[43, 120, 121]. Our murine model of aIL7R expression could similarly be applied to investigate its role in initiating T-ALL or altering early thymocyte development by crossing to T-cell-specific Cre strains. As discussed previously, IL-7R signaling and expression is dynamically regulated in the DN and DP thymocyte stages, so we may need to knock-in aIL7R into the endogenous locus as opposed to *Rosa26* to reflect this physiology. Selecting the most relevant Cre strains is also likely to be important. It would be interesting to evaluate aIL7R both alone and in concert with the Vav-Hoxa9 mouse model[122] of moderate *Hoxa9* overexpression that is predisposed to ETP-ALL to assess potential synergistic effects. Indeed, recent work from Scott Durum's group indicates that DN murine thymocytes transduced to overexpress Hoxa9 and mutant human IL-7R can induce T-ALL *in vivo* when adoptively transferred into irradiated Rag-/- mice[123], supporting this concept.

We have shown that murine and human IL-7R-mutant B-ALLs display activation of JAK/STAT, mTOR, and a unique "BCR-like" signaling program characterized by SYK phosphorylation. As discussed earlier, it is currently unclear what is driving the activation of this "BCR-like" signature. Furthermore, the role of aIL7R and/or WT IL-7R in "BCR-like" activation remains undefined. Our phosphoproteomics data indicates that acute (15 mins) IL-7 stimulation has little impact on the relative phosphorylation levels of Syk and its downstream targets (i.e. Btk, Pik3ap1, Cbl, etc.; Figure **II.7c-g**), suggesting no direct role for IL-7R signals. Alternatively, aIL7R/IL-7R may indirectly influence the upstream events that mediate Syk

activation. Integrins are an intriguing candidate to induce "BCR-like" signaling and evidence suggests they can be regulated by IL-7R signals. In naïve human T cells, 72 hours of IL-7 stimulation can induce the expression of the integrin α4β7 and its binding to MAdCAM-1[124], while in Th17 cells IL-7R and α2β1 cooperate to drive adhesion to collagen and IL-17 production[125]. Importantly, both studies found JAK/STAT and PI3K pathways are required for these functional effects. Moreover, in murine pro-B cells, IL-7R blockade results in decreased FAK expression and increased motility, suggesting that IL-7R signals promote integrin-mediated adhesion to IL-7-producing stromal cells in the bone marrow[126]. These data indicate that future signaling studies using murine aIL7R progenitors, leukemias, and human Ph-like ALLs treated with anti-IL-7R and/or anti-integrin blocking antibodies may add clarity to the "BCR-like" activation signature.

Ph-like ALL remains associated with high rates of relapse and chemotherapy resistance and more effective therapies are urgently needed. Preclinical studies have demonstrated reduced *in vivo* survival and growth of Ph-like ALL xenografts, including the IL-7R/SH2B3-mutant (PALJDL), in response to ruxolitinib and rapamycin treatment[68]. We demonstrate that targeted inhibition of active signaling pathways (Jak/Stat, mTOR, and Syk) in primary aIL7R tumors impaired their survival *in vitro* (Figure **II.6b**, **II.7h-j**, and **II.S8**). *In vivo*, however, while rapamycin treatment alone delayed tumor growth it was not sufficient to eliminate disease in either the murine leukemia or human PDX setting (Figures **II.6c-i** and **II.S5g-i**) and entospletinib treatment alone showed no inhibitory effect on the PALJDL xenograft (Figure **II.S9**). These findings are consistent with CRLF2-rearranged Ph-like xenografts, where targeting single candidate pathways (JAK/STAT, PI3-K, or BCR-like) is insufficient as monotherapy[127]. Only triple pathway therapy (ruxolitinib + parsaclisib + dasatanib), or dual therapy in combination with steroids (ruxolitinib + parsaclisib + dexamethasone) provided effective control *in vivo*[127]. Dual JAKi and PI3-Ki treatment also extended the survival of *Sh2b3*$^{-/-}$ *Trp53*$^{-/-}$ B-ALL recipients compared to single agent therapy[56]. Our results suggest that *in vivo* combinatorial testing of targeted therapeutics could be a useful next step for both the

aIL7R murine leukemias and the PALJDL Ph-like PDX model and that rapamycin, ruxolitinib, and entospletinib represent logical initial candidates.

Overall, the data from this study demonstrates how early B cell development is impacted by activated IL-7R expression and establishes aIL7R, but not heterozygous Sh2b3 or Ikzf1 loss, as a leukemia-initiating mutation. Our novel B-ALL GEMMs will be a useful *in vivo* system to further investigate the mechanisms by which cytokine-driven B cell leukemias develop and persist, as well as to test combinatorial therapies that may treat primary aIL7R B-ALL. These important preclinical experiments represent a crucial first step in the path towards improving outcomes for patients with IL-7R-mutant leukemias.

Chapter IV. Glossary

aIL7R – Activated murine IL-7R mutant (PPCL insertion)

ALL – Acute lymphoblastic leukemia

B-ALL – B cell acute lymphoblastic leukemia

BCR – B cell receptor

BM – Bone marrow

CLP – Common lymphoid progenitor

CRLF2 - Cytokine Receptor Like Factor 2 (aka TSLP receptor)

EdU – 5-ethynyl-2'-deoxyuridine

IL-7R – Interleukin-7 receptor

LNK – lymphocyte adapter protein (aka SH2B3)

FM – Follicular mature B cells

MS – Mass spectrometry

MZ – Marginal zone B cells

MZp – Marginal zone precursor B cells

PDX – Patient-derived xenograft

Ph+ - Philadelphia chromosome+

Ph-like – Philadelphia chromosome-like

SH2B3 – Src homology 2-B adapter protein 3

T1 – Transitional type 1 B cells

T2 – Transitional type 2 B cells

TSLP – Thymic stromal lymphopoietin

WT - Wildtype

Chapter V. References

1. Clark MR, Mandal M, Ochiai K, Singh H. Orchestrating B cell lymphopoiesis through interplay of IL-7 receptor and pre-B cell receptor signalling. *Nature Reviews Immunology* 2014 Feb; **14**(2)**:** 69-80.

2. Funk PE, Varas A, Witte PL. ACTIVITY OF STEM-CELL FACTOR AND IL-7 IN COMBINATION ON NORMAL BONE-MARROW B-LINEAGE CELLS. *Journal of Immunology* 1993 Feb; **150**(3)**:** 748-752.

3. Ray RJ, Paige CJ, Furlonger C, Lyman SD, Rottapel R. Flt3 ligand supports the differentiation of early B cell progenitors in the presence of interleukin-11 and interleukin-7. *European Journal of Immunology* 1996 Jul; **26**(7)**:** 1504-1510.

4. Tokoyoda K, Egawa T, Sugiyama T, Choi BI, Nagasawa T. Cellular niches controlling B lymphocyte behavior within bone marrow during development. *Immunity* 2004 Jun; **20**(6)**:** 707-718.

5. Tsukada S, Saffran DC, Rawlings DJ, Parolini O, Allen RC, Klisak I*, et al.* DEFICIENT EXPRESSION OF A B-CELL CYTOPLASMIC TYROSINE KINASE IN HUMAN X-LINKED AGAMMAGLOBULINEMIA. *Cell* 1993 Jan; **72**(2)**:** 279-290.

6. Conley ME, Broides A, Hernandez-Trujillo V, Howard V, Kanegane H, Miyawaki T*, et al.* Genetic analysis of patients with defects in early B-cell development. *Immunological Reviews* 2005 Feb; **203:** 216-234.

7. McDonnell TJ, Deane N, Platt FM, Nunez G, Jaeger U, McKearn JP*, et al.* BCL-2-IMMUNOGLOBULIN TRANSGENIC MICE DEMONSTRATE EXTENDED B-CELL SURVIVAL AND FOLLICULAR LYMPHOPROLIFERATION. *Cell* 1989 Apr; **57**(1)**:** 79-88.

8. Mullighan CG, Goorha S, Radtke I, Miller CB, Coustan-Smith E, Dalton JD*, et al.* Genome-wide analysis of genetic alterations in acute lymphoblastic leukaemia. *Nature* 2007 Apr; **446**(7137)**:** 758-764.

9. Kuiper RP, Schoenmakers E, van Reijmersdal SV, Hehir-Kwa JY, van Kessel AG, van Leeuwen FN*, et al.* High-resolution genomic profiling of childhood ALL reveals novel recurrent genetic lesions affecting pathways involved in lymphocyte differentiation and cell cycle progression. *Leukemia* 2007 Jun; **21**(6)**:** 1258-1266.

10. Prasad MAJ, Ungerback J, Ahsberg J, Somasundaram R, Strid T, Larsson M*, et al.* Ebf1 heterozygosity results in increased DNA damage in pro-B cells and their synergistic transformation by Pax5 haploinsufficiency. *Blood* 2015 Jun; **125**(26)**:** 4052-4059.

11. Ta VBT, de Bruijn MJW, ter Brugge PJ, van Hamburg JP, Diepstraten HJA, van Loo PF*, et al.* Malignant transformation of Slp65-deficient pre-B cells involves disruption of the Arf-Mdm2-p53 tumor suppressor pathway. *Blood* 2010 Feb; **115**(7)**:** 1385-1393.

12. Perentesis JP, Bhatia S, Boyle E, Shao Y, Shu XO, Steinbuch M*, et al.* RAS oncogene mutations and outcome of therapy for childhood acute lymphoblastic leukemia. *Leukemia* 2004 Apr; **18**(4)**:** 685-692.

13. Roberts KG, Li Y, Payne-Turner D, Harvey RC, Yang YL, Pei D*, et al.* Targetable Kinase-Activating Lesions in Ph-like Acute Lymphoblastic Leukemia. *New England Journal of Medicine* 2014 Sep; **371**(11)**:** 1005-1015.

14. Reshmi SC, Harvey RC, Roberts KG, Stonerock E, Smith A, Jenkins H*, et al.* Targetable kinase gene fusions in high-risk B-ALL: a study from the Children's Oncology Group. *Blood* 2017 Jun; **129**(25)**:** 3352-3361.

15. Roberts KG, Reshmi SC, Harvey RC, Chen IM, Patel K, Stonerock E*, et al.* Genomic and outcome analyses of Ph-like ALL in NCI standard-risk patients: a report from the Children's Oncology Group. *Blood* 2018 Aug; **132**(8)**:** 815-824.

16. Frisch A, Ofran Y. How I diagnose and manage Philadelphia chromosome-like acute lymphoblastic leukemia. *Haematologica* 2019 Oct; **104**(11)**:** 2135-2143.

17. Barata JT, Durum SK, Seddon B. Flip the coin: IL-7 and IL-7R in health and disease. *Nature Immunology* 2019 Dec; **20**(12)**:** 1584-1593.

18. Kondo M, Weissman IL, Akashi K. Identification of clonogenic common lymphoid progenitors in mouse bone marrow. *Cell* 1997 Nov; **91**(5)**:** 661-672.

19. Dias S, Silva H, Cumano A, Vieira P. Interleukin-7 is necessary to maintain the B cell potential in common lymphoid progenitors. *Journal of Experimental Medicine* 2005 Mar; **201**(6)**:** 971-979.

20. Boudil A, Matei IR, Shih HY, Bogdanoski G, Yuan JS, Chang SG*, et al.* IL-7 coordinates proliferation, differentiation and Tcra recombination during thymocyte beta-selection. *Nature Immunology* 2015 Apr; **16**(4)**:** 397-405.

21. Seddon B, Zamoyska R. TCR and IL-7 receptor signals can operate independently or synergize to promote lymphopenia-induced expansion of naive T cells. *Journal of Immunology* 2002 Oct; **169**(7)**:** 3752-3759.

22. Yu Q, Park JH, Doan LL, Erman B, Feigenbaum L, Singer A. Cytokine signal transduction is suppressed in preselection double-positive thymocytes and restored by positive selection. *Journal of Experimental Medicine* 2006 Jan; **203**(1)**:** 165-175.

23. Pearson C, Silva A, Seddon B. Exogenous Amino Acids Are Essential for Interleukin-7 Induced CD8 T Cell Gowth. *Plos One* 2012 Apr; **7**(4).

24. Kaech SM, Tan JT, Wherry EJ, Konieczny BT, Surh CD, Ahmed R. Selective expression of the interleukin 7 receptor identifies effector CD8 T cells that give rise to long-lived memory cells. *Nature Immunology* 2003 Dec; **4**(12)**:** 1191-1198.

25. Corfe SA, Paige CJ. The many roles of IL-7 in B cell development; Mediator of survival, proliferation and differentiation. *Seminars in Immunology* 2012 Jun; **24**(3)**:** 198-208.

26. Ochiai K, Maienschein-Cline M, Mandal M, Triggs JR, Bertolino E, Sciammas R*, et al.* A self-reinforcing regulatory network triggered by limiting IL-7 activates pre-BCR signaling and differentiation. *Nature Immunology* 2012 Mar; **13**(3)**:** 300-U124.

27. Hendriks RW, deBruijn M, Maas A, Dingjan GM, Karis A, Grosveld F. Inactivation of Btk by insertion of lacZ reveals defects in B cell development only past the pre-B cell stage. *Embo Journal* 1996 Sep; **15**(18)**:** 4862-4872.

28. Rheingold SR, Brown VI, Fang JJ, Kim JM, Grupp SA. Role of the BCR complex in B cell development, activation, and leukemic transformation. *Immunologic Research* 2003; **27**(2-3)**:** 309-329.

29. Herzog S, Storch B, Jumaa H. Dual role of the adaptor protein SLP-65 - Organizer of signal transduction and tumor suppressor of pre-B cell leukemia. *Immunologic Research* 2006; **34**(2)**:** 143-155.

30. Fry TJ, Mackall CL. Interleukin-7: from bench to clinic. *Blood* 2002 Jun; **99**(11)**:** 3892-3904.

31. Mazzucchelli RI, Riva A, Durum SK. The human IL-7 receptor gene: Deletions, polymorphisms and mutations. *Seminars in Immunology* 2012 Jun; **24**(3)**:** 225-230.

32. Mullighan CG. Molecular genetics of B-precursor acute lymphoblastic leukemia. *Journal of Clinical Investigation* 2012 Oct; **122**(10)**:** 3407-3415.

33. Mullighan CG. The genomic landscape of acute lymphoblastic leukemia in children and young adults. *Hematology-American Society of Hematology Education Program* 2014 Dec**:** 174-180.

34. Andersson A, Eden P, Lindgren D, Nilsson J, Lassen C, Heldrup J*, et al.* Gene expression profiling of leukemic cell lines reveals conserved molecular signatures among subtypes with specific genetic aberrations. *Leukemia* 2005 Jun; **19**(6)**:** 1042-1050.

35. Li JF, Dai YT, Lilljebjorn H, Shen SH, Cui BW, Bai L*, et al.* Transcriptional landscape of B cell precursor acute lymphoblastic leukemia based on an international study of 1,223 cases. *Proceedings of the National Academy of Sciences of the United States of America* 2018 Dec; **115**(50)**:** E11711-E11720.

36. Harvey RC, Mullighan CG, Wang XF, Dobbin KK, Davidson GS, Bedrick EJ*, et al.* Identification of novel cluster groups in pediatric high-risk B-precursor acute lymphoblastic leukemia with gene expression profiling: correlation with genome-wide DNA copy number alterations, clinical characteristics, and outcome. *Blood* 2010 Dec; **116**(23)**:** 4874-4884.

37. Den Boer ML, van Slegtenhorst M, De Menezes RX, Cheok MH, Buijs-Gladdines J, Peters S*, et al.* A subtype of childhood acute lymphoblastic leukaemia with poor treatment outcome: a genome-wide classification study. *Lancet Oncology* 2009 Feb; **10**(2)**:** 125-134.

38. Feldhahn N, Klein F, Mooster JL, Hadweh P, Sprangers M, Wartenberg M*, et al.* Mimicry of a constitutively active pre-B cell receptor in acute lymphoblastic leukemia cells. *Journal of Experimental Medicine* 2005 Jun; **201**(11)**:** 1837-1852.

39. Tasian SK, Loh ML, Hunger SP. Philadelphia chromosome-like acute lymphoblastic leukemia. *Blood* 2017 Nov; **130**(19)**:** 2064-2072.

40. Russell LJ, Capasso M, Vater I, Akasaka T, Bernard OA, Calasanz MJ*, et al.* Deregulated expression of cytokine receptor gene, CRLF2, is involved in lymphoid transformation in B-cell precursor acute lymphoblastic leukemia. *Blood* 2009 Sep; **114**(13)**:** 2688-2698.

41. Roberts KG, Morin RD, Zhang JH, Hirst M, Zhao YJ, Su XP*, et al.* Genetic Alterations Activating Kinase and Cytokine Receptor Signaling in High-Risk Acute Lymphoblastic Leukemia. *Cancer Cell* 2012 Aug; **22**(2)**:** 153-166.

42. Herold T, Schneider S, Metzeler KH, Neumann M, Hartmann L, Roberts KG*, et al.* Adults with Philadelphia chromosome-like acute lymphoblastic leukemia frequently have IGH-CRLF2 and JAK2 mutations, persistence of minimal residual disease and poor prognosis. *Haematologica* 2017 Jan; **102**(1)**:** 130-138.

43. Zenatti PP, Ribeiro D, Li WQ, Zuurbier L, Silva MC, Paganin M*, et al.* Oncogenic IL7R gain-of-function mutations in childhood T-cell acute lymphoblastic leukemia. *Nature Genetics* 2011 Oct; **43**(10)**:** 932-U931.

44. Shochat C, Tal N, Bandapalli OR, Palmi C, Ganmore I, Kronnie GT*, et al.* Gain-of-function mutations in interleukin-7 receptor-alpha (IL7R) in childhood acute lymphoblastic leukemias. *Journal of Experimental Medicine* 2011 May; **208**(5)**:** 901-908.

45. Shochat C, Tal N, Gryshkova V, Birger Y, Bandapalli OR, Cazzaniga G*, et al.* Novel activating mutations lacking cysteine in type I cytokine receptors in acute lymphoblastic leukemia. *Blood* 2014 Jul; **124**(1)**:** 106-110.

46. Geron I, Savino AMS, Tal N, Brown J, Turati V, James C*, et al.* An instructive role for IL7RA in the development of human B-cell precursor leukemia. BioRxiv; 2020.

47. Buchner M, Swaminathan S, Chen ZS, Muschen M. Mechanisms of pre-B-cell receptor checkpoint control and its oncogenic subversion in acute lymphoblastic leukemia. *Immunological Reviews* 2015 Jan; **263**(1)**:** 192-209.

48. Treanor LM, Zhou S, Janke L, Churchman ML, Ma ZJ, Lu TH*, et al.* Interleukin-7 receptor mutants initiate early T cell precursor leukemia in murine thymocyte progenitors with multipotent potential. *Journal of Experimental Medicine* 2014 Apr; **211**(4)**:** 701-713.

49. Yokoyama K, Yokoyama N, Izawa K, Kotani A, Harashima A, Hozumi K*, et al.* In vivo leukemogenic potential of an interleukin 7 receptor alpha chain mutant in hematopoietic stem and progenitor cells. *Blood* 2013 Dec; **122**(26)**:** 4259-4263.

50. Takaki S, Sauer K, Iritani BM, Chien S, Ebihara Y, Tsuji K*, et al.* Control of B cell production by the adaptor protein Lnk: Definition of a conserved family of signal-modulating proteins. *Immunity* 2000 Nov; **13**(5)**:** 599-609.

51. Tong W, Zhang J, Lodish HF. Lnk inhibits erythropoiesis and Epo-dependent JAK2 activation and downstream signaling pathways. *Blood* 2005 Jun; **105**(12)**:** 4604-4612.

52. Takaki S, Morita H, Tezuka Y, Takatsu K. Enhanced Hematopoiesis by hematopoietic progenitor cells lacking intracellular adaptor protein, Lnk. *Journal of Experimental Medicine* 2002 Jan; **195**(2)**:** 151-160.

53. Velazquez L, Cheng AM, Fleming HE, Furlonger C, Vesely S, Bernstein A*, et al.* Cytokine signaling and hematopoietic homeostasis are disrupted in Lnk-deficient mice. *Journal of Experimental Medicine* 2002 Jun; **195**(12)**:** 1599-1611.

54. Tong W, Lodish HE. Lnk inhibits Tpo-mpl signaling and Tpo-mediated megakaryocytopoiesis. *Journal of Experimental Medicine* 2004 Sep; **200**(5)**:** 569-580.

55. Mori T, Iwasaki Y, Seki Y, Iseki M, Katayama H, Yamamoto K*, et al.* Lnk/Sh2b3 Controls the Production and Function of Dendritic Cells and Regulates the Induction of IFN-gamma-Producing T Cells. *Journal of Immunology* 2014 Aug; **193**(4)**:** 1728-1736.

56. Cheng Y, Chikwava K, Wu C, Zhang HB, Bhagat A, Pei DH*, et al.* LNK/SH2B3 regulates IL-7 receptor signaling in normal and malignant B-progenitors. *Journal of Clinical Investigation* 2016 Apr; **126**(4)**:** 1267-1281.

57. Bersenev A, Wu C, Balcerek J, Tong W. Lnk Controls Hematopoietic Stem Cell Self-Renewal through Direct Interactions with JAK2 and Contributes to Oncogenic JAK2-Induced Myeloproliferative Diseases in Mice. *Blood* 2008 Nov; **112**(11)**:** 329-329.

58. Ge Z, Gu Y, Xiao LC, Han Q, Li JY, Chen BA*, et al.* Co-existence of IL7R high and SH2B3 low expression distinguishes a novel high-risk acute lymphoblastic leukemia with Ikaros dysfunction. *Oncotarget* 2016 Jul; **7**(29)**:** 46014-46027.

59. Georgopoulos K, Bigby M, Wang JH, Molnar A, Wu P, Winandy S*, et al.* THE IKAROS GENE IS REQUIRED FOR THE DEVELOPMENT OF ALL LYMPHOID LINEAGES. *Cell* 1994 Oct; **79**(1)**:** 143-156.

60. Wang JH, Nichogiannopoulou A, Wu L, Sun L, Sharpe AH, Bigby M*, et al.* Selective defects in the development of the fetal and adult lymphoid system in mice with an Ikaros null mutation. *Immunity* 1996 Dec; **5**(6)**:** 537-549.

61. Schwickert TA, Tagoh H, Gultekin S, Dakic A, Axelsson E, Minnich M*, et al.* Stage-specific control of early B cell development by the transcription factor Ikaros. *Nature Immunology* 2014 Mar; **15**(3)**:** 283-293.

62. Alkhatib A, Werner M, Hug E, Herzog S, Eschbach C, Faraidun H*, et al.* FoxO1 induces Ikaros splicing to promote immunoglobulin gene recombination. *Journal of Experimental Medicine* 2012 Feb; **209**(2)**:** 395-406.

63. Nera KP, Alinikula J, Terho P, Narvi E, Tornquist K, Kurosaki T*, et al.* Ikaros has a crucial role in regulation of B cell receptor signaling. *European Journal of Immunology* 2006 Mar; **36**(3)**:** 516-525.

64. Thompson EC, Cobb BS, Sabbattini P, Meixlsperger S, Parelho V, Liberg D*, et al.* Ikaros DNA-binding proteins as integral components of B cell developmental-stage-specific regulatory circuits. *Immunity* 2007 Mar; **26**(3)**:** 335-344.

65. Katerndahl CDS, Heltemes-Harris LM, Willette MJL, Henzler CM, Frietze S, Yang RD*, et al.* Antagonism of B cell enhancer networks by STAT5 drives leukemia and poor patient survival. *Nature Immunology* 2017 Jun; **18**(6)**:** 694-+.

66. Holmfeldt L, Wei L, Diaz-Flores E, Walsh M, Zhang JH, Ding L*, et al.* The genomic landscape of hypodiploid acute lymphoblastic leukemia. *Nature Genetics* 2013 Mar; **45**(3)**:** 242-252.

67. Maude SL, Tasian SK, Vincent T, Hall JW, Collins-Underwood R, Mullighan CG*, et al.* Targeting mTOR and JAK2 in Xenograft Models of CRLF2-Overexpressing Acute Lymphoblastic Leukemia (ALL). *Blood* 2011 Nov; **118**(21)**:** 113-114.

68. Maude SL, Tasian SK, Vincent T, Hall JW, Sheen C, Roberts KG*, et al.* Targeting JAK1/2 and mTOR in murine xenograft models of Ph-like acute lymphoblastic leukemia. *Blood* 2012 Oct; **120**(17)**:** 3510-3518.

69. Chen ZS, Shojaee S, Buchner M, Geng HM, Lee J, Klemm L*, et al.* Signalling thresholds and negative B-cell selection in acute lymphoblastic leukaemia. *Nature* 2015 May; **521**(7552)**:** 357-+.

70. Muschen M. Rationale for targeting the pre-B-cell receptor signaling pathway in acute lymphoblastic leukemia. *Blood* 2015 Jun; **125**(24)**:** 3688-3693.

71. Yoshida T, Ng SYM, Zuniga-Pflucker JC, Georgopoulos K. Early hematopoietic lineage restrictions directed by Ikaros. *Nature Immunology* 2006 Apr; **7**(4)**:** 382-391.

72. Joshi I, Yoshida T, Jena N, Qi XQ, Zhang JW, Van Etten RA*, et al.* Loss of Ikaros DNA-binding function confers integrin-dependent survival on pre-B cells and progression to acute lymphoblastic leukemia. *Nature Immunology* 2014 Mar; **15**(3)**:** 294-304.

73. Allenspach E, Shubin N, Cerosaletti K, Mikacenic C, Gorman J, MacQuivey M*, et al.* The autoimmune risk R262W variant of the adaptor SH2B3 improves survival in sepsis. *Journal of Immunology [In preparation/revision]* 2020.

74. Mullighan CG, Su XP, Zhang JH, Radtke I, Phillips LAA, Miller CB*, et al.* Deletion of IKZF1 and Prognosis in Acute Lymphoblastic Leukemia. *New England Journal of Medicine* 2009 Jan; **360**(5)**:** 470-480.

75. Meffre E, Fougereau M, Argenson JN, Aubaniac JM, Schiff C. Cell surface expression of surrogate light chain (Psi L) in the absence of mu on human pro-B cell lines and normal pro-B cells. *European Journal of Immunology* 1996 Sep; **26**(9)**:** 2172-2180.

76. Lemmers B, Arnoulet C, Fossat C, Chambost H, Sainty D, Gabert J*, et al.* Fine characterization of childhood and adult acute lymphoblastic leukemia (ALL) by a proB and preB surrogate light chain-specific mAb and a proposal for a new B cell ALL classification. *Leukemia* 2000 Dec; **14**(12)**:** 2103-2111.

77. Lemmers B, Gauthier L, Guelpa-Fonlupt V, Fougereau M, Schiff C. The human (Psi L+mu(-)) proB complex: Cell surface expression and biochemical structure of a putative transducing receptor. *Blood* 1999 Jun; **93**(12)**:** 4336-4346.

78. Goldberg L, Gough SM, Lee F, Dang C, Walker RL, Zhu YLJ*, et al.* Somatic mutations in murine models of leukemia and lymphoma: Disease specificity and clinical relevance. *Genes Chromosomes & Cancer* 2017 Jun; **56**(6)**:** 472-483.

79. Gough SM, Goldberg L, Pineda M, Walker RL, Zhu YJ, Bilke S*, et al.* Progenitor B-1 B-cell acute lymphoblastic leukemia is associated with collaborative mutations in 3 critical pathways. *Blood Advances* 2017 Sep; **1**(20)**:** 1749-1759.

80. Lu LW, Chaudhury P, Osmond DG. Regulation of cell survival during B lymphopoiesis: Apoptosis and Bcl-2/Bax content of precursor B cells in bone marrow of mice with altered expression of IL-7 and recombinase-activating gene-2. *Journal of Immunology* 1999 Feb; **162**(4)**:** 1931-1940.

81. Malin S, McManus S, Cobaleda C, Novatchkova M, Delogu A, Bouillet P*, et al.* Role of STAT5 in controlling cell survival and immunoglobulin gene recombination during pro-B cell development. *Nature Immunology* 2010 Feb; **11**(2)**:** 171-U197.

82. Grillot DAM, Merino R, Pena JC, Fanslow WC, Finkelman FD, Thompson CB*, et al.* bcl-x exhibits regulated expression during B cell development and activation and modulates lymphocyte survival in transgenic mice. *Journal of Experimental Medicine* 1996 Feb; **183**(2)**:** 381-391.

83. Tasian SK, Doral MY, Borowitz MJ, Wood BL, Chen IM, Harvey RC*, et al.* Aberrant STAT5 and PI3K/mTOR pathway signaling occurs in human CRLF2-rearranged B-precursor acute lymphoblastic leukemia. *Blood* 2012 Jul; **120**(4)**:** 833-842.

84. Tasian SK, Teachey DT, Li Y, Shen F, Harvey RC, Chen IM*, et al.* Potent efficacy of combined PI3K/mTOR and JAK or ABL inhibition in murine xenograft models of Ph-like acute lymphoblastic leukemia. *Blood* 2017 Jan; **129**(2)**:** 177-187.

85. Hurtz C, Wertheim GB, Loftus JP, Blumenthal D, Lehman A, Li Y*, et al.* Oncogene-independent BCR-like signaling adaptation confers drug resistance in Ph-like ALL. *The Journal of clinical investigation* 2020 2020-Jul-01; **130**(7)**:** 3637-3653.

86. Cramer SD, Hixon JA, Andrews C, Porter RJ, Rodrigues GOL, Wu XL*, et al.* Mutant IL-7R alpha and mutant NRas are sufficient to induce murine T cell acute lymphoblastic leukemia. *Leukemia* 2018 Aug; **32**(8)**:** 1795-1799.

87. Damia G, Komschlies KL, Faltynek CR, Ruscetti FW, Wiltrout RH. ADMINISTRATION OF RECOMBINANT HUMAN INTERLEUKIN-7 ALTERS THE FREQUENCY AND NUMBER OF MYELOID PROGENITOR CELLS IN THE BONE-MARROW AND SPLEEN OF MICE. *Blood* 1992 Mar; **79**(5)**:** 1121-1129.

88. Komschlies KL, Gregorio TA, Gruys ME, Back TC, Faltynek CR, Wiltrout RH. ADMINISTRATION OF RECOMBINANT HUMAN IL-7 TO MICE ALTERS THE COMPOSITION OF B-LINEAGE CELLS AND T-CELL SUBSETS, ENHANCES T-CELL FUNCTION, AND INDUCES REGRESSION OF ESTABLISHED METASTASES. *Journal of Immunology* 1994 Jun; **152**(12)**:** 5776-5784.

89. Morrissey PJ, Conlon P, Braddy S, Williams DE, Namen AE, Mochizuki DY. ADMINISTRATION OF IL-7 TO MICE WITH CYCLOPHOSPHAMIDE-INDUCED LYMPHOPENIA ACCELERATES LYMPHOCYTE REPOPULATION. *Journal of Immunology* 1991 Mar; **146**(5)**:** 1547-1552.

90. Digel W, Schmid M, Heil G, Conrad P, Gillis S, Porzsolt F. HUMAN INTERLEUKIN-7 INDUCES PROLIFERATION OF NEOPLASTIC-CELLS FROM CHRONIC LYMPHOCYTIC-LEUKEMIA AND ACUTE LEUKEMIAS. *Blood* 1991 Aug; **78**(3)**:** 753-759.

91. Martin-Lorenzo A, Hauer J, Vicente-Duenas C, Auer F, Gonzalez-Herrero I, Garcia-Ramirez I*, et al.* Infection Exposure Is a Causal Factor in B-cell Precursor Acute Lymphoblastic Leukemia as a Result of Pax5-Inherited Susceptibility. *Cancer Discovery* 2015 Dec; **5**(12)**:** 1328-1343.

92. Nakayama J, Yamamoto M, Hayashi K, Satoh H, Bundo K, Kubo M*, et al.* BLNK suppresses pre-B-cell leukemogenesis through inhibition of JAK3. *Blood* 2009 Feb; **113**(7)**:** 1483-1492.

93. Appelmann I, Rillahan CD, de Stanchina E, Carbonetti G, Chen C, Lowe SW*, et al.* Janus kinase inhibition by ruxolitinib extends dasatinib- and dexamethasone-induced remissions in a mouse model of Ph plus ALL. *Blood* 2015 Feb; **125**(9)**:** 1444-1451.

94. Abdelrasoul H, Vadakumchery A, Werner M, Lenk L, Khadour A, Young M*, et al.* Synergism between IL7R and CXCR4 drives BCR-ABL induced transformation in Philadelphia chromosome-positive acute lymphoblastic leukemia. *Nature Communications* 2020 Jun; **11**(1)**:** 12.

95. Mocsai A, Ruland J, Tybulewicz VLJ. The SYK tyrosine kinase: a crucial player in diverse biological functions. *Nature Reviews Immunology* 2010 Jun; **10**(6)**:** 387-402.

96. Loftus JP, Yahiaoui A, Brown PA, Niswander LM, Bagashev A, Wang M*, et al.* Combinatorial efficacy of entospletinib and chemotherapy in patient-derived xenograft models of infant acute lymphoblastic leukemia. *Haematologica* 2020 2020-May-15.

97. Hobeika E, Thiemann S, Storch B, Jumaa H, Nielsen PJ, Pelanda R*, et al.* Testing gene function early in the B cell lineage in mb1-cre mice. *Proceedings of the National Academy of Sciences of the United States of America* 2006 Sep; **103**(37)**:** 13789-13794.

98. Rickert RC, Roes J, Rajewsky K. B lymphocyte-specific, Cre-mediated mutagenesis in mice. *Nucleic Acids Research* 1997 Mar; **25**(6)**:** 1317-1318.

99. Becker-Herman S, Meyer-Bahlburg A, Schwartz MA, Jackson SW, Hudkins KL, Liu CH*, et al.* WASp-deficient B cells play a critical, cell-intrinsic role in triggering autoimmunity. *Journal of Experimental Medicine* 2011 Sep; **208**(10)**:** 2033-2042.

100. Wray-Dutra MN, Chawla R, Thomas KR, Seymour BJ, Arkatkar T, Sommer KM*, et al.* Activated CARD11 accelerates germinal center kinetics, promoting mTORC1 and terminal differentiation. *Journal of Experimental Medicine* 2018 Sep; **215**(9)**:** 2445-2461.

101. Bandaranayake AD, Correnti C, Ryu BY, Brault M, Strong RK, Rawlings DJ. Daedalus: a robust, turnkey platform for rapid production of decigram quantities of active recombinant proteins in human cell lines using novel lentiviral vectors. *Nucleic Acids Research* 2011 Nov; **39**(21).

102. Schwartz MA, Kolhatkar NS, Thouvenel C, Khim S, Rawlings DJ. CD4(+) T Cells and CD40 Participate in Selection and Homeostasis of Peripheral B Cells. *Journal of Immunology* 2014 Oct; **193**(7)**:** 3492-3502.

103. McKenna A, Hanna M, Banks E, Sivachenko A, Cibulskis K, Kernytsky A*, et al.* The Genome Analysis Toolkit: A MapReduce framework for analyzing next-generation DNA sequencing data. *Genome Research* 2010 Sep; **20**(9)**:** 1297-1303.

104. Dunn T, Berry G, Emig-Agius D, Jiang Y, Lei S, Iyer A*, et al.* Pisces: an accurate and versatile variant caller for somatic and germline next-generation sequencing data. *Bioinformatics* 2019 May; **35**(9)**:** 1579-1581.

105. Wang K, Li MY, Hakonarson H. ANNOVAR: functional annotation of genetic variants from high-throughput sequencing data. *Nucleic Acids Research* 2010 Sep; **38**(16)**:** 7.

106. Hale M, Lee B, Honaker Y, Leung WH, Grier AE, Jacobs HM*, et al.* Homology-Directed Recombination for Enhanced Engineering of Chimeric Antigen Receptor T Cells. *Molecular Therapy-Methods & Clinical Development* 2017 Mar; **4:** 192-203.

107. Eng JK, Jahan TA, Hoopmann MR. Comet: An open-source MS/MS sequence database search tool. *Proteomics* 2013 Jan; **13**(1)**:** 22-24.

108. Deutsch EW, Mendoza L, Shteynberg D, Farrah T, Lam H, Tasman N*, et al.* A guided tour of the Trans-Proteomic Pipeline. *Proteomics* 2010 Mar; **10**(6)**:** 1150-1159.

109. MacLean B, Tomazela DM, Shulman N, Chambers M, Finney GL, Frewen B*, et al.* Skyline: an open source document editor for creating and analyzing targeted proteomics experiments. *Bioinformatics* 2010 Apr; **26**(7)**:** 966-968.

110. Perez-Riverol Y, Csordas A, Bai JW, Bernal-Llinares M, Hewapathirana S, Kundu DJ*, et al.* The PRIDE database and related tools and resources in 2019: improving support for quantification data. *Nucleic Acids Research* 2019 Jan; **47**(D1)**:** D442-D450.

111. Perez-Garcia A, Ambesi-Impiombato A, Hadler M, Rigo I, LeDuc CA, Kelly K*, et al.* Genetic loss of SH2B3 in acute lymphoblastic leukemia. *Blood* 2013 Oct; **122**(14)**:** 2425-2432.

112. Olsson L, Albitar F, Castor A, Behrendtz M, Biloglav A, Paulsson K*, et al.* Cooperative Genetic Changes in Pediatric B-Cell Precursor Acute Lymphoblastic Leukemia with Deletions or Mutations of IKZF1. *Genes Chromosomes & Cancer* 2015 May; **54**(5)**:** 315-325.

113. Yano M, Imamura T, Asai D, Deguchi T, Hashii Y, Endo M*, et al.* Clinical significance of SH2B3 (LNK) expression in paediatric B-cell precursor acute lymphoblastic leukaemia. *British Journal of Haematology* 2018 Oct; **183**(2)**:** 327-330.

114. Kersseboom R, Middendorp S, Dingjan GM, Dahlenborg K, Reth M, Jumaa H*, et al.* Bruton's tyrosine kinase cooperates with the B cell linker protein SLP-65 as a tumor suppressor in pre-B cells. *Journal of Experimental Medicine* 2003 Jul; **198**(1)**:** 91-98.

115. Mombaerts P, Iacomini J, Johnson RS, Herrup K, Tonegawa S, Papaioannou VE. RAG-1-DEFICIENT MICE HAVE NO MATURE LYMPHOCYTES-B AND LYMPHOCYTES-T. *Cell* 1992 Mar; **68**(5)**:** 869-877.

116. Shinkai Y, Rathbun G, Lam KP, Oltz EM, Stewart V, Mendelsohn M*, et al.* RAG-2-DEFICIENT MICE LACK MATURE LYMPHOCYTES OWING TO INABILITY TO INITIATE V(D)J REARRANGEMENT. *Cell* 1992 Mar; **68**(5)**:** 855-867.

117. Kitamura D, Roes J, Kuhn R, Rajewsky K. A B-CELL-DEFICIENT MOUSE BY TARGETED DISRUPTION OF THE MEMBRANE EXON OF THE IMMUNOGLOBULIN MU-CHAIN GENE. *Nature* 1991 Apr; **350**(6317)**:** 423-426.

118. Peschon JJ, Morrissey PJ, Grabstein KH, Ramsdell FJ, Maraskovsky E, Gliniak BC*, et al.* EARLY LYMPHOCYTE EXPANSION IS SEVERELY IMPAIRED IN INTERLEUKIN-7 RECEPTOR-DEFICIENT MICE. *Journal of Experimental Medicine* 1994 Nov; **180**(5)**:** 1955-1960.

119. Barata JT, Keenan TD, Silva A, Nadler LM, Boussiotis VA, Cardoso AA. Common gamma chain-signaling cytokines promote proliferation of T-cell acute lymphoblastic leukemia. *Haematologica* 2004 Dec; **89**(12)**:** 1459-1467.

120. Zhang JH, Ding L, Holmfeldt L, Wu G, Heatley SL, Payne-Turner D*, et al.* The genetic basis of early T-cell precursor acute lymphoblastic leukaemia. *Nature* 2012 Jan; **481**(7380)**:** 157-163.

121. Liu Y, Easton J, Shao Y, Maciaszek J, Wang ZM, Wilkinson MR*, et al.* The genomic landscape of pediatric and young adult T-lineage acute lymphoblastic leukemia. *Nature Genetics* 2017 Aug; **49**(8)**:** 1211-+.

122. Beachy SH, Onozawa M, Silverman D, Chung YJ, Rivera MM, Aplan PD. Isolated Hoxa9 overexpression predisposes to the development of lymphoid but not myeloid leukemia. *Experimental Hematology* 2013 Jun; **41**(6)**:** 518-529.

123. Rodrigues GOL, Hixon J, Winer H, Li WQ, Durum S. Overexpression of TLX3 or HOXA9 in association mutant IL7R alpha are sufficient to generate T-ALL in vivo. *Cancer Research* 2020 Jul; **80**(14)**:** 103-104.

124. Cimbro R, Vassena L, Arthos J, Cicala C, Kehrl JH, Park C*, et al.* IL-7 induces expression and activation of integrin alpha 4 beta 7 promoting naive T-cell homing to the intestinal mucosa. *Blood* 2012 Sep; **120**(13)**:** 2610-2619.

125. El Azreq MA, Arseneault C, Boisvert M, Page N, Allaeys I, Poubelle PE*, et al.* Cooperation between IL-7 Receptor and Integrin alpha 2 beta 1 (CD49b) Drives Th17-Mediated Bone Loss. *Journal of Immunology* 2015 Nov; **195**(9)**:** 4198-4209.

126. Fistonich C, Zehentmeier S, Bednarski JJ, Miao RF, Schjerven H, Sleckman BP*, et al.* Cell circuits between B cell progenitors and IL-7(+) mesenchymal progenitor cells control B cell development. *Journal of Experimental Medicine* 2018 Oct; **215**(10)**:** 2586-2599.

127. Hurtz C, Wertheim G, Loftus JP, Blumenthal D, Lehman A, Li Y*, et al.* Oncogene-Independent Adaptation of Pre-B Cell Receptor Signaling Confers Drug Resistance and Signaling Plasticity in Ph-like ALL. *Blood* 2019 Nov; **134:** 4.